

**Analyses on the diversity of drought tolerance in
grasses of the genus *Panicum***

Dissertation
Zur Erlangung des Doktorgrades
der Naturwissenschaften

vorgelegt beim Fachbereich Biowissenschaften
der Johann Wolfgang Goethe-Universität
in Frankfurt am Main

von
Tanja Jungcurt

aus Frankfurt am Main, Deutschland

Frankfurt am Main 2014

(D 30)

Vom Fachbereich..... der
Johann Wolfgang Goethe-Universität als Dissertation angenommen.

Dekan.....

Gutachter.....

Datum der Disputation

*Look deep into nature,
and then you will understand
everything better.*

Albert Einstein

Table of contents

1	Introduction	1
1.1	Climate change and its impact on plants.....	1
1.2	C ₃ and C ₄ photosynthesis in plants	3
1.2.1	Morphology of C ₄ plants	3
1.2.2	Physiology of C ₄ plants.....	4
1.2.2.1	The NAD-ME subtype of C ₄ photosynthesis	4
1.3	The genus <i>Panicum</i> L.	6
1.3.1	<i>P. bisulcatum</i> Thunb.....	6
1.3.2	<i>P. laetum</i> Kunth	7
1.3.3	<i>P. miliaceum</i> L.	7
1.3.4	<i>P. turgidum</i> Forssk.....	8
1.4	The impact of drought stress on plants	8
1.4.1	Physiological reactions to drought stress	9
1.4.2	Molecular reactions to drought stress	10
1.5	Aim	11
2	Material and Methods.....	13
2.1	Plants and experimental setup	13
2.1.1	Seed origin.....	13
2.1.2	Plant cultivation.....	13
2.1.3	Soil composition.....	14
2.1.4	Drought stress treatment	14
2.1.5	Sampling	15
2.1.6	Leaf tissue homogenisation.....	15
2.2	Physiological analyses	16
2.2.1	Determination of the relative water content of leaves.....	16
2.2.2	Gas exchange measurements	16
2.2.3	Leaf water use efficiency	17
2.2.4	Chlorophyll a fluorescence measurements	17
2.3	Molecular analyses	19
2.3.1	Protein analyses	19
2.3.1.1	Protein isolation	19
2.3.1.2	Protein quantification.....	20
2.3.1.3	SDS-PAGE.....	21

2.3.1.4. Western Blot.....	22
2.3.1.5. Immunodetection	22
2.3.1.6. Evaluation of protein bands	23
2.3.2 Transcriptomics.....	23
2.3.2.1. RNA isolation	23
2.3.2.2. DNase digestion	23
2.3.2.3. RNA purification.....	24
2.3.2.4. RNA concentration measurements.....	24
2.3.2.5. Gel electrophoresis on agarose basis.....	24
2.3.2.6. HT-SuperSAGE	24
2.3.2.7. 3' RACE.....	30
2.3.2.8. BLAST	31
2.3.2.9. qPCR.....	32
2.4 Data processing and statistical analyses	35
3 Results.....	37
3.1 Physiological analyses	37
3.1.1 Relative leaf water content.....	37
3.1.2 Gas exchange measurements.....	39
3.1.3 Leaf water use efficiency.....	41
3.1.4 Chlorophyll a fluorescence analyses.....	42
3.2 Molecular analyses	48
3.2.1 Protein analyses	48
3.2.2 Transcriptomics.....	51
3.2.2.1. Isolation of RNA.....	51
3.2.2.2. HT-SuperSAGE	52
3.2.2.3. BLAST search	62
3.2.2.4. 3' RACE.....	63
3.2.2.5. BLAST search for gene annotation	64
3.2.2.6. Gene expression analysis by qPCR.....	66
4 Discussion.....	75
4.1 Physiological analyses	75
4.1.1 Relative leaf water content.....	75
4.1.2 Photosynthesis rate, stomatal conductance and transpiration rate.....	76
4.1.3 Leaf Water use efficiency	78

4.1.4	Chlorophyll a fluorescence transients and JIP-test parameter.....	79
4.2	Molecular analyses	87
4.2.1	Analyses of the content of selected proteins.....	87
4.2.2	Transcriptomics	89
4.2.2.1.	Gene expression profiling by HT-SuperSAGE	89
4.2.2.2.	ABA-dependent and ABA-independent gene expression	91
4.2.2.3.	The MAPKinase pathways	96
4.2.2.4.	Calcium signals and protective proteins	97
4.2.2.5.	Species-comprehensive analyses	98
4.2.2.6.	Fold-change regulation of HT-SuperSAGE tags	100
4.2.2.7.	BLAST and qPCR results	101
5	Summary	107
6	Zusammenfassung.....	109
7	References	115
8	List of figures	129
9	List of tables	131
10	Abbreviations	133
11	Appendix	137
11.1	3' RACE.....	137
	Acknowledgments	143
	Curriculum vitae	145

1 Introduction

Against the background of climate change, the analysis on the plant's reactions to drought stress preserve augmented significance. Increasing numbers of inhabitants in already dry areas of the world have to be nourished and biotechnological as well as breeding approaches have to find new genotypes able to grow under limited water resources. Investigating the plant's reactions to drought stress can additionally give an insight into future global plant distribution. It is therefore of great importance to understand why certain plants – in this study grasses of the genus *Panicum* – can survive under severe drought stress while others can't. In the following chapters, a short introduction about the predicted climate change, the plants analysed in this dissertation and the physiological as well as molecular reactions of plants to drought stress will be given.

1.1 Climate change and its impact on plants

The Intergovernmental Panel on Climate Change (IPCC) released a new report on climate change in 2013 stating that “it is virtually certain that there will be more frequent hot and fewer cold temperature extremes over most land areas on daily and seasonal timescales as global mean temperatures increase. It is very likely that heat waves will occur with a higher frequency and duration.” (IPCC 2013). With changing temperatures the precipitation pattern is also altered leading to less precipitation especially in southern Europe, northern, western and southern Africa and central – as well as northern parts of South America (Fig. 1). In contrast, precipitation could increase up to 50 % in the arctic regions (“worst case scenario”) boosting ice melting and rising sea levels. Besides the effects of temperature and precipitation, also the concentration of carbon dioxide plays an important part when it comes to plant biodiversity and distribution. It is stated in the fifth IPCC assessment report that “carbon dioxide concentrations have increased by 40 % since pre-industrial times, primarily from fossil fuel emissions and secondarily from net land use change emissions” peaking at 391 ppm in 2011 (IPCC 2013).

Consequences of these changes are – amongst others – a diminished biodiversity and a redistribution of flora and fauna in the affected areas as the ongoing climatic changes happen too fast for the herbal - and animal adaptation. These changes have – in the end – also an impact on humanity.

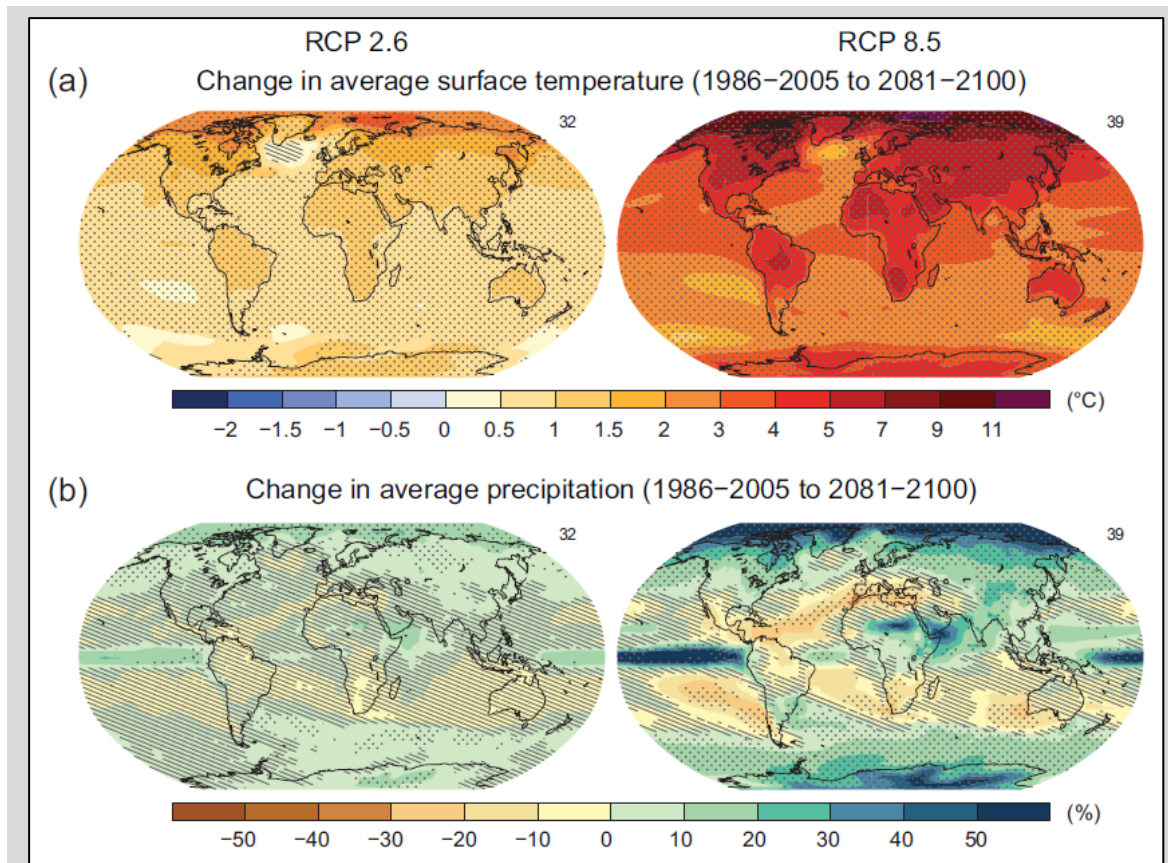


Fig. 1: Maps of Coupled Model Intercomparison Project Phase 5 (CMIP5) multi-model mean results for the scenarios “Representative Concentration Pathway” (RCP) RCP2.6 (“best case”) and RCP8.5 (“worst case”) in 2081–2100 of (a) annual mean surface temperature change and (b) average percent change in annual mean precipitation. Changes in panels (a) and (b) are shown relative to 1986–2005. The number of CMIP5 models used to calculate the multi-model mean is indicated in the upper right corner of each panel. For panels (a) and (b), hatching indicates regions where the multi-model mean is small compared to natural internal variability (i.e., less than one standard deviation of natural internal variability in 20-year means). Stippling indicates regions where the multi-model mean is large compared to natural internal variability (i.e., greater than two standard deviations of natural internal variability in 20-year means) and where at least 90 % of models agree on the sign of change (according to IPCC 2013).

As plants are sessile creatures they are exposed to the environmental conditions around them. Biotic as well as abiotic factors like pest infestation, water shortage, heat, cold or salinity stress can have great impact on plant development and growth. When climatic conditions deviate from the “normal”, plants experience stress situations. To counteract these stress situations plants have developed a myriad of adaptation – and defence mechanisms on cellular, physiological, metabolic and molecular levels enabling the plant to survive up to a certain (plant specific) impact of stress (LAWLOR 2009). Among these mechanisms, the utilization of the type of photosynthesis plays an important part in drought stress adaptation.

1.2 C₃ and C₄ photosynthesis in plants

Three different photosynthesis types exist in plants – the C₃ type of photosynthesis, the C₄ type of photosynthesis and the crassulacean acid metabolism (CAM). The C₃ metabolism is used by about 90 % of the angiosperm species, followed by the CAM being used by about 7 % and then by the C₄ metabolism which is found in about 3 % of all known angiosperm species (SAGE 2004). Despite this small species number its contribution to global primary production reaches 25 % (STILL et al. 2003) and around 30 % of terrestrial carbon is fixed by C₄ species (LLOYD & FARQUHAR 1994). In warmer and drier regions C₄ plants have competitive advantages over C₃ species as they have a better water use efficiency (WUE). This is due to morphological (1.2.1) and physiological (1.2.2) differences which evolved in the course of evolution. Their nomenclature derives from the first stable metabolite formed during CO₂ fixation – a C₃ molecule in C₃ plants and a C₄ molecule in C₄ plants.

1.2.1 Morphology of C₄ plants

Leaves of C₄ plants possess two different types of photosynthetically active tissue – the bundle sheath cells (BSC) and the mesophyll cells (MC). The vascular bundle is thereby surrounded by the BSC which itself are surrounded by the MC having contact with the gaseous room of the leaf. This C₄ characteristic leaf anatomy is called *Kranz* anatomy (HABERLAND 1984).

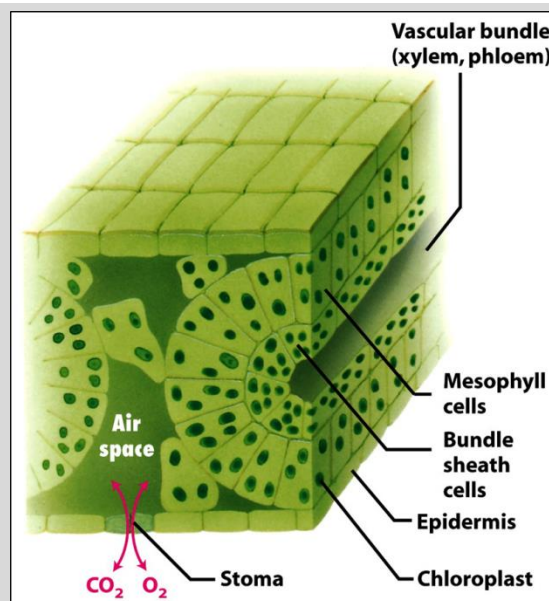


Fig. 2: Anatomy of a C₄ leaf (Kranz anatomy). The vascular bundle is surrounded by mesophyll cells which are circular surrounded by mesophyll cells (MC). The MC are in contact with the gaseous room of the leaf (according to LODISH et al. 2008).

Both photosynthetic active cell types possess grana thylakoids and the enzymes of the Calvin cycle. An exception can be found in the C₄ NADP-malate enzyme (NADP-ME) subtype showing a chloroplast dimorphism. Its BSC lack grana and the MC lack the enzymes of the Calvin cycle.

1.2.2 Physiology of C₄ plants

As mentioned above, C₄ plants have a competitive advantage in warmer and drier areas which can be ascribed to their morphological characteristics. The enzyme ribulose-1,5-bisphosphate carboxylase/oxygenase (RubisCO), which is the initial CO₂ fixing enzyme in C₃ plants, is found in the chloroplasts of the BSC in C₄ plants as a carboxylating enzyme. The initial CO₂ fixation in C₄ species is carried out in the MC by the enzyme phosphoenolpyruvate carboxylase (PEPC). The fixed CO₂ is then transported into the BSC and released to be used by the RubisCO (HATCH 1987). This “pre-fixation” leads to a high CO₂ concentration around RubisCO suppressing its oxygenic function (photorespiration). The photosynthetic capacity of C₄ plants is therefore higher than in C₃ plants when surrounding temperatures reach 30-45°C as the oxygenic function is suppressed. In contrast to C₃ plants, C₄ species do not lack CO₂ when closing their stomata to prevent excess loss of water during dry and hot days. These characteristics lead to a two - three times higher water use efficiency of C₄ plants and enable them to dominate warmer and drier regions of the world.

Besides the NAD-ME subtype of C₄ photosynthesis two more subtypes exist, the NADP-ME - and the phosphoenolpyruvate carboxykinase (PCK) subtype. Also diverse crossovers between the C₃ and C₄ subtypes and within the C₄ subtypes exist differing in morphological as well as biochemical attributes (MOSS et al. 1969).

1.2.2.1. The NAD-ME subtype of C₄ photosynthesis

As the C₄ *Panicum* species analysed in this dissertation all use the NAD-ME subtype of photosynthesis, it will be introduced in detail below (Fig. 3).

In plants using the C₄ NAD-ME subtype the bundle sheath chloroplasts have thylakoid membranes with developed grana stackings and photosystem II (PS II).

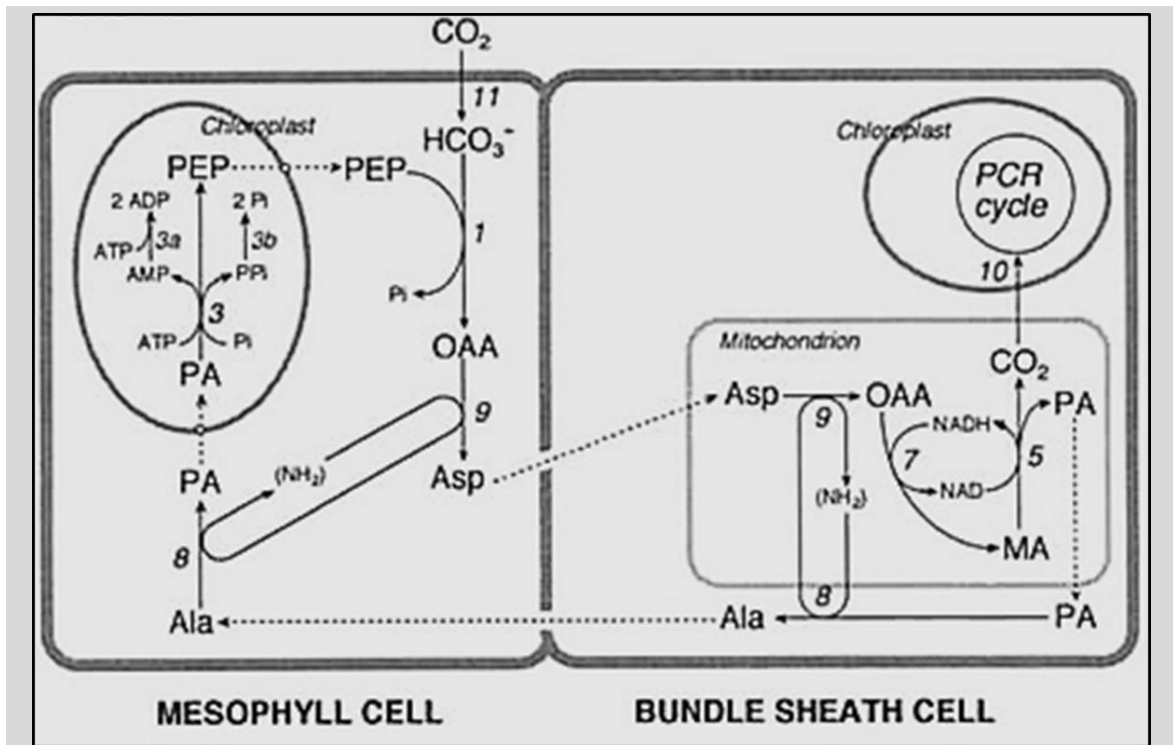


Fig. 3: NAD-ME subtype of C₄ photosynthesis. Abbreviations: OAA – oxaloacetate, Asp – aspartate, MA – malate, PA – pyruvate, Ala – alanine, PEP – phosphoenolpyruvate, Pi – orthophosphate, PPi – pyrophosphate. Enzyme abbreviations: 1 – phosphoenolpyruvate carboxylase (PEPC), 3 – pyruvate phosphate dikinase, 3a – adenylate kinase, 3b – pyrophosphatase, 5 – NAD-malic enzyme (NAD-ME), 7 – NAD-malate dehydrogenase, 8 – alanine aminotransferase, 9 – aspartate aminotransferase, 10 – RuBP carboxylase, 11 – carbonic anhydrase (according to KANAI & EDWARDS 1999).

In the mesophyll cells (MC) the enzyme phosphoenolpyruvate carboxylase (PEPC) carboxylates the phosphoenolpyruvate (PEP) to oxaloacetate (OAA) using the HCO_3^- generated from the CO_2 in the gaseous room. This reaction is carried out in the cytosol of the MC. OAA is then transaminated into aspartate as the main initial product of CO_2 -fixation. Aspartate itself is transported via a diffusion gradient into the mitochondria of the bundle sheath cells (BSC). In the BSC the aspartate is deaminated to OAA again and this is used by the enzyme NAD-malate dehydrogenase to form malate. Malate is now decarboxylated to pyruvate by the NAD-malate enzyme (NAD-ME) thereby forming CO_2 . The reduction equivalents ($\text{NADH} + \text{H}^+$) used in the previous step are also regenerated. The released CO_2 is transported into the chloroplast of the BSC where it is used as substrate by the RubisCO. The pyruvate (PA) is released into the cytosol of the BSC, transaminated to alanine (Ala) and as such transported to the MC where it is deaminated again to PA. PA is then transported into the chloroplast of the MC and converted to PEP - available for the PEPC.

1.3 The genus *Panicum* L.

The genus *Panicum* L. was first described in 1753 by C. Linnaeus as the genus “Panicgrass”. It belongs to the Paniceae and is the most important genus in this tribe (SEDE et al. 2009), which comprises important crops like foxtail millet (*Setaria italica*), pearl millet (*Pennisetum glaucum*) and proso millet (*Panicum miliaceum*). Its nearly 450 species inherit the C₃ type of photosynthesis and all C₄ subtypes and have a worldwide distribution in diverse habitats with the dominant occurrence in tropical and subtropical regions (WEBSTER 1988). The selected species investigated in this dissertation *P. laetum* Kunth, *P. miliaceum* L. and *P. turgidum* Forssk. are phylogenetically grouped in the subtribe Panicinae (subfamily Panicoideae) of the Paniceae s.s. clade and are closely related to each other (MORRONE et al. 2012, ZIMMERMANN et al. 2013) whereas *P. bisulcatum* Thunb. belongs to clade B of Paniceae s.s. (ZIMMERMANN et al. 2013). This phylogenetic relationship is also reflected by the photosynthesis types these species use as *P. laetum*, *P. miliaceum* and *P. turgidum* all possess the C₄ NAD-ME photosynthesis subtype and *P. bisulcatum* conducts C₃ photosynthesis. It has been the subject of discussion for some years to restrict those species clustering into the subtribe Panicinae as the “true Panicum” with all appending species conducting C₄ NAD-ME photosynthesis (ALISCIONI et al. 2003, CHRISTIN et al. 2009, MORRONE et al. 2012).

1.3.1 *P. bisulcatum* Thunb.

P. bisulcatum (black seed panic grass) is an annual grass growing up to heights of 180 cm with linear leaf blades and much branching panicles. It grows in moist places up to 1.600 m a.m. in temperate regions like the USA, China and East-Asia and tropical regions like India and South-East Asia down to Australia (CLAYTON et al. 2006). *P. bisulcatum* has been described as a grass used for erosion control (LAZARIDES & HINCE 1993) and forage production (KOYAMA 1987) but besides these qualities it is of low economic and ecologic significance. Its scientific importance is reflected in publications by diverse authors (ALFONSO & BRÜGGEMANN 2012, FLADUNG & HESSELBACH 1986, PINTO et al. 2011) where it has also been recommended as a C₃ model grass organism in the genus *Panicum*. In this dissertation *P. bisulcatum* was used as a representative grass for the metabolism type of C₃ photosynthesis being sensitive to drought.

1.3.2 *P. laetum* Kunth

P. laetum (wild fonio) is an annual summer-green grass growing up to 70 cm of height with lanceolate leaf blades and an open panicle (CLAYTON et al. 2006). It is a much branching grass that typically grows in dips with damp soils near seasonal wetlands where it can form immense meadows extending into the desert along rivers (ADAM 1966). It favours sunny places and is distributed in the African countries southerly of the Sahara in the Sahel zone. It is found from Mauretania in the west to Sudan in the east where it can be found up to 1300 m a.m. (CLAYTON et al. 2006, BRINK 2006 and references therein). *P. laetum* is of ecological importance as it is used for the restoring of over-grazed desert pastures in semi-arid regions (WILLIAM & FARIAS 1972). It has also a very high economic importance as being one of the so called “lost crops of Africa”, crops not actively cultivated by the people but harvested in times of scarcity (IRVINE 1955). Grains collected by the nomadic people are also sold at higher prices in markets than cultivated millets (BROWN et al. 2009). *P. laetum* is furthermore used as fodder for stock (BROWN et al. 2009) and is suitable for the production of hay and silage (BRINK 2006 and references therein). Even though *P. laetum* is of high ecologic and economic importance, it has not been of high scientific interest and only few publications can be found. In this dissertation *P. laetum* is investigated as a representative of the NAD-ME C₄ photosynthesis subtype being semi-tolerant to drought.

1.3.3 *P. miliaceum* L.

P. miliaceum (proso millet, broom millet) is an annual grass growing up to 150 cm of height with linear leaves and a drooping panicle (CLAYTON et al. 2006). It is a modest plant with little demands for water cultivated preferentially in temperate regions on every continent of this planet up to 3000 m a.m. (even in the Himalaya region). *P. miliaceum* has been cultivated for over 5000 years in central and eastern Asia where it is still a major crop today. It is of great ecologic importance as it can grow in semi-arid areas, where hardly any other cereal can be cultivated (BRINK 2006 and references therein). For human consumption its grains are used to produce flour or porridge or are cooked like rice. The plant has also medical qualities and grains are used to cure abscesses while stem and root decoctions are used to treat haematuria. Grains of *P. miliaceum* are also used as fodder but the plant's forage quality is very poor (BRINK 2006 and references therein). The plant is furthermore of high economic importance as the international trade with *P. miliaceum* in the years of 1999 - 2003 summed up to 170.000 t / year having a significant economic impact (BRINK 2006 and references therein). In addition to its great ecologic and economic impact, *P. miliaceum* is

also of scientific interest and several studies have been conducted with that species (ALFONSO & BRÜGGEMANN 2012, EMENDACK et al. 2011, HU et al. 2008, KARYUDI & FLETCHER 2002). In this dissertation *P. miliaceum* is investigated as a representative of the NAD-ME C₄ photosynthesis subtype being tolerant to drought.

1.3.4 *P. turgidum* Forssk.

P. turgidum (desert grass) is a perennial tussock grass growing up to 100 cm of height with linear - lanceolate leaf blades and an open, pyramidal panicle (CLAYTON et al. 2006). It is mainly dispersed in northern Africa and the Middle East (WILLIAM & FARIAS 1972) where it can be found up to 3200 m a.m. (BRINK 2006 and references therein). Like *P. laetum* it is a “lost crop of Africa” and the grains are harvested by nomadic people as a supplementary crop (IRVINE 1955). *P. turgidum* is also used as fodder as it has an excellent forage quality and a high nutritive value (WILLIAM & FARIAS 1972). Some people also use the powder of ground stems for wound-dressing (BRINK 2006 and references therein). Its ecological value is augmented by its extreme drought and salt tolerance and sand-binding characteristics which facilitate cultivation and counteract desertification in dry habitats (WILLIAM & FARIAS 1972). Besides its use as supplementary crop, *P. turgidum* is of little economic value only being described as a potential plant for ethanol production (ABIDEEN et al. 2011). Even though being extremely drought tolerant, *P. turgidum* has only been the subject of few scientific research activities (EL-KEBLAWY et al. 2011, ASHRAF & YASMIN 1995). In this dissertation *P. turgidum* is investigated as a representative of the NAD-ME C₄ photosynthesis subtype being extremely tolerant to drought.

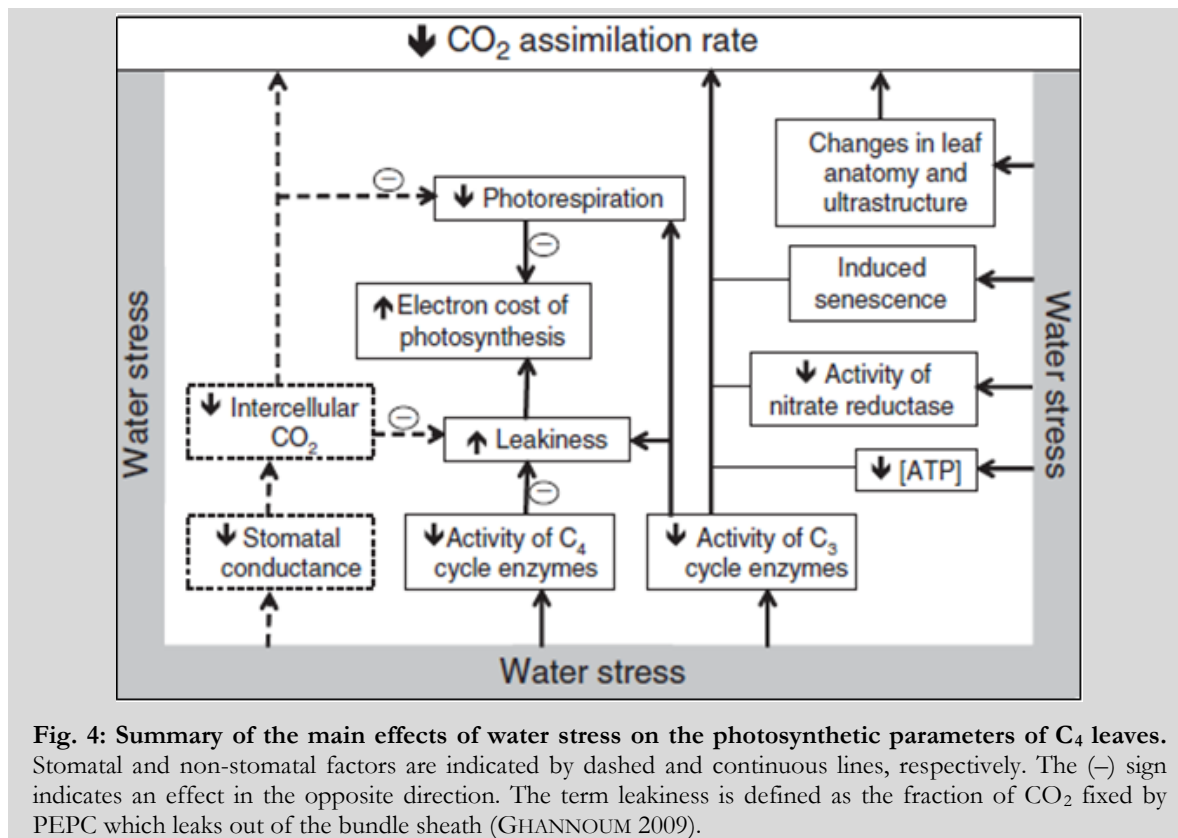
1.4 The impact of drought stress on plants

The impact of drought and other abiotic stresses is the main cause of crop failure worldwide, reducing yields by more than 50 % (BRAY et al. 2000). Monetary losses reach millions of dollars per year due to reduced – or no crop productivity at all. It is therefore of great importance to gain knowledge of the plant’s reactions and adaptation to arid soil to counteract reduced crop productivity. Drought stress affects the plant on all “levels”, from physiological reactions up to gene expression. As analyses in this dissertation focused on physiological as well as molecular reactions to drought stress, the two topics will be introduced below.

1.4.1 Physiological reactions to drought stress

In C_3 as well as in C_4 plants physiological reactions to drought stress undergo different phases in correlation with declining relative leaf water content (RWC). In C_3 plants stomatal- as well as non-stomatal inhibition has been postulated to limit net photosynthesis rate (LAWLOR & TEZARA 2009). In C_4 plants however, the effects of drought stress are less well studied. In plants using C_4 photosynthesis, the initial phase, also called stomatal phase, is marked by a RWC above 70 % and declining CO_2 assimilation rate is mainly the result of decreased intercellular CO_2 concentrations due to closed stomata and stomatal conductance (GHANNOUM 2009). The second phase is characterized by a mixed stomatal and non-stomatal phase and the third phase is characterized by mainly non-stomatal limitations (GHANNOUM 2009). The non-stomatal phase is found when the RWC falls below 70 % and CO_2 assimilation rate is inhibited due to metabolic limitations and not due to declining CO_2 concentrations – this phase is also called the metabolic inhibition.

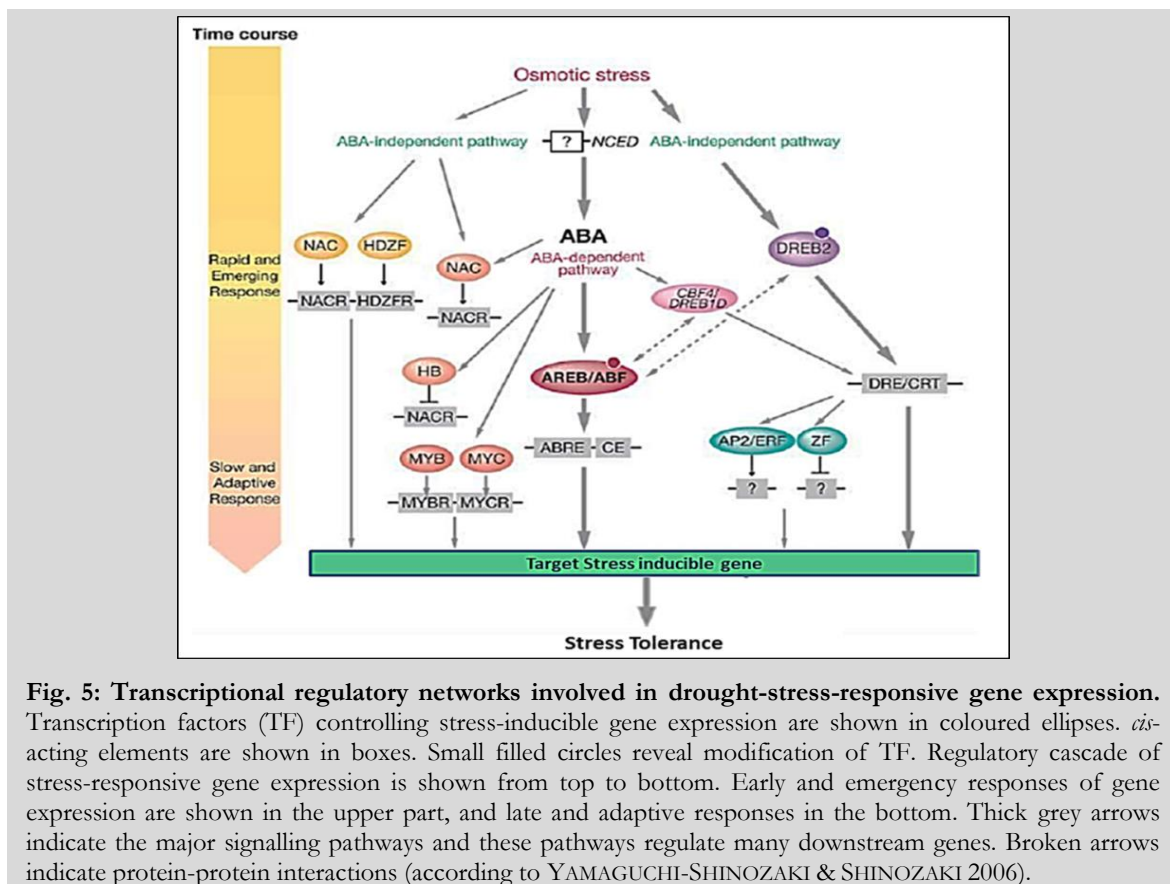
GHANNOUM (2009) stated that “the stomatal factors refer to the downstream effects of CO_2 limitation on photosynthetic activity. The non-stomatal factors encompass everything else, including the direct effects of reduced leaf and cellular water status on the activity of enzymes involved in the CO_2 fixation and electron transport reactions, induction of early senescence, and changes to leaf anatomy and ultrastructure” (Fig. 4)



As mentioned above, the *C₄ Panicum* species investigated in this dissertation all belong to the NAD-ME subtype. It is therefore remarkable that their “robustness” to drought differs in such an extreme way. As their physiology is similar, differences must also be found on a molecular level explaining the different adaptation mechanisms.

1.4.2 Molecular reactions to drought stress

In plants suffering from drought stress a differential gene expression profile can be observed compared to control plants. Drought stress induces a variety of genes in different species (INGRAM & BARTELS 1996) and the products of these genes take over different functions – e.g. regulation of gene expression, signal transductions or stress tolerance (SHINOZAKI et al. 2003). Drought induced gene expression is regulated by an abscisic acid - (ABA) independent or an ABA-dependent pathway suggesting that the phytohormone ABA plays an important role in parts of the drought stress response (SHINOZAKI et al. 2003). Both signalling pathways induce a variety of transcription factors (TF) and *cis*-acting elements which in turn induce stress inducible genes. Products of this gene expression (e.g. proteins or metabolites) then function in stress adaptation and stress tolerance (Fig. 5). For a detailed description of the individual TF and elements see also 4.2.2.1 - 4.2.2.3.



Proteins involved in drought stress are e.g. late embryogenesis abundant (LEA) proteins, heat shock proteins (HSPs) or aquaporins protecting the plant proteome under stress or regulating water flow within the tissue (see also 4.2.2.4). All these mechanisms together – physiological, metabolic, proteomic and molecular – enable the plants to survive under water shortage up to a plant-specific point.

1.5 Aim

In this dissertation the impact of drought stress on different *Panicum* species was investigated. Grasses of the genus *Panicum* were chosen as investigation objects due to their economic and ecologic importance, especially in West-Africa. Especially the species *P. laetum* and *P. turgidum* are of great significance as wild growing stocks are still harvested by the people when cultivated cereals (e.g. *S. bicolor*, *Z. mays*) wither in the dry season.

The *Panicum* species analysed in this dissertation were subjected to different severities of drought stress and their reactions were investigated using diverse approaches on molecular as well as on physiological levels. Even though the C₄ *Panicum* species *P. laetum*, *P. miliaceum* and *P. turgidum* all use the NAD-malate enzyme (NAD-ME) subtype of C₄ photosynthesis they are differentially adapted to drought stress as explained in 1.3.2, 1.3.3 and 1.3.4. *P. bisulcatum* as a species using C₃ photosynthesis was incorporated into the studies as a “control” since C₃-plants are known to be more sensitive to drought than C₄ plants (see 1.3.1). The species investigated were selected in correspondence to their scientific, ecologic and economic importance, their habitat, their difference in drought adaptation and their cultivation ability (1.3.1-1.3.4). The aim was to deepen the understanding of the diverse reactions to drought stress. In contrast to focused investigations on a mostly molecular level, this dissertation aimed to combine physiological as well as molecular data to give a broad overview of the plants behaviour under drought stress and recovery. As climate change models predict increasing temperatures and longer lasting droughts, the comprehension of the grasses adaptation mechanisms to drought can help improve breeding and biotechnological approaches.

2 Material and Methods

2.1 Plants and experimental setup

In the chapters below, the origin of the seeds and plants, their cultivation and the experimental setup for the drought stress treatment are explained. Also the homogenisation procedure of the collected samples is described.

2.1.1 Seed origin

Seeds / plants from the different species were partly obtained from the botanical garden Frankfurt / Main or collected in their habitat (Table 1).

Table 1: Origin of seeds / plants.

Species	Origin	Coordinates	Collector
<i>P. bisulcatum</i>	Botanical garden, Goethe-University Frankfurt (D)	unknown	unknown
<i>P. laetum</i>	Burkina Faso	See THIOMBIANO et al. (2012)	Marco Schmidt
<i>P. miliaceum</i>	Botanical garden, Goethe-University Frankfurt (D)	unknown	unknown
<i>P. turgidum</i>	Tunisia, Touzeur, As-Sabihah (Plants)	34,3160 N / 7,9348 E	Wolfgang Brüggemann

2.1.2 Plant cultivation

For germination, seeds from *P. bisulcatum*, *P. laetum* and *P. miliaceum* (1.3.1, 1.3.2, 1.3.3) were dispersed on damp Vermiculite without coverage and left in the climate chamber (Viessmann) for several days. Conditions in the climate chamber were set up similar to the natural conditions where seeds would germinate (see Table 2) with a light intensity of ca. $300 \mu\text{mol m}^{-2}\text{s}^{-1}$ at the height of the germinating seeds.

Table 2: Climate chamber setup. Parameters were set to mimic conditions of the species' habitats.

Parameter	Modulation
Humidity	70 %
Day / night rhythm	14 h / 10 h
Temperature day / night	25°C / 22°C
Dusk / dawn	1 h each
Max. light intensity	1000 $\mu\text{mol m}^{-2}\text{s}^{-1}$

After germination seedlings of a size of ca. 4 -5 cm were transferred into plastic pots with a diameter of 21 cm and a height of 15 cm containing 3 kg soil (for soil composition see

2.1.3). For better root development and stress avoidance, roots were transferred with Vermiculite guaranteeing sufficient water supply. In each pot three seedlings were planted and grown for 3 - 4 weeks in the climate chamber (ca. $400 - 500 \mu\text{mol m}^{-2}\text{s}^{-1}$, Table 2) until leaves were fully developed. Plants were fertilized once a week with 1 % “Wuxal 12-4-6-Normal solution” (Schering) until 5 days before onset of the stress treatment (2.1.4). For the procedure of the drought stress treatment plants were chosen by eye according to a similar developmental state (similar size and leaf number) to ensure comparable conditions. *P. turgidum* plants collected in Tunisia and conveyed to Germany (1.3.4) were planted in plastic pots with a diameter of 21 cm and a height of 15 cm containing 3 kg soil (for soil composition see 2.1.3). Plants growing in the climate chamber (Table 2) under a light intensity of ca. $500 \mu\text{mol m}^{-2}\text{s}^{-1}$ were fertilized every two weeks with the same fertilizer described for *P. bisulcatum*, *P. laetum* and *P. miliaceum*.

2.1.3 Soil composition

Soil used for the drought stress experiments in this dissertation was composed of 39 % sand, 17 % humus, 34 % clay / loam and 10 % of Perligran 0-6 (Knauf Perlite). Soil was stored at 4°C in the dark until usage to prevent cultivation of microbes.

2.1.4 Drought stress treatment

The evening before onset of the drought stress treatment, plants were well watered. Drought stress was induced by completely withholding water for a defined time, depending on the time point the species showed a significant reduction in turgescence. For *P. bisulcatum* irrigation was stopped for five days, whereas for *P. laetum* irrigation was withheld for seven days and for *P. miliaceum* the time without water supply was eight days. For *P. turgidum* water was withheld for 11 days corresponding to the strong adaptation to drought this plant inherits. For each species (except *P. turgidum*) three pots with three individuals per pot (see 2.1.2) were subjected to drought stress (stress group, $n = 3$) and three pots with three individuals / pot were watered over the complete experiment time (control group, $n = 3$). For *P. turgidum* only two individuals were subjected to drought stress due to a limited number of plants. The first day of the drought stress treatment (day 1) was the day following the vespertine irrigation.

2.1.5 Sampling

Light adapted leaf samples (the youngest fully developed leaves, ca. 2 h after onset of light) were taken at day 1 (control) and every following second day until the end of the drought stress treatment (stress). Additionally, “recovery” samples were taken 2 h after rewatering the plants. Due to a very limited number of leaf blades, *P. turgidum* was only sampled once during drought stress treatment and not every second day like *P. bisulcatum*, *P. laetum* and *P. miliaceum* (Table 3). Leaf samples of mixed ages (the youngest 2-3 fully developed leaves) were taken from all three individuals / pot (pooled samples) to guarantee sufficient amounts of leaf tissue for all notional analyses.

Table 3: Sampling scheme. Leaf tissue samples were taken every second day (except *P. miliaceum* Day 8 and *P. turgidum*), frozen in liquid nitrogen immediately and stored at -80°C.

Species	Day 1 Control	Day 3	Day 5	Day 7	Day 8	Day 11	Recovery (+2 h)
<i>P. bisulcatum</i>	x	x	x				x
<i>P. laetum</i>	x	x	x	x			x
<i>P. miliaceum</i>	x	x	x	x	x		x
<i>P. turgidum</i>	x					x	x

Cut tissues were immediately collected in aluminium foil bags and frozen in liquid nitrogen. Leaf samples were stored at -80°C until use.

Leaf sampling was carried out in 2011 and 2012 to guarantee for sufficient leaf material for the molecular analyses.

2.1.6 Leaf tissue homogenisation

Leaf tissue homogenisation was carried out for all molecular analyses, be it protein analyses like Western Blots (2.3.1.4) and Immunodetection (2.3.1.5) or RNA analyses like HT-SuperSAGE (2.3.2.6) or qPCR (2.3.2.9). Therefore microcentrifuge tubes and the steel ball were cooled in liquid nitrogen, 100 mg of frozen leaf tissue (fresh weight, FW) from the pooled samples were weighed in the cold microcentrifuge tube together with a steel ball, clamped into the swing mill (Retsch MM 301) and shaken for 30 sec and 30 shakes / sec to grind the leaf tissue. To guarantee a representative cross section through the pooled samples, pieces from every single leaf were transferred into the microcentrifuge tube until 100 mg leaf tissue were reached. Ground leaf tissue was stored at -80°C. Using the pebble mill guaranteed a constant grinding of the leaf tissues and therefore a constant material quality.

2.2 Physiological analyses

In the chapters below the conducted gas exchange measurements, the leaf water use efficiency and the chlorophyll a measurements are described.

2.2.1 Determination of the relative water content of leaves

The relative water content (RWC) was determined for every pooled leaf sample taken according to BARRS & WEATHERLEY (1962). Therefore cuttings of ca. 1 cm² fresh leaf tissue were weighed (FW), then weighed again after saturation by floating on water in petri dishes at 4°C overnight (turgid weight, TW) and finally after drying in an oven at 80°C overnight (dry weight, DW). The RWC was calculated according to the following equation:

$$RWC [\%] = \frac{(FW - DW)}{(TW - DW)} * 100$$

2.2.2 Gas exchange measurements

Gas exchange measurements were conducted using the “Portable Gas Exchange Fluorescence System” (GFS-3000, Heinz Walz GmbH). The GFS-3000 is a gas exchange analyser based on the measurement of changes in CO₂ concentration and water vapour in the measuring chamber. The system calculates gas exchange parameters like the photosynthesis rate P_N [$\mu\text{mol m}^{-2} \text{s}^{-1}$], the stomatal conductance to water vapour $g_{\text{H}_2\text{O}}$ [$\text{mmol m}^{-2} \text{s}^{-1}$] and the transpiration rate T [$\text{mmol m}^{-2} \text{s}^{-1}$] *in vivo*. Gas exchange parameters were calculated according to CAEMMERER and FARQUHAR (1981). The parameter $g_{\text{H}_2\text{O}}$ can be converted into stomatal conductance to CO₂ by division ($g_{\text{CO}_2} = g_{\text{H}_2\text{O}}/1.56$) as the conductance for CO₂ depends on the conductance for H₂O. As the GFS-3000 calculates $g_{\text{H}_2\text{O}}$ this parameter was used for analyses. Measuring programs were written with the software GFS-Win 3.23 (Walz). Parameters for the GFS-3000 measuring chamber were set according to the conditions obtained in the climate chamber (CO₂: 400 ppm, relative humidity: 70 %, temperature: 25°C, light intensity: 2000 $\mu\text{mol m}^{-2}\text{s}^{-1}$) and according to the manufacturers instruction. A leaf adaptation interval of 10 min and a measuring interval of 1 min (with a total of 6 measuring points of 10 sec each) were set to quantify the gas exchange parameters described above. Measurements were performed on the youngest fully developed leaf of control, stress and recovery plants of *P. bisulcatum*, *P. laetum* and *P. miliaceum* (n = 3). For *P. turgidum* no gas exchange parameters were recorded.

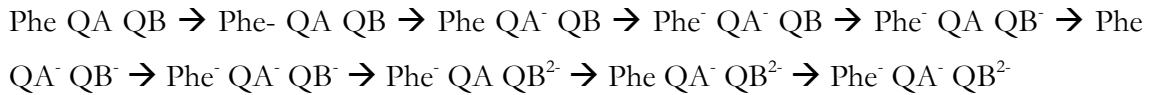
2.2.3 Leaf water use efficiency

The leaf water use efficiency (WUE) describes the relation between the amount of fixed carbon and transpired water and was calculated as follows:

$$WUE [\mu\text{mol CO}_2 / \text{mmol H}_2\text{O}] = \frac{\text{Photosynthesis rate } [\mu\text{mol CO}_2 \text{ m}^{-2} \text{ s}^{-1}]}{\text{Transpiration rate } [\text{mmol H}_2\text{O} \text{ m}^{-2} \text{ s}^{-1}]}$$

2.2.4 Chlorophyll a fluorescence measurements

If a dark adapted leaf is exposed to a saturating light impulse, the absorbed energy is either trapped in reaction centres (RCs) and converted to chemical components or dissipated as heat or fluorescence. This chlorophyll fluorescence is mainly emitted by the Chl a's of PS II where PS I only plays a negligible role (BAKER & WEBBER, 1987). Upon light exposure, the electron chain in a dark adapted leaf (all RCs are oxidized, in an "open" state) is reduced up to the acceptor site of PS I, reducing pheophytine (Phe), quinone A (QA) and quinone B (QB) in PS II consecutively until all RCs are reduced and in a "closed" state. STRASSER & STIRBET (2001) generated a model for the reduction of Phe, QA and QB in PS II:



In this model the four electrons successively released by the oxygen evolving complex reduce Phe, QA and QB subsequently with QA being re-oxidized ("turnover") multiple times reflecting the primary reactions of PS II. The more RCs are closed, the higher is the Chl a fluorescence dissipated by PS II. Any dark adapted photosynthetic sample will display a fast fluorescence rise (10 μs – 1 s) from an initial fluorescence intensity F_0 to a maximal fluorescence intensity F_M when given saturating light (STRASSER et al. 2004). The fast fluorescence transient shows several steps at different times namely called O (0.05 ms), J (2 ms), I (30 ms) and P (300 ms) which can be allocated to different redox stages of PS II during electron transport (STRASSER et al. 1999). Based on these OJIP parameters, STRASSER & STRASSER (1995) designed a test called the JIP-test. If there is a physiological change of state, it will also be visible in the shape of the fast polyphasic fluorescence transient generated from the experimental values provided from the JIP-test (STRASSER et al. 2000).

The induction transients of Chl a were followed using the Plant Efficiency Analyser (Pocket PEA, Hansatech Instruments Ltd.) with measurements taken “predawn” to have the longest dark adaptation possible. Data acquisition was conducted before applying gas exchange measurements (2.2.1). According to STRASSER et al. (2000, 2004) F_0 was set to the fluorescence intensity at 50 μs ($F_{50\mu\text{s}} = F_0$) within the PEA Plus 1.0.0.1 Software. The Pocket PEA used in this dissertation measures the fast fluorescence kinetic for 1s applying 3 x 650 nm saturating light impulses, each one with a light intensity of 3500 $\mu\text{mol quanta m}^{-2}\text{s}^{-1}$. Data are recorded every 10 μs for the first 300 μs , every 0.1 ms until 3 ms, every 1 ms until 30 ms, every 10 ms until 300 ms and every following 100 ms until 1 s has been reached. There are four prominent steps in the fast fluorescence rise of chl a, O, J, I and P (O: fluorescence intensity at 50 μs = F_0 , J: fluorescence intensity at 2 ms = F_J , I: fluorescence intensity at 300 ms = F_I and P: maximal fluorescence intensity = F_M). Different chl a fluorescence parameters describing energy fluxes, quantum yield and performance indices (PI) were analysed using the Biolyzer HP3 software and the JIP-test equations (STRASSER et al. 2010), for detailed description of all analysed parameters see Table 4. Differential induction curves (control - stress, control - recovery) were calculated from data points recorded by the Pocket PEA according to YORDANOV et al. (2008):

$$\Delta V_{OP}(t) = [(F_t - F_0) \text{ stress} / (F_M - F_0) \text{ stress}] - [(F_t - F_0) \text{ control} / (F_M - F_0) \text{ control}]$$

Table 4: Experimental values provided by the JIP-test.

$F_0 = F_{50\mu\text{s}}$	Minimal fluorescence intensity at 50 μs – all RC are open / in oxidized state
F_V	Difference of minimal and maximal fluorescence intensity $F_V = F_M - F_0$
F_M	Maximal fluorescence intensity – all RC are closed / in reduced state
M_0	Initial slope of the induction curve. $M_0 = 4 (F_{300\mu\text{s}} - F_0) / (F_M - F_0)$
V_J	Relative variable fluorescence intensity at 2 ms $V_J = (F_{2\text{ms}} - F_0) / (F_M - F_0)$
V_I	Relative variable fluorescence intensity at 30 ms $V_I = (F_{30\text{ms}} - F_0) / (F_M - F_0)$
$V_{OJ, 300\mu\text{s}}$	Relative variable fluorescence intensity of the OJ phase at 300 μs . $V_{OJ, 300\mu\text{s}} = (F_{300\mu\text{s}} - F_0) / (F_{2\text{ms}} - F_0)$
$V_{OK, 150\mu\text{s}}$	Relative variable fluorescence intensity of the OK phase at 150 μs . $V_{OK, 150\mu\text{s}} = (F_{150\mu\text{s}} - F_0) / (F_{300\mu\text{s}} - F_0)$
ϕP_0	Quantum efficiency of primary photochemistry. ϕP_0 expresses the probability of Q_A reduction. $\phi P_0 = TR_0 / ABS = F_V / F_m$
ϕE_0	Quantum efficiency of electron transport. ϕE_0 Expresses the probability of an electron transport further than Q_A . $\phi E_0 = ET_0 / ABS$
ϕD_0	Probability that the energy of an absorbed photon is dissipated as heat. $\phi D_0 = 1 - \phi P_0$
ϕR_0	Probability that the PS I end acceptor is reduced. $\phi R_0 = RE_0 / ABS = 1 - F_I / F_M$
δR_0	Probability that an electron from the intersystem electron carriers is transported to the PS I end acceptor. $\delta R_0 = (F_M - F_I) / (F_M - F_0)$

Area	Integrated area between the induction curve and F_M
S_M	Normalized area. $S_M = \text{Area}/(F_M - F_0)$
ABS/RC	Absorption flux, effective antenna size of an active RC. $\text{ABS/RC} = M_0 (1/V_j) (1/\varphi P_0)$
TR ₀ /RC	Trapped energy flux leading to the reduction of Q_A . $\text{TR}_0/\text{RC} = M_0 (1/V_j)$
ET ₀ /RC	Electron transport flux further than Q_A . $\text{ET}_0/\text{RC} = M_0 (1/V_j) (1 - V_j)$
DI ₀ /RC	Dissipation flux. $\text{DI}_0/\text{RC} = \text{ABS/RC} - \text{TR}_0/\text{RC}$
RE ₀ /RC	Electron flux leading to the reduction of the PS I end acceptor. $\text{RE}_0/\text{RC} = M_0 (1/V_j) (1 - V_I)$
PI _{abs}	Performance Index. Efficiency of energy conservation from absorbed photons to reduction of intersystem electron carriers. $(\text{RC}/\text{ABS}) [(F_v/F_m)/1 - (F_v/F_m)] [(1 - V_j)/(1 - (1 - V_j))]$
PI _{tot}	Efficiency of energy conservation from absorbed photons to the reduction of the PS I end acceptor. $\text{PI}_{\text{tot}} = \text{PI}_{\text{abs}} \varphi R_0 / (1 - \varphi R_0)$
RC/CS ₀	Active reaction centre per excited cross section. $\text{RC}/\text{CS}_0 = \varphi P_0 (V_j/M_0) F_0$

2.3 Molecular analyses

In the following chapters the molecular methods conducted are described starting from protein- to transcriptomic analyses.

2.3.1 Protein analyses

In this chapter the methods for protein isolation, quantification and visualisation are described.

2.3.1.1. Protein isolation

Protein isolation of soluble proteins was carried out according to ASHOUB et al. (2011). To 100 mg ground plant tissue (see 2.1.6) 900 μl of ice cold ethanol containing 10 mM DTT were added and mixed well for 5 sec. Proteins were precipitated at -80°C for 1 h before a centrifugation step at 13.000 rpm for 15 min at 3°C was conducted. The supernatant was discarded and the pellet was washed twice with 900 μl of ice cold ethanol containing 10 mM DTT by 5 sec of mixing and a precipitation step for 1 h at -80°C . After these two washing steps, the supernatant was discarded, 900 μl of ethanol with 10 mM DTT were added to the pellet, mixed well and left at -80°C overnight. When the pellet was white it was left to dry in a vacuum centrifuge (Univapo 100h, UniEquip) for 10 min. The pellet was resuspended in 500 μl resuspension solution containing 7 M urea, 2 M thiourea and 2 % NP-40 (v/v) by mixing for 5 min at RT. The solution was centrifuged at 13.000 rpm for 10 min at RT before the supernatant was transferred to a new microcentrifuge tube (for

purification of the solution containing the soluble proteins this step was repeated once) and stored at -80°C .

The resulting pellet containing the membrane proteins (and cell debris) was washed three times with sodium borate buffer containing 50 mM sodium borate and 50 mM ascorbic acid (centrifugation step of 15 min at 4°C and 13.000 rpm).

2.3.1.2. Protein quantification

For protein concentration determination the Bradford protein assay was performed (BRADFORD 1976). A standard curve was established by measuring protein solutions (BSA solutions) with a known concentration. Therefore different amounts of BSA solution [40 $\mu\text{g} / \text{ml}$] were mixed with water, Quick Start™ Bradford Reagent (BioRad) and resuspension solution (2.3.1.1) in a total volume of 1 ml in quartz cuvettes (Hellma, Table 5). The absorption at 595 nm was detected on a UV spectrophotometer (U-2900, Hitachi).

Table 5: Pipetting scheme for the standard curve of the Bradford protein assay. Protein solutions with a known concentration were mixed with water, Bradford reagent and resuspension solution to determine a standard curve based on the absorbance change of the resuspension solution.

BSA (40 $\mu\text{g}/\text{ml}$) [μl]	H ₂ O [μl]	Bradford reagent [μl]	Resuspension solution [μl]	Final protein conc. [$\mu\text{g}/\mu\text{l}$]
0	800	200	2	0
12.5	787.5	200	2	0.5
25	775	200	2	1
50	750	200	2	2
100	700	200	2	4
150	650	200	2	6
200	600	200	2	8
250	550	200	2	10
300	500	200	2	12

The absorption at 595 nm was plotted against the appending protein concentration and a linear trend line was applied crossing x- and y axis at (0/0). The trend line formula ($y = 0.06x$) was used to determine protein concentrations of samples containing 2 μl protein suspension by incorporating it in the following formula:

$$\text{Protein concentration } [\mu\text{g} / \mu\text{l}] = \text{Abs}_{595} / 0.06 / 2$$

For every sample, three replicates were analysed to ensure statistical significance of the results ($n = 3$).

2.3.1.3. SDS-PAGE

Sodium dodecyl sulphate polyacrylamide gel electrophoresis (SDS-PAGE) was conducted according to LAEMMLI (1970) to determine the quality of isolated soluble proteins and for subsequent western blotting analyses (2.3.1.4). For quality examination, 12.5 % separation- / 4 % stacking gels were casted (Table 6) using the Mini-PROTEAN® Tetra Cell (BioRad) following the manufacturer's instructions.

Table 6: Pipetting scheme for different SDS-PAGs. 12.5 % and 15 % separation gels were used both with 4 % stacking gel. 30 % acrylamide solution was obtained from Roth (Rotiphorese® Gel 30 (37.5:1)). Final amounts of gel solutions were sufficient for one mini gel (BioRad). SDS = sodium dodecyl sulphate, TEMED = N,N,N',N'-tetramethylethylenediamin, APS = ammonium persulfate.

Components	12.5 % separation gel	15 % separation gel	4 % stacking gel
H ₂ O	2.0 ml	1.5 ml	1.8 ml
1.5 M Tris-HCl, pH 8.8; 0.4 % SDS (v/v)	1.5 ml	1.5 ml	-
0.5 M Tris-HCl, pH 6.8; 0.4 % SDS (v/v)	-	-	750 µl
30 % acrylamid solution	2.5 ml	3.0 ml	450 µl
TEMED	3.4 µl	3.4 µl	3.0 µl
APS	60.0 µl	60.0 µl	36.0 µl

Gels were placed in the electrophoresis chamber and covered with running buffer (25 mM Tris; 192 mM glycine; 0.1 % SDS (w/v)) before removing the combs. For the SDS-PAGE, extracted proteins needed to be treated with (4x) denaturing buffer (300 mM Tris-HCl, pH 6,8; 8 % SDS (w/v); 40 % glycerine (w/v); 20 % β-mercaptoethanol (v/v); 0.2 % bromphenolblue (w/v)) and were left at 95°C for 5 min. After heat treatment, samples were put on ice until usage. For quality control and all subsequent analyses based on SDS-PAGE, 20 µg protein were applied to the SDS-PAGs. A size standard (PageRuler Prestained Protein Ladder, Thermo Scientific) was applied to every SDS-PAG for approximation of separated protein sizes. Gels were run at 80 V (stacking gel) and 120 V (separation gel) respectively until the bromphenolblue emerged the gel.

Gels designated for quality control were stained with coomassie brilliant blue solution (0.25 % Coomassie Brilliant Blue R250 (w/v); 50 % methanol (v/v); 7 % acetic acid (v/v)) for 30 min and destained with destaining solution (50 % methanol (v/v); 10 % acetic acid (v/v)) for several hours. When gels were fully destained, a scan was taken for digitalization of the results. For subsequent analyses like western blotting (2.3.1.4), gels were used directly without further treatment.

2.3.1.4. Western Blot

Western blots (and the subsequent Immunodetection, see 2.3.1.5, TOWBIN et al. 1979) were carried out for detection of specific proteins in control, stress and recovery leaf tissue samples. Therefore, the proteins subjected to SDS-PAGE (2.3.1.3) were transferred (blotted) onto a PVDF membrane (Immobilon-P Transfer Membrane, Merck Milipore) for better accessibility. A semi-dry blotting system was used (Trans-Blot® SD Semi-Dry Electrophoretic Transfer Cell, BioRad) and membrane and SDS-PAGs were sandwiched between one layer of extra thick blot Paper (Criterion Size, BioRad) saturated in single buffer (48 mM Tris; 39 mM glycine; 20 % methanol (v/v); 1 mM SDS) with the PVDF membrane placed closer to the anode and the SDS-PAGE placed closer to the cathode. Before use the PVDF membrane had to be equilibrated in methanol for 20 sec and afterwards in single buffer for 1 min. The system was run at 1.5 mA / cm² for one hour. Proteins blotted onto the PVDF membrane were visualized with amido black solution (0.1 % amido-black (w/v); 45 % methanol (v/v); 10 % acetic acid (v/v)) and the membranes were left to dry overnight.

2.3.1.5. Immunodetection

For immunodetection the PVDF membranes subjected to western blotting (2.3.1.4) were blocked for one hour with TBST buffer (20 mM Tris-HCl, pH 7.5; 0.15 M NaCl; 0.05 % Tween 20 (v/v)) comprising 5 % skimmed milk powder (0.4 ml / cm²). A primary antibody specific to a certain target protein (see Table 7) was given to the TBST-milk powder solution (1:5000) and PVDF membranes were incubated for one hour.

Table 7: List of primary antibodies used for immunodetection. PEPC = phosphoenolpyruvate carboxylase, RubisCO = ribulose-1,5-bisphosphate carboxylase/oxygenase, LSU/SSU = large/small subunit, OEC = oxygen evolving complex.

Target protein	Antibody
PEPC	α -PEPC (T. Berberich)
RubisCO (LSU, SSU)	135-IV-II Anti-RubisCO holoenzyme from <i>S. cereale</i> (T. Berberich)
Dehydrin 1	Rabbit Anti-Dehydrin (AS07 20, Agrisera)
OEC (PsbO)	Rabbit Anti-33 KDa OEC (PsbO) (AS06 142-33, Agrisera)

Three subsequent washing steps were conducted, each for 10 min. with TBST before a second antibody (horseradish peroxidase, HRP, Pierce) was applied (1:10,000) in TBST only (0.4 ml / cm²). Membranes were incubated for one hour and three washing steps with TBST (each 10 min) were carried out afterwards. For chemiluminescent visualization of the antibody-bound proteins, membranes were left for 1 min in Pierce ECL Western Blotting

Substrate (Thermo Scientific) according to the manufacturer's instructions. Then membranes were sandwiched between two acetate sheets in a photo-cassette and an X-ray film (Medical X-Ray Screen Film Blue Sensitive, CEA) was exposed for 30 sec - 30 min. For development, the X-ray films were put into developer solution (Roentogen liquid, Entwickler Konzentrat, Tetenal) for 1 min, transferred to a stopper solution (5 % acetic acid in H₂O) for 30 sec and again transferred to a fixer solution (Roentogen liquid, Fixier Konzentrat, Tetenal) for 2 min. Films had to be washed in H₂O for 15 min before drying them over night.

2.3.1.6. Evaluation of protein bands

To quantify the bands generated by Immunodetection, their pixels were counted using the freeware ImageJ (Wayne Rasband, <http://rsb.info.nih.gov/ij/>). The output then underwent statistical analyses (2.4).

2.3.2 Transcriptomics

In this dissertation transcriptomic analyses were carried out by HT-SuperSAGE (2.3.2.6) generating a “tag - library”. From this library a small amount of tags was chosen to conduct 3' rapid amplification of cDNA ends (3' RACE, 2.3.2.7) and resultant outcomes were used for BLAST searches (2.3.2.8). To confirm the HT-SuperSAGE results, the expression of selected genes was analysed by qPCR analyses (2.3.2.9).

Below the methods for RNA isolation and clean-up are described, followed by the different methods used for transcriptomic analyses.

2.3.2.1. RNA isolation

Total RNA was isolated using the peqGOLD TriFast™ buffer (Pepqlab) according to the manufacturer's instructions using 100 mg of frozen ground plant tissue. 44 µl of RNase-free water were added to the generated pellet to resolve it.

2.3.2.2. DNase digestion

A subsequent DNase digestion was carried out (TURBO DNA-free™ Kit, life technologies) to remove DNA carryovers from RNA isolation according to the manufacturer's instructions. The liquid phase containing the DNA-free RNA was transferred to a new microcentrifuge tube.

2.3.2.3. RNA purification

Subsequently to the DNase treatment RNA was purified to eliminate DNase enzyme leftovers using the NucleoSpin® RNA Clean-up kit (Macherey-Nagel) following the manufacturer's instructions and an elution of the RNA from the column by adding 20 µl RNase-free H₂O.

2.3.2.4. RNA concentration measurements

RNA concentration and purity were measured on a NanoDrop 2000c (Thermo Scientific) by applying 1 µl of DNase treated RNA to the detector. A clear absorbance peak at a wavelength of 260 nm should be visible for high quality RNA. Furthermore the absorbance ratio $A_{260/280}$ should be ~2 to guarantee for protein-free RNA.

2.3.2.5. Gel electrophoresis on agarose basis

To check the RNA (or cDNA, DNA) quality 1 µg total RNA (or cDNA, DNA) (in a total volume of 5 µl, adding 1 µl of 6x loading dye, Fermentas) was run on a 1-2 % agarose gel in TAE buffer (Tris-HCl, pH 8.0; 20 mM acetic acid; 1 mM EDTA, pH 8.0) at 100 mA for 25 min. The gel was stained in ethidiumbromide solution (7.5 µl ethidiumbromide in 100 ml H₂O) for 15 min. and fluorescence was visualized on a UV screen (UVstar, Biometra). For documentation a photo was taken before disposal of the gel.

2.3.2.6. HT-SuperSAGE

HT-Super SAGE (high throughput-super serial analyses of gene expression) was conducted to generate a 26 bp tag library of expressed mRNAs from drought treated samples of different *Panicum* species according to MATSUMURA et al. (2010). In summary, total RNA from *P. bisulcatum*, *P. laetum*, *P. miliaceum* and *P. turgidum* samples (control, stress and recovery) was isolated according to material and methods (2.3.2.1) and double-stranded (ds) cDNA was transcribed. This ds cDNA was digested with *Nla*III, a restriction enzyme (RE) with the very common recognition site 5'-CATG-3' and an adapter sequence (adapter 2) was ligated to the 5'-CATG-3' sticky end harbouring the recognition site of a second restriction enzyme - EcoP15I. EcoP15I cuts 26 - 27 bp downstream of its recognition site, leaving a sticky end just like *Nla*III. A second digestion with the RE EcoP15I was conducted, leaving an "adapter 2 - 26 bp ds cDNA" ("adapter 2 - 26 bp tag") fragment. To the sticky end of this fragment a second adapter (adapter 1) was ligated to form an "adapter

2 - 26 bp tag - adapter 1" fragment of ca. 125 bp. This fragment was first amplified by PCR (polymerase chain reaction) and then used as a template for the sequencing reaction by the Illumina Genome Analyser II to generate a "26 bp tag library" based on expressed mRNAs. Sequence reads were then analysed *in silico*. For a detailed description of the method and the kits used see below and see Fig. 6.

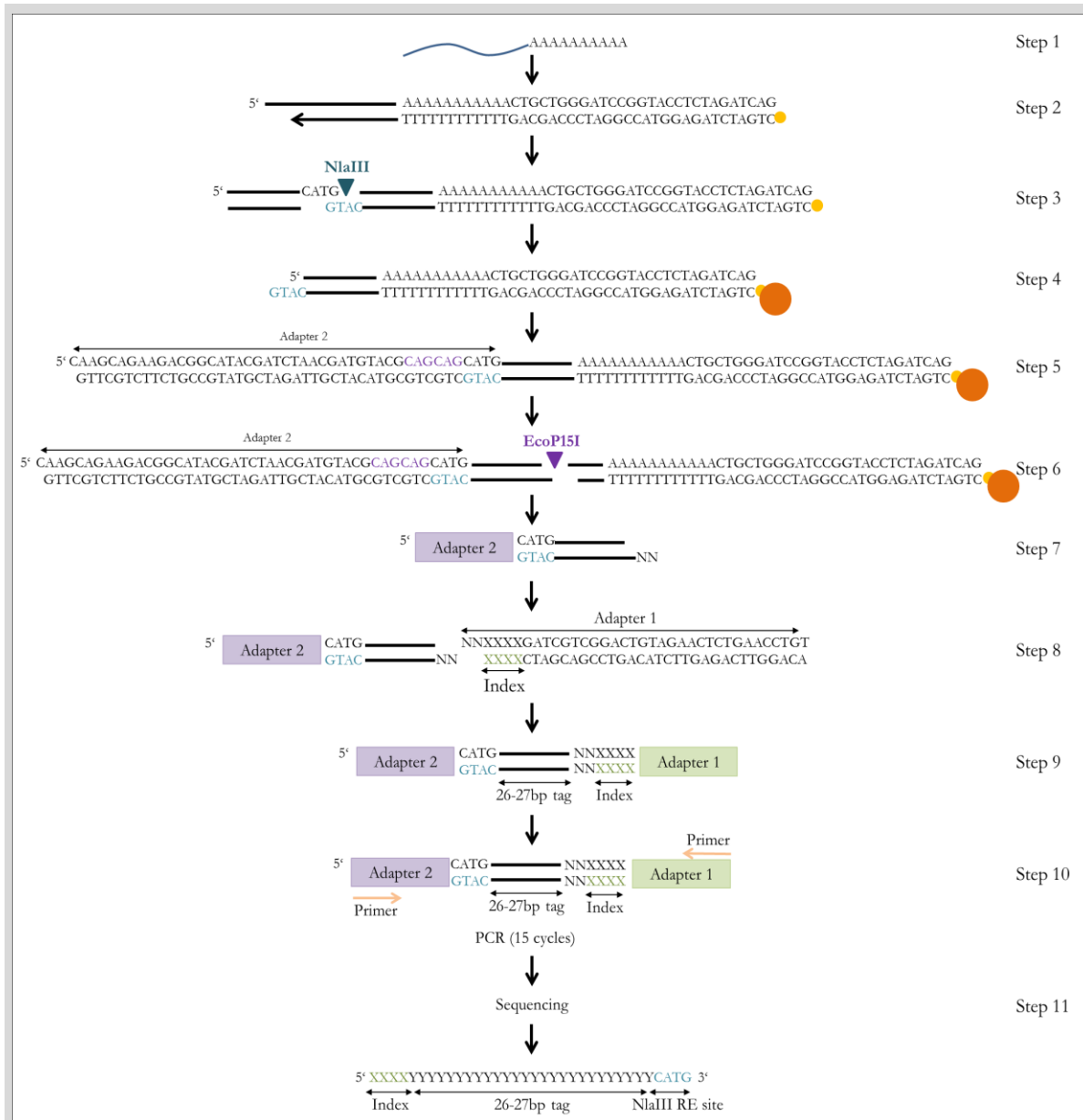


Fig. 6: Selected steps of the HT-SuperSAGE method according to MATSUMURA et al. (2010). The yellow circles in step 2-6 symbolise the biotin, the orange circles in step 4-6 symbolise the dynabeads bound to the biotin. Total mRNA was used for reverse transcription (step 1, 2) and digested with the restriction enzyme *Nla*III (step 3). Restricted fragments were bound to magnetic dynabeads (step 4) and an adapter was ligated to the fragment (step 5). A second digestion with the restriction enzyme *Eco*P15I was conducted (step 6, 7) and a second adapter harbouring an index sequence was ligated (step 9). The sequence was amplified by PCR (step 10) and sequenced (step 11).

From control, stress and recovery samples of *P. bisulcatum*, *P. laetum*, *P. miliaceum* and *P. turgidum*, total RNA was isolated from 100 mg frozen leaf tissues (see 2.1.6, 2.3.2.1 - 2.3.2.3) and stored at -80°C (step 1, Fig. 6). For the synthesis of first- and second strand cDNA from mRNA, 2 - 10 µg of total RNA (in a total volume of 10 µl DEPC H₂O) were used according to the manufacturer's instruction (SuperScript® Double-Stranded cDNA Synthesis Kit, Invitrogen). An elongated and biotinylated oligo dT reverse transcription primer (5'-bio-CTGATCTAGAGGTACCGGATCCCAGCAGT₍₁₈₎-3') was used, containing the 5'-CAGCAG-3' recognition site of the type III restriction enzyme EcoP15I (MATSUMURA et al. 2003) (step 2, Fig. 1). After first- and second strand cDNA synthesis, ds cDNA samples were purified using the QIAquick® PCR Purification Kit (Qiagen) following the manufacturer's instructions and eluted in 50 µl TE buffer (10 mM Tris-HCl, pH 8.0; 1 mM EDTA). For the following digestion by the restriction enzyme *Nla*III (New England BioLabs) samples were prepared according to the manufacturer's instruction. *Nla*III RE digestion was carried out to generate a sticky end (3'-GTAC-5') at all ds cDNAs to facilitate the ligation of an adapter (step 3, Fig. 6). For the ligation of an adapter 100 µl of streptavidin coated magnetic beads (dynabeads® M-270 Streptavidin, life technologies) were washed in siliconised microcentrifuge tubes with 200 µl bind and wash (B&W) buffer (10 mM Tris-HCl, pH 7.5; 1 mM EDTA; 2 M NaCl). Dynabeads were magnetically collected at the wall of the microcentrifuge tube for 1 min before removal of the supernatant. The *Nla*III RE digested ds cDNA was given into the microcentrifuge tube with 200 µl of 2x B&W buffer and mixed gently. The solution was left at RT for 20 min for the association of the biotin-labelled ds cDNA to the streptavidin coated magnetic beads. Four subsequent washing steps were carried out with the first two steps consisting of 200 µl 1x B&W buffer and the last two steps consisting of 200 µl TE buffer. The ds cDNA with the *Nla*III RE site closest to the poly-A tail was tightly bound to the dynabeads after this step (step 4, Fig. 6). For the ligation of an adapter (adapter 2) to the 3'-GTAC-5' *Nla*III RE site of the ds cDNA, 21 µl of TE buffer, 6 µl of 5x T4 DNA ligase buffer (Invitrogen) and 1 µl of a 20 pM adapter 2 solution were given into the microcentrifuge tubes and carefully mixed by pipetting up and down several times (adapter 2 sequence: 5'-CAAGCAGAAGACGGCATACGATCTAACGTAGTACGCA-GCAGCATG-3' harbouring the recognition site 5'-CAGCAG-3' of the RE EcoP15I) (step 5, Fig. 6). The bead suspension was incubated at 50°C for 2 min and then kept at RT for 15 min. 2 µl of T4 DNA Ligase (1 U / µl, Invitrogen) were added and the bead suspension was left at 16°C for at least 2 h by repeated mixing every 20 - 30 min. After the complete ligation of adapter

2 the bead suspension was washed four times with 200 μ l B&W buffer followed by three washing steps of 200 μ l NE buffer 3 (50 mM Tris-HCl pH 7.9; 10 mM MgCl₂; 100 mM NaCl, 1 mM DTT). For the following digestion of the ds cDNA with the RE EcoP15I (which cuts 25-27 bp downstream of its recognition site) 10 μ l of 10x NE buffer 3, 10 μ l of 10x ADP, 1 μ l of 100x BSA, 74 μ l of sterile H₂O and 5 μ l of EcoP15I RE were given to the washed magnetic beads and mixed by pipetting up and down several times. The suspension was left at 37°C for 2 h by mixing every 20 - 30 min (step 6, Fig. 6). After the complete digestion, tubes were placed on the magnetic stand to collect the “adaptor 2 - 26 bp tag” fragment and the supernatant was transferred to a new microcentrifuge tube. To ensure the complete transfer of EcoP15I digested fragments, dynabeads were mixed with 100 μ l of 1x B&W buffer, beads were magnetically collected and the supernatant was transferred into the same microcentrifuge tube as before. For complete clear-off of magnetic beads, ds cDNA was extracted by giving 100 μ l of phenol / chloroform to the solution. After mixing and centrifugation for 5 min at 10.000 rpm the upper phase was collected in a new microcentrifuge tube. For ds cDNA precipitation, 100 μ l of 10 M ammonium acetate, 3 μ l of glycogen and 900 μ l of ice cold ethanol were added and left at -80°C for 1 h before centrifugation at 4°C and 13.000 rpm for 40 min. The resulting pellet was washed twice with 200 μ l of 70 % ethanol and centrifugation at 4°C and 13.000 rpm for 2 min. The clean pellet was dried under vacuum centrifugation for 5 min and then dissolved in 10 μ l TE buffer (step 7, Fig. 6). For the ligation of another adaptor (adaptor 1), additional preparations had to be carried out. 10 μ l of 100 pmol / μ l sense and complementary anti-sense adaptor oligonucleotides were mixed with 6 μ l 5x T4 ligase buffer and 4 μ l TE buffer and left for denaturation at 94°C for 4 min before cooling down (80°C - 10 sec; 70°C - 20 sec; 60°C - 30 sec; 20°C - 10 min; 4°C - ∞). To minimise analyses costs and maximise sample throughput, different ds cDNA libraries (samples) were mixed together for a single sequencing run. For later *in silico* separation of the libraries, a four to six bp long unique index fragment was implemented in adaptor 1 which itself was then ligated to the “26 bp - adaptor 2” fragment isolated before. The first four to six bases of the sequence read encode the unique index sequence followed by the 26 - 27 nucleotides of the “tag” (MATSUMURA et al. 2010). The following adaptor 1 sequences with unique indices / sample were prepared (Table 8).

Table 8: Adapter 1 indices. The different indices were used to distinguish between the samples analysed by HT-SuperSAGE in a one shot sequencing run. C = control, S = stress, R = recovery.

Sample name	Index sequence
<i>P. miliaceum</i> C	CCAAAA
<i>P. miliaceum</i> S	CCTAAT
<i>P. miliaceum</i> R	GCGC
<i>P. turgidum</i> C	CCGAAG
<i>P. turgidum</i> S	CGAATA
<i>P. turgidum</i> R	CGTATT
<i>P. bisulcatum</i> C	CGCATC
<i>P. bisulcatum</i> S	GACC
<i>P. bisulcatum</i> R	GACA
<i>P. laetum</i> C	GCGT
<i>P. laetum</i> S	GCGG
<i>P. laetum</i> R	GCGA

The following ligation of adapter 1 to the isolated sequence was conducted by adding 3 µl 5x T4 ligase buffer and 0.5 µl of adapter 1 solution and incubation at 50°C for 2 min. After heat treatment samples were left at RT for 15 min before 1.5 µl T4 ligase were added and incubated at 16°C for 2 h (step 8, Fig. 6). Fragments were purified using the MinElute PCR Purification Kit (Qiagen) following the manufacturer's instructions and eluted in 20 µl TE buffer (step 9, Fig. 6). The purified fragments were then used as template for PCR. For amplification by PCR 4 µl of 5x Phusion HF buffer (Finnzymes), 0.4 µl 10 mM dNTPs, 0.2 µl 100 µM adapter 1 / 2 primer, 0.5 µl 50 mM MgCl₂, 0.2 µl Phusion® High-Fidelity DNA Polymerase (Finnzyme) and 1 µl template were mixed in a total volume of 20 µl. Cyclor program was set to 98°C - 2 min, [98°C - 20 sec, 60°C - 30 sec (15 cycles)], 10°C - ∞. To check the size of the fragment and the amplification amount an 8 % polyacrylamide gel (PAG) was run with 3.5 ml 40 % acrylamide / bis-acrylamid solution, 350 µl 50x TAE buffer, 175 µl APS and 15 µl TEMED in a total volume of 17.54 ml. 1.5 µl of a 20 bp DNA ladder and 15 µl of PCR product mixed with 3 µl loading dye were loaded onto the PAG and run at 10 mA for 10 min and 30 mA for further 10 min until the loading dye had migrated $\frac{2}{3}$ through the gel. After gel electrophoresis, the PAG was stained using SYBR green (Takara Bio) for visualization of ds cDNA. If a band of approximately 120 bp size ("adapter 1 - 26 bp tag - adapter 2") was visible, samples were used for the continuous workflow. To increase the amount of "adapter 1 - 26 bp tag - adapter 2" fragments, a PCR with 8 replicates was conducted according to the setup described above (step 10, Fig. 6). After PCR, samples were collected in one microcentrifuge tube and purified using the MinElute PCR Purification Kit (Qiagen) according to the manufacturer's instructions and eluted with 10 µl TE buffer. A second 8 % PAG was prepared and the 10 µl of purified PRC product, mixed with 2 µl loading dye were loaded onto the gel following the setup

described above. After SYBR Green staining, bands with a size of ca. 120 bp were cut out of the gel and immediately resuspended in 300 µl TE buffer at 37°C for 2 h. Gel solution was then transferred to a Spin-X Centrifuge Tube Filter (Corning) and centrifuged at 15,000 rpm for 20 min. A phenol / chloroform extraction was carried out and the resulting pellet was dissolved in 10 µl TE buffer. To check the quality of the extracted “adapter 1 - 26 bp tag - adapter 2” fragment, the PCR product was directly transformed in electrocompetent *E. coli* cells using the TOPO[®] TA Cloning[®] Kit (Invitrogen) following the manufacturer’s instructions. 50 µl of transformed competent *E. coli* cells were then plated on LB medium containing 100 µg / ml ampicillin, 20 µg / ml X-gal, and 0.1 mM IPTG and left at 37°C over night. Fragments inserted in the TOPO vector were amplified by colony PCR by collecting 3 - 5 colonies and dissolving in 10 µl H₂O. 10 µl of colony PCR master mix (including M13F and M13R primer) were added according to the manufacturer’s instruction and a general PCR program was run (95°C - 1 min, [95°C - 15 sec, 55°C - 15 sec, 72°C - 30 sec (35 cycles)], 72°C - 7 min, 4°C - ∞). 5 µl of the PCR product were run on a 1 % agarose gel with the expected size of the fragment being ~300 bp. If amplification was positive, bands were cut out of the gel, purified (QIAquick[®] PCR Purification Kit (Qiagen) following the manufacturer’s instructions) and sequenced using the M13F primer. If the *in silico* sequences showed the ~26 b “tag” flanked by the index sequence (5’) and the - CATG- *Nla*III RE site (3’) ds cDNA concentration and quality was analysed using the Agilent High Sensitivity DNA Kit following the manufacturer’s instructions on an Agilent 2100 Bioanalyzer (Agilent Technologies). For the HT-SuperSAGE analyses, all samples were combined in one microcentrifuge tube with a concentration of 4 ng / sample and purified using the MinElute PCR Purification Kit (Qiagen) according to the manufacturer’s instructions and eluted with 12 µl elution buffer. Combined HT-SuperSAGE samples were given to Kentaro Yoshida (Iwate Biotechnology Research Centre, Narita 22-174-4, Kitakami, Iwate, 024-0003, Japan) for sequencing on the Illumina Genome Analyser II and following *in silico* bioinformatics analyses (step 11, Fig. 6). For the sorting of sequenced fragments according to their index sequence and further *in silico* analyses scripts written in Perl (www.perl.org) were applied (MATSUMURA et al. 2010). As output large excel files listing all the identified 26 b “tag” sequences with the according count numbers (5’-CATG-22 b-3’) were generated. A nucleotide - protein BLAST search (2.3.2.8) against the genome of *P. virgatum* (the only *Panicum* genome completely sequenced and available online at that time) was carried out and excel files were generated listing the “tag” sequence, the according count number and the annotated gene. As annotation numbers for the species

were relatively low due to differences in the genomes, highly regulated “tags” without annotations were used to carry out 3’ RACE (2.3.2.7) for further analyses.

2.3.2.7. 3’ RACE

The rapid amplification of cDNA ends (RACE) is a method to amplify either the 5’- or the 3’ ends of cDNA (FROHMAN et al. 1988). In this dissertation only the 3’ ends of synthesised ss cDNA were amplified as it was assumed that the 26 bp “tags” generated by HT-Super SAGE (2.3.2.6) were located close to the 3’ end. 3’ RACE was carried out to elongate the 26 bp sequences generated by HT-SuperSAGE (as described in 2.3.2.6.) for better gene / protein annotation. Therefore 400 ng total RNA (2.3.2.1 - 2.3.2.4), 1 µl 100 mM 3’ RACE primer (oligo dT with adapter sequence, 5’GGCCAC-GCGTCGACTAGTAC-3’), 1 µl 10 mM dNTPs in a total volume of 14.5 µl was left at 65°C for 5 min. and immediately transferred on ice. 4 µl 5x RT buffer (Maxima First Strand cDNA Synthesis Kit, Thermo Scientific), 0.5 µl RiboLock RNase inhibitor and 1 µl Maxima Reverse Transcriptase were added and left for 30 min at 50°C. For enzyme degradation, samples were put to 85°C for 5 min before transferred to ice and stored at -20°C (step 1 - 3, Fig. 7). For sequence amplification by PCR 24 highly differentially expressed 26 bp “tags” which could not be annotated to a specific protein were selected to synthesise primers for every species (Table 26, Table 27). In total 96 primers were synthesised and PCR was conducted at the following conditions: 14.1 µl H₂O, 4 µl 5x buffer (Promega), 0.4 µl 10 mM dNTPs, 0.2 µl 100 mM Primer (forward - 26bp tag primer / R - adapter primer), 0.1 µl GoTaq Polymerase (Promega), 1 µl template. Cyclor Program (Mastercycler ProS PCR Thermal Cycler, Eppendorf) was set to 98°C - 30 sec, [98°C - 10 sec, 50°C - 20 sec, 72°C - 1 min (35 cycles)], 72°C - 5 min (step 4, Fig. 7). After the PCR run the reaction mix (the total of 20 µl) was loaded onto a 1.5 % agarose gel (for comparison see 2.3.2.5) and visible bands were cut out of the gel and eluted in 50 µl H₂O (Gene Jet Gel Extraction Kit, following the manufacturer’s instructions). Samples were sequenced using the 26 bp “tag” primer only at the BiK-F laboratory (Frankfurt, Germany). The generated sequences (step 5, Fig. 7) were used for a nucleotide - nucleotide BLAST (2.3.2.8) for gene annotation and a subsequent nucleotide - protein BLAST (2.3.2.8) for protein annotation.

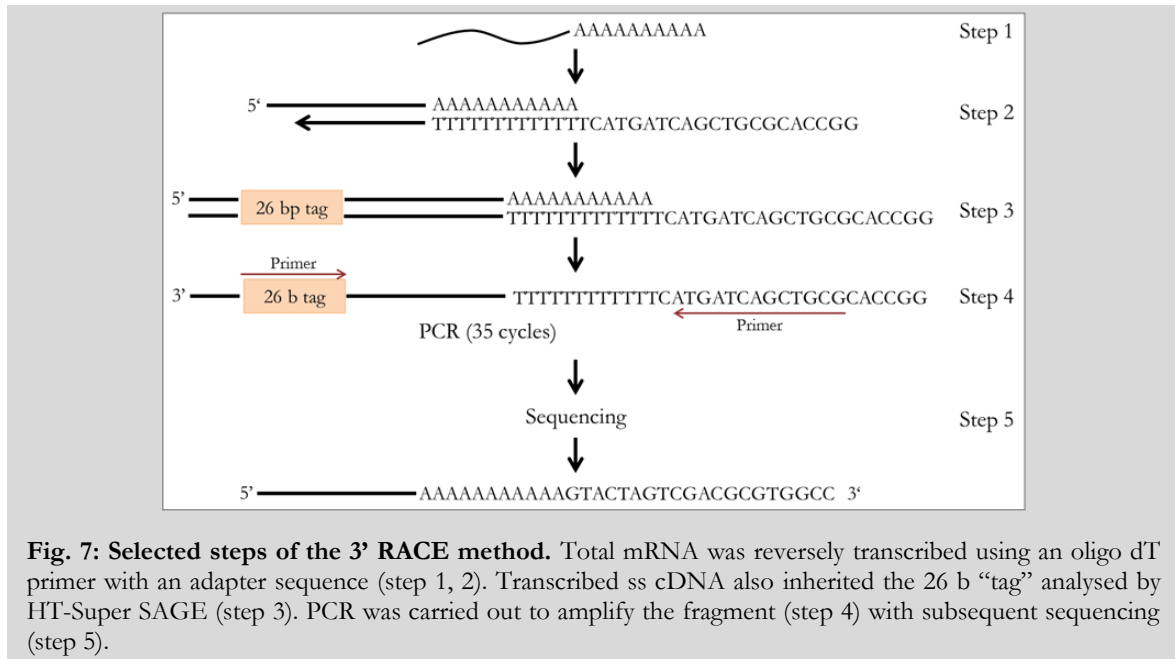


Fig. 7: Selected steps of the 3' RACE method. Total mRNA was reversely transcribed using an oligo dT primer with an adapter sequence (step 1, 2). Transcribed ss cDNA also inherited the 26 b "tag" analysed by HT-Super SAGE (step 3). PCR was carried out to amplify the fragment (step 4) with subsequent sequencing (step 5).

2.3.2.8. BLAST

„The Basic Local Alignment Search Tool (BLAST) is a bioinformatics tool that finds regions of local similarity between sequences. The program compares nucleotide or protein sequences to sequence databases and calculates the statistical significance of matches. BLAST can be used to infer functional and evolutionary relationships between sequences as well as help identify members of gene families” (<http://blast.ncbi.nlm.nih.gov/>). It was developed by ALTSCHUL et al. (1990) and has been a very powerful and often used tool in the last ca. 20 years. In this dissertation the nucleotide BLAST (BLASTn) was used to compare an extracted nucleotide sequence of unknown function (nucleotide query) to the GenBank nucleotide database using the BLAST tool on the NCBI (National Centre for Biotechnology Information) homepage (<http://blast.ncbi.nlm.nih.gov/>). For comparison of the 3' RACE sequences (see 2.3.2.7) to the GenBank database (see also MATSUMURA et al. 2003), the expressed sequence tag (EST) database was chosen (Fig. 8). ESTs are short sequences of 100 - 800 bp size generated from mRNA sequenced either from the 5' or 3' end of the cDNA. Since HT-SuperSAGE (2.3.2.6) and 3' RACE (2.3.2.7) were conducted on the basis of mRNA, the EST database was the optimal nucleotide database for a nucleotide BLAST search. A megablast algorithm search was carried out to find highly similar sequences (instead of a discontinuous megablast to find more dissimilar sequences or a BLASTn to find somewhat similar sequences, <http://blast.ncbi.nlm.nih.gov/>). The result is a list of sequences similar to the entered query sequence with a given score (the

higher the better), an e-value (significance value, the smaller the better) and an accession link to the listed sequence.

The sequence with the highest score and lowest e-value found for the entered unknown 3' RACE sequence was then used for a second megablast against the nr / nt (non-redundant / nucleotide) database to find the appending gene sequence (Fig. 8). This sequence was then translated to a protein query using the open reading frame finder (ORF finder) from the NCBI homepage (<http://www.ncbi.nlm.nih.gov/projects/gorf/orfig.cgi>). The protein query could then be utilized for a protein BLAST (BLASTp) similar to the BLASTn search. The blastp algorithm compares the unknown protein sequence to a protein database of non-redundant protein sequences and returns a list of similar sequences also inheriting a score and an e-value. It additionally delivers a graphical summary of specific hits, superfamilies and multi-domains fitting to the entered unknown protein sequence. Based on these steps, the 3' RACE sequence was annotated to a protein sequence of known function (Fig. 8).

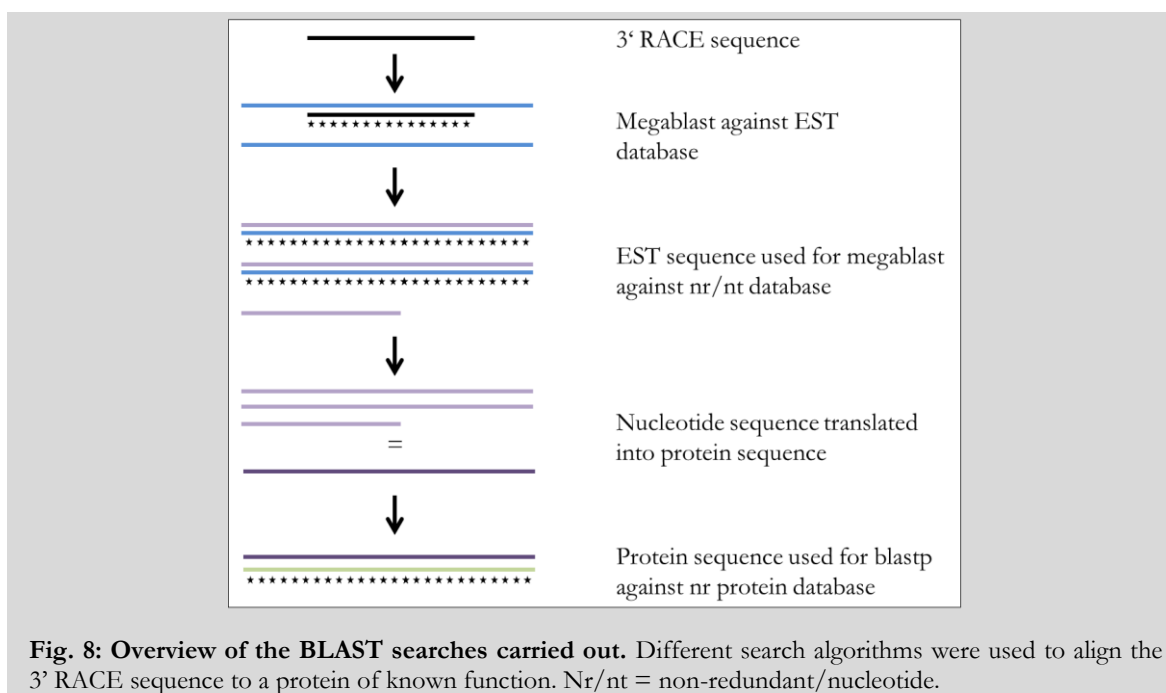


Fig. 8: Overview of the BLAST searches carried out. Different search algorithms were used to align the 3' RACE sequence to a protein of known function. Nr/nt = non-redundant/nucleotide.

2.3.2.9. qPCR

The quantitative real-time PCR (qPCR) was conducted to verify the results from the HT-SuperSAGE analyses displaying gene expression levels based on mRNA amounts. The method is based on the measurement of increasing fluorescence intensity through amplification of ds cDNA and inclusion of a fluorescence marker (SYBR Green I) over

time. For amplification of specific genes of interest, primers were generated referring to the sequences generated by 3' RACE (2.3.2.7) and the subsequent BLAST search for tag annotation (2.3.2.8). For primer generation, special software was used to guarantee for optimal primer design established by ROZEN and SKALETSKY (2000) (Primer3, <http://frodo.wi.mit.edu/>). As the qPCR is based on the amplification of ds nucleotide chains, mRNA had to be reversely transcribed before starting the experiment. The preparation of a standard curve for primer efficiency determination was also conducted before running first comparative real-time experiments.

For reverse transcription of isolated RNA (2.3.2.1 - 2.3.2.3) the iScript™ cDNA Synthesis Kit (BioRad) was used. According to the manufacturer's instructions 0.5 µg of total RNA were mixed with 4 µl 5x iScript mix and 1 µl reverse transcriptase (BioRad) in a total volume of 20 µl. Samples were left at 25°C for 5 min before standing at 42°C for 30 min. The enzyme was degraded by heating the samples at 85°C for 5 min.

Synthesized cDNA was first used to check the primer quality by normal PCR. Therefore 13.7 µl H₂O, 4 µl 5x iProof™ HF buffer (BioRad), 6.4 µl 100mM dNTP mix, 0.5 µl DMSO and 0.2 µl iProof™ High Fidelity DNA Polymerase (BioRad) and 1 µl cDNA template were mixed together and the following program was run on a Thermal Cycler (Arktik Thermal Cycler, Thermo Scientific): 95°C - 5 min, [95°C - 20 sec, 55°C - 20 sec, 72°C - 10 sec (35 cycles)], 72°C - 2 min. PCR mix was put on a 2 % agarose gel (2.3.2.5) and screened for a single band at a size of ca. 110 bp.

For qPCR the efficiencies for each primer pair had to be evaluated. A dilution row of 1:1, 1:2, 1:4, 1:8 and 1:16 diluted cDNA was prepared starting with 6 µl cDNA template and a subsequent dilution row of 3 µl cDNA + 3 µl H₂O (and so forth). A mix of 10 µl SensiFAST SYBR Lo-ROX reaction mix (Bioline), 8 µl H₂O, 0.5 µl Primer forward / reverse and 1 µl (diluted) template was applied to 0.2 ml microcentrifuge tubes and the following program was run on a quantitative real time PCR thermo cycler (Mx3005p, Agilent Technologies): 95°C - 5 min, [95°C - 20 sec, 55°C - 20 sec, 72°C - 10 sec (40 cycles)] with a subsequent melting curve of 95°C - 1 min, 55°C - 30 sec, 95°C - 30 sec (melting curve data is collected during a ramp from 55°C to 95°C). For each template 3 replica (control of internal variation) were prepared (Fig. 9). Dilution row measurements were not only conducted to calculate the primer efficiency but also for optimal template concentration determination (Ct values between 15 - 25 cycles).

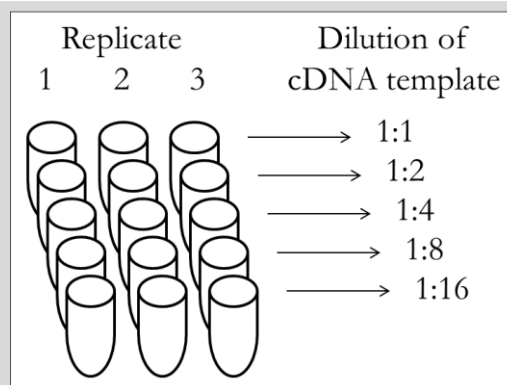


Fig. 9: Schematic description of primer efficiency measurement setup. The cDNA template used for the primer efficiency measurement was diluted 1:1, 1:2, 1:4, 1:8 and 1:16 with three internal replicates per dilution.

For the qPCR setup additional samples containing either water as template (no template control, NTC) or RNA instead of cDNA as template (no real-time, no RT) were run. NTC samples were run to guarantee for the pureness of the reactions, NRT samples were run to ensure that generated cDNA was not contaminated with DNA assuring the cleanliness of isolated RNA and avoiding amplification of DNA instead of cDNA. RNA for the NRT samples was diluted to 0.02 $\mu\text{g}/\mu\text{l}$ comparable with the amount of cDNA applied for qPCR.

The qPCR was conducted using the SensiFAST SYBR Lo-ROX Kit (Bioline). A mix of 10 μl SensiFAST SYBR Lo-ROX reaction mix, 8 μl H_2O , 0.5 μl Primer forward / reverse and 1 μl template was applied to 0.2 ml microcentrifuge tubes and the following program was run on a quantitative real time PCR thermo cycler (Mx3005p, Agilent Technologies): 95°C - 5 min, [95°C - 20 sec, 55°C - 20 sec, 72°C - 10 sec (40 cycles)] with a subsequent melting curve (as described above). For the analyses of a single gene including control, stress and recovery sample (in triplicate for internal variation control), a master mix (21-fold) had to be pipetted. Plate setup included the control sample as the “calibrator” (set to 1.0) and the stress and recovery samples as “unknown”. Additionally no RT samples were run for every template (C, S, R) and one NTC sample was run. For an internal calibration, a second set of samples had to be included in every qPCR run with primers amplifying a reference gene (house-keeping gene) equally expressed in all samples - the cap-binding protein 20 (CPB 20) - as the normalizing assay (Fig. 10). Plate setup was carried out according to the manufacturer’s instructions (MxPro QPCR Software for Mx3000P and Mx3005P QPCR Systems, Agilent Technologies).

All	1	2	3	4	5	6	7	8	9	10	11	12
	Calibrator	Calibrator	Calibrator	No RT	No RT	No RT	Calibrator	Calibrator	Calibrator	No RT	No RT	No RT
A	REF	REF	REF	REF	REF	REF	REF	REF	REF	REF	REF	REF
	NORM	NORM	NORM	NORM	NORM	NORM	Pm 3	Pm 3	Pm 3	Pm 3	Pm 3	Pm 3
B	Unknown	Unknown	Unknown	No RT	No RT	No RT	Unknown	Unknown	Unknown	No RT	No RT	No RT
	REF	REF	REF	REF	REF	REF	REF	REF	REF	REF	REF	REF
	NORM	NORM	NORM	NORM	NORM	NORM	Pm 3	Pm 3	Pm 3	Pm 3	Pm 3	Pm 3
C	Unknown	Unknown	Unknown	No RT	No RT	No RT	Unknown	Unknown	Unknown	No RT	No RT	No RT
	REF	REF	REF	REF	REF	REF	REF	REF	REF	REF	REF	REF
	NORM	NORM	NORM	NORM	NORM	NORM	Pm 3	Pm 3	Pm 3	Pm 3	Pm 3	Pm 3
D	NTC	NTC	NTC	Not in Use	Not in Use	Not in Use	NTC	NTC	NTC			
	REF	REF	REF	REF	REF	REF	REF	REF	REF			
	NORM	NORM	NORM	CPB20	CPB20	CPB20	Pm 3	Pm 3	Pm 3			

Fig. 10: Plate setup for a qPCR experiment. The “calibrator” contains the control sample, the “unknowns” contain stress and recovery samples (three internal replicates per sample). No RT (no real-time) comprises control, stress and recovery templates (RNA). NTC (no template control) only has water as template. Samples A-D and 1-6 were run with primers specific for the house-keeping gene CPB 20 as the “normalizing assay” (NORM), samples A-D and 7-12 were run with a specific primer for the 9-cis-epoxacarotenoid dioxygenase 1 (NCED 1, here called Pm 3).

Subsequently to the qPCR run, samples were loaded on a 2 % agarose gel (2.3.2.5) and checked for the amplification of a single band with the size of ca. 110 bp.

2.4 Data processing and statistical analyses

Data processing was carried out in the specific programs described for each device. Data analyses were carried out in Microsoft Excel 2010 (Microsoft Corporation, Redmond, USA) and additional graphical depictions were generated in GraphPad Prism 5.04 (GraphPad Software, San Diego, USA). For statistical analyses (calculation of significances) the unpaired t-test was applied in GraphPad Prism with * $p < 0.05$, ** $p < 0.01$ and *** $p < 0.001$ as depicted and described in figures and captions.

3 Results

In this dissertation the reaction of different grasses from the genus *Panicum* subjected to drought stress was analysed. Diverse measurements and analyses were conducted to obtain a holistic picture of the reactions to drought stress on different “levels” from physiology to gene expression in closely related grasses.

There are diverse approaches to compare the reactions to drought stress within species differentially adapted to drought. Sample selection (and comparison) was based on the relative leaf water content (RWC) of the collected tissues, resulting in four “groups” to be analysed: a control group, a moderate stress group, a severe stress group and a recovery group. Analyses on the base of the RWC made sure, that all species were suffering from an equally strong degree of leaf dehydration, independent from the duration they needed to reach the specific RWC levels.

3.1 Physiological analyses

Physiological analyses (2.2) were conducted to obtain a picture of physiological changes during drought stress within the species and in comparison to each other. Gas exchange measurements undertaken with the GFS 3000 were carried out on *P. bisulcatum*, *P. laetum* and *P. miliaceum* only and not on *P. turgidum* due to limited leaf material during the measuring period.

3.1.1 Relative leaf water content

The determination of the relative leaf water content (RWC) was carried out according to BARRS & WEATHERLEY (1962) as an easy method to measure the water balance in sampled leaves. The selection of samples used for molecular analyses in this dissertation was based on the RWC to make comparison between the different species more reasonable as the level of leaf dehydration was similar.

Table 9: RWC values of samples. For *P. bisulcatum*, *P. laetum* and *P. miliaceum* n = 5 samples were subjected to RWC measurements (n = 3 for moderate stress), for *P. turgidum* n = 2 samples were subjected to RWC measurements. * p < 0.05, ** p < 0.01, *** p < 0.001 vs. control (unpaired t-test).

Species / RWC [%]	Control	Moderate stress	Stress	Recovery
<i>P. bisulcatum</i>	82,02	76,94	46,66 ***	78,59
<i>P. laetum</i>	89,86	71,94 ***	49,18 ***	86,29 *
<i>P. miliaceum</i>	91,53	75,59 **	51,01 ***	86,21
<i>P. turgidum</i>	89,12	-	53,72 *	86,97
Mean value RWC	88,13 ± 5.66	74,82 ± 7.22	50,14 ± 5.62	84,52 ± 5.62

For better visualization of the treatment period / RWC correlation, results were also illustrated as a graphical summary in Fig. 11 in correspondence to Table 3 where the sampling scheme is listed.

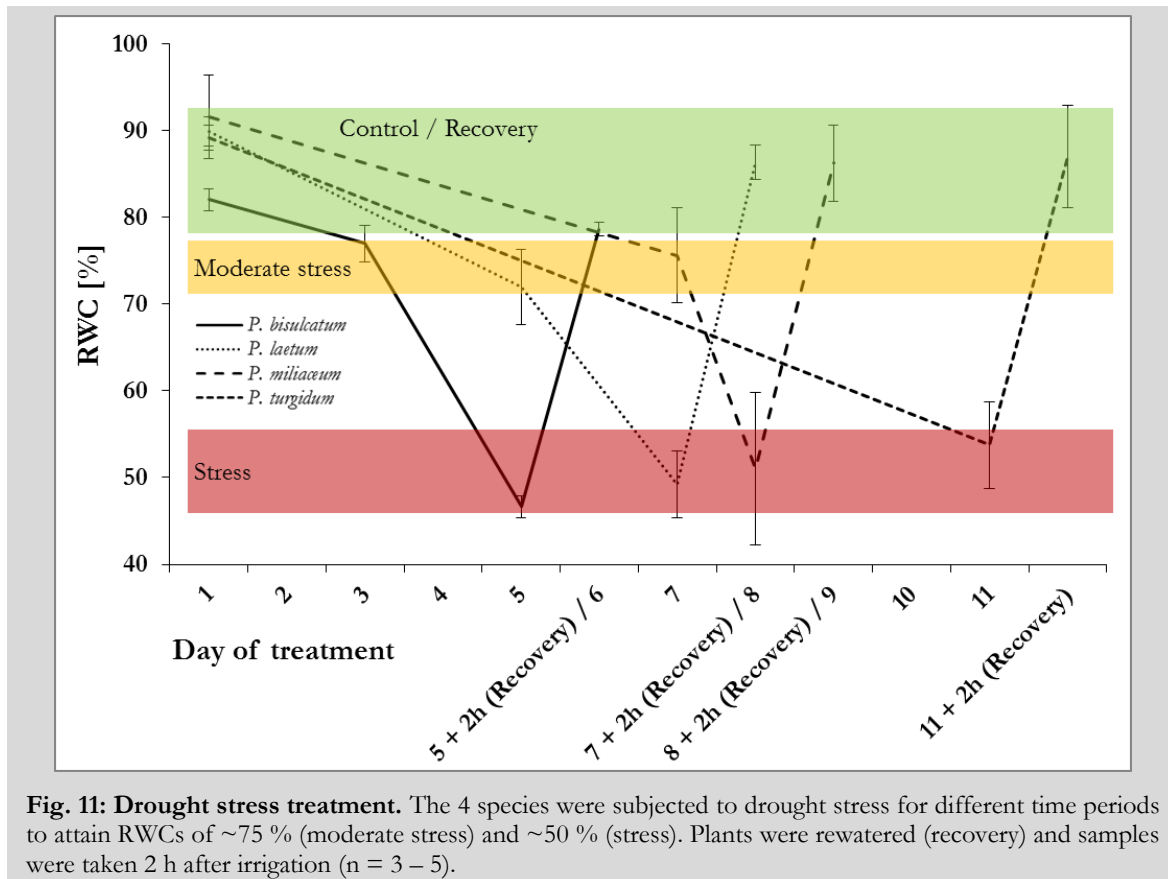


Fig. 11: Drought stress treatment. The 4 species were subjected to drought stress for different time periods to attain RWCs of ~75 % (moderate stress) and ~50 % (stress). Plants were rewatered (recovery) and samples were taken 2 h after irrigation (n = 3 – 5).

The relative leaf water content decreased from ~90 % on the control day to ~75 % at the “moderate stress” day. On the “stress” day, relative leaf water content had attained ~50 % ($p < 0.05$ for *P. turgidum* and $p < 0.001$ for all other samples control vs. stress, unpaired t-test, Table 9). Recovery samples showed RWC levels of ~85 % similar to the control conditions (Table 9, Fig. 11). It is clearly visible that *P. bisulcatum* was subjected to drought stress for the shortest time. Its RWC was 77 % at day 3 and 47 % at day 5 whereas *P. laetum* reached a RWC of 72 % at day 5 and 49 % at day 7 respectively. *P. miliaceum* showed a RWC of 76 % at day 7 and 51 % at day 8 and *P. turgidum* had to be subjected to drought stress for 11 days to reach a RWC of 54 % (no samples were collected for a RWC of ~75 %). The water status of the different samples collected was very similar on all sampling days resulting in a uniform population of samples, allowing the comparison of the different species to the given sampling points.

3.1.2 Gas exchange measurements

Gas exchange measurements were conducted to monitor the photosynthesis rate (P_N), stomatal conductance to water vapour (g_{H_2O}) and transpiration rate (T) in *P. bisulcatum*, *P. laetum* and *P. miliaceum* over the drought stress experiment time. Parameters were recorded at a light intensity of $2000 \mu\text{mol m}^{-2} \text{s}^{-1}$ and a CO_2 concentration of 400 ppm to ensure for light saturation and natural CO_2 concentration.

In all three analysed *Panicum* species there was a significant reduction of the net photosynthetic rate (P_N) in the course of drought stress application visible (Fig. 12 A-C). The reduction was strongest in *P. bisulcatum* during the early phase of water stress as well as during severe drought stress (Fig. 12 A). P_N was on average reduced by $16 \mu\text{mol m}^{-2} \text{s}^{-1}$ (71 %) and $23 \mu\text{mol m}^{-2} \text{s}^{-1}$ (101 %) respectively (due to negative values). Recovery values were reduced by $17 \mu\text{mol m}^{-2} \text{s}^{-1}$ (72 %). In *P. laetum* P_N was reduced by $11 \mu\text{mol m}^{-2} \text{s}^{-1}$ (37 %) during moderate stress, $28 \mu\text{mol m}^{-2} \text{s}^{-1}$ (91 %) during stress and $19 \mu\text{mol m}^{-2} \text{s}^{-1}$ (61 %) during recovery (Fig. 12 B) whereas in *P. miliaceum* the photosynthesis rate was reduced by $10 \mu\text{mol m}^{-2} \text{s}^{-1}$ (37 %), $21 \mu\text{mol m}^{-2} \text{s}^{-1}$ (77 %) and $13 \mu\text{mol m}^{-2} \text{s}^{-1}$ (46 %) respectively (Fig. 12 C).

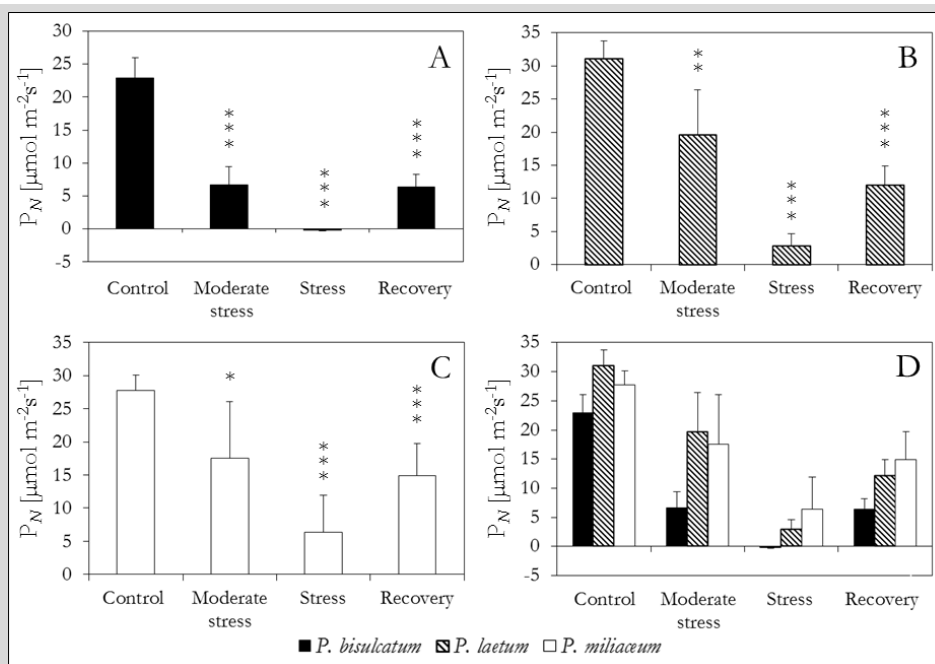


Fig. 12: Photosynthesis rate (P_N) recorded in three *Panicum* species under drought stress treatment. A) *P. bisulcatum*, B) *P. laetum*, C) *P. miliaceum*. Control (n = 6), moderate stress, stress and recovery (n = 3) with appending SD (black bars). * p < 0.05, ** p < 0.01, * p < 0.001 vs. control (unpaired t-test).**

When comparing the species with each other (Fig. 12 D) the C_3 species *P. bisulcatum* had a significantly ($p < 0.001$ for *P. laetum* vs. *P. bisulcatum* and $p < 0.05$ for *P. miliaceum* vs.

P. bisulcatum, unpaired t-test) lower photosynthesis rate at the control day than the C₄ species *P. laetum* and *P. miliaceum*. At the time of severest drought stress only photorespiration could be recorded for *P. bisulcatum* (negative photosynthesis rate), however it was still possible to measure (albeit small) positive photosynthesis rates for *P. laetum* and *P. miliaceum* (Fig. 12 A-D). During recovery P_N increased in all three species but values were still significantly higher in the C₄ species *P. laetum* and *P. miliaceum* than in the C₃ species *P. bisulcatum* ($p < 0.05$ for *P. laetum* and *P. miliaceum* vs. *P. bisulcatum*, unpaired t-test).

The stomatal conductance to water vapour (g_{H_2O}) is a parameter describing the rate of gas exchange through the stomata. In the course of drought stress, stomatal conductance significantly decreased in all three analysed *Panicum* species due to stomatal closure (Fig. 13 A-C). During moderate and severe stress g_{H_2O} was reduced by 165 mmol m⁻²s⁻¹ (78 %) and 197 mmol m⁻²s⁻¹ (93 %) respectively in *P. bisulcatum*, recovery values 2 h after irrigation were reduced by 160 mmol m⁻²s⁻¹ (75 %) (Fig. 13 A). In *Panicum laetum* g_{H_2O} was reduced by 81 mmol m⁻²s⁻¹ (51 %) during moderate stress and 139 mmol m⁻²s⁻¹ (88 %) during severe stress where recovery values were reduced by 95 mmol m⁻²s⁻¹ (59 %) (Fig. 13 B). The smallest reduction was recorded for *P. miliaceum* where g_{H_2O} was reduced by 92 mmol m⁻²s⁻¹ (50 %) during moderate stress, 138 mmol m⁻²s⁻¹ (75 %) in severe stress and 97 mmol m⁻²s⁻¹ (53 %) 2 h after irrigation (Fig. 13 C).

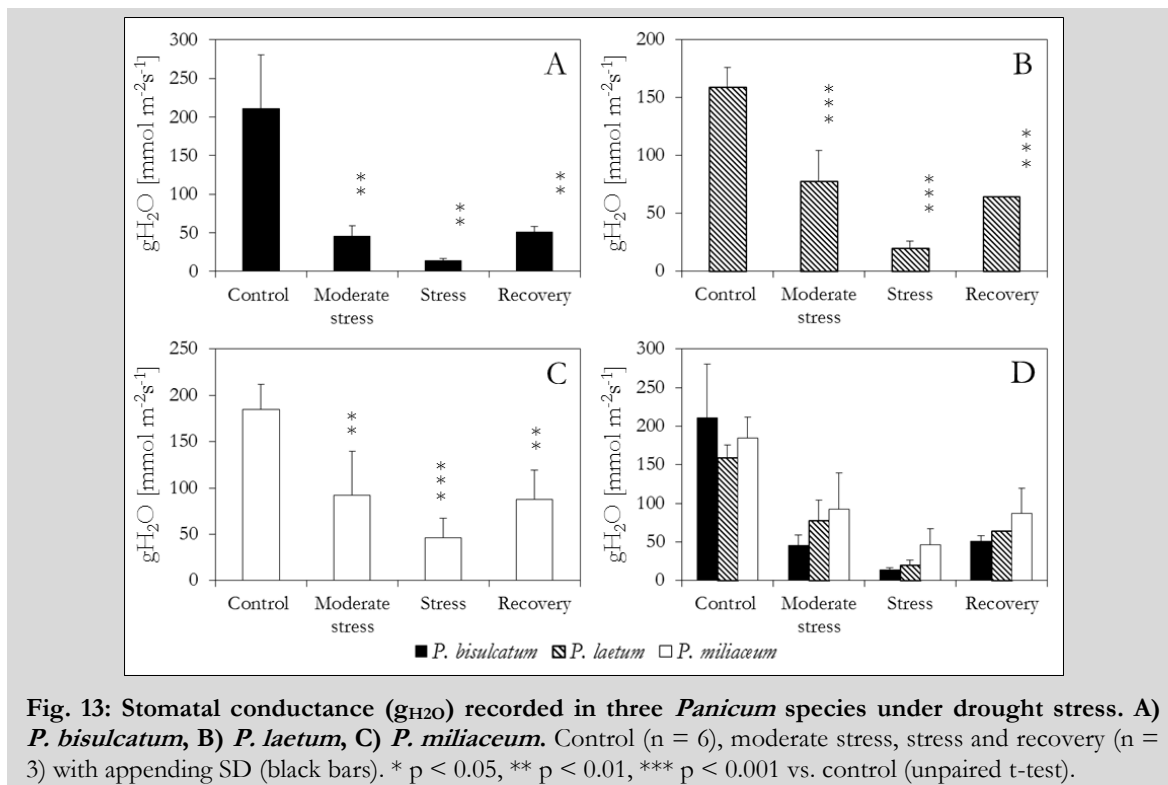


Fig. 13: Stomatal conductance (g_{H_2O}) recorded in three *Panicum* species under drought stress. **A)** *P. bisulcatum*, **B)** *P. laetum*, **C)** *P. miliaceum*. Control ($n = 6$), moderate stress, stress and recovery ($n = 3$) with appending SD (black bars). * $p < 0.05$, ** $p < 0.01$, *** $p < 0.001$ vs. control (unpaired t-test).

When comparing the species with each other (Fig. 13 D) there cannot be found any significant differences during all phases of drought stress and recovery. Even though *P. bisulcatum* showed the highest values for g_{H_2O} during control conditions (compared to *P. laetum* and *P. miliaceum*) and the smallest values during drought stress, changes in stomatal conductance did not significantly differ between the species.

Reactions analysing the transpiration rate (T) approximated g_{H_2O} measurements as these were conducted under equal conditions (data not shown).

3.1.3 Leaf water use efficiency

The water use efficiency (WUE) describes the proportion of fixed carbon dioxide to transpired water through the stomata and was calculated as P_N/T . In Table 10 the mean values calculated for each species at the different levels of drought stress are given with their appending standard deviation (SD). Under moderate stress conditions (RWC ~75 %) WUE was only significantly higher in *P. miliaceum* (Control vs. moderate stress, $p < 0.05$, unpaired t-test) but increases (not significant) in mean WUE values could also be recorded for *P. bisulcatum* and *P. laetum*. Under severe stress conditions (RWC ~50 %) a significant decrease in WUE could only be recorded for *P. bisulcatum* (control vs. stress, $p < 0.001$, unpaired t-test) where negative values were calculated due to negative P_N (Fig. 12 A). For *P. laetum* and *P. miliaceum* slight (not significant) reductions of the mean WUE values could be recorded. Recovery and control values were similar for all species (Table 10).

Table 10: Water use efficiency (WUE) [$\mu\text{mol CO}_2 / \text{mmol H}_2\text{O}$] of analysed *Panicum* species under different water regimes. Control (n = 6), moderate stress, severe stress and recovery (n = 3). Significant intraspecific differences were only apparent in *P. bisulcatum* control vs. stress (** $p < 0.001$) and *P. miliaceum* control vs. moderate stress (* $p < 0.05$), unpaired t-test.

	Control	Moderate stress	Severe stress	Recovery
<i>P. bisulcatum</i>	8.3 \pm 0.6	9.3 \pm 1.4	-0.7 \pm 0.5 ***	7.3 \pm 0.7
<i>P. laetum</i>	13.9 \pm 0.7	16.2 \pm 1.3	9.8 \pm 3.6	13.2 \pm 0.9
<i>P. miliaceum</i>	12.0 \pm 0.9	15.2 \pm 0.9 *	9.5 \pm 5.7	12.9 \pm 0.2

When comparing the C_4 species' WUE with each other no significant differences between the values of the NAD-ME species *P. laetum* and *P. miliaceum* could be found at any time of the drought stress treatment.

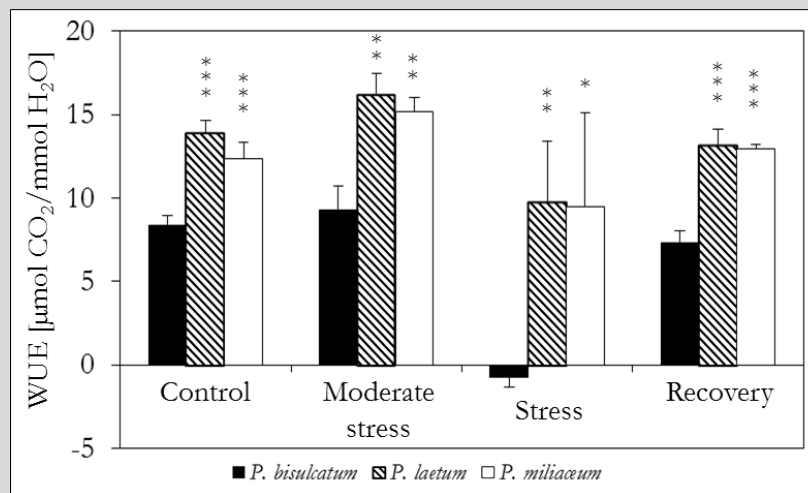


Fig. 14: Water use efficiency (WUE) of *Panicum* species under different water regimes. Control (n = 6), Moderate stress, Stress and Recovery (n = 3). Significant interspecific differences were found at all measuring time points (*P. bisulcatum* vs. *P. laetum*, *P. bisulcatum* vs. *P. miliaceum*). * p < 0.05, ** p < 0.01, *** p < 0.001, unpaired t-test). Statistical results for *P. laetum* vs. *P. miliaceum* (unpaired t-test) were ns at all times.

On the contrary significantly higher WUE values between the C₃ species *P. bisulcatum* and the C₄ species *P. laetum* and *P. miliaceum* (Fig. 14) could be detected during all measuring points of the drought stress experiment.

3.1.4 Chlorophyll a fluorescence analyses

Sunlight is used by plants to convert light energy into chemical components during photosynthesis. Excess light energy is thereby either dissipated as heat or – to a much lesser extend – as fluorescence. This chlorophyll a (Chl a) fluorescence quickly rises to a maximum which was recorded by the Plant Efficiency Analyser (PEA, 2.2.4). The Chl a fluorescence transients recorded during control, severe drought stress and recovery can be analysed and their “interpretation can provide information about the photosynthetic capacity and the vitality of the plant material” (STRASSER et al. 2010). The analyses give detailed information about the photosystems efficiency and performance under optimal and non-optimal conditions and were used as a non-invasive screening of the photosynthetic apparatus of the grasses investigated in this dissertation.

The fast polyphasic Chl a fluorescence rise starts at the fluorescence (F) intensity $F_0 = 50\mu\text{s}$ ($F_{50\mu\text{s}}$) and reaches a maximal value under saturating light conditions (F_M) at around 500ms. All parameters shown in this dissertation were calculated from these values and the fluorescence values at a given time F_t .

Chl a transients were first normalized to $F_{50\mu\text{s}} = 1$ for better comparison (Fig. 15) of the polyphasic rise of the transients recorded under different water regimes (F_t/F_0). The

different “steps” described in 2.2.4 ($O = F_0 = F_{50\mu s}$, $J = F_{2ms}$, $I = F_{30ms}$ and $P = F_{300ms}$) were clearly visible in the control transients (open triangles) of all four species investigated in this dissertation (shown in Fig. 15 A by vertical grey lines). During severe stress (filled circle) Chl a fluorescence transients altered their appearance and the fluorescence intensity dropped, particularly visible in the lower maximal fluorescence F_M emitted around 500 ms (Fig. 15) in all four grasses investigated in this dissertation. When looking at the Chl a fluorescence transients recorded during recovery (open square), *P. bisulcatum* and *P. laetum* did not show great changes compared to the “stress transients” (Fig. 15 A, B) whereas *P. miliaceum* exhibited a transient with even lower Chl a fluorescence at F_M under recovery conditions (Fig. 15 C) compared to control and stress measurements. Only the Chl a fluorescence transient of *P. turgidum* (Fig. 15 D) approximated to the transient measured under control conditions. The illustration of the transients normalized to $F_{50\mu s}$ gives information about the efficiency of the samples primary photochemistry under control, drought stress and recovery conditions.

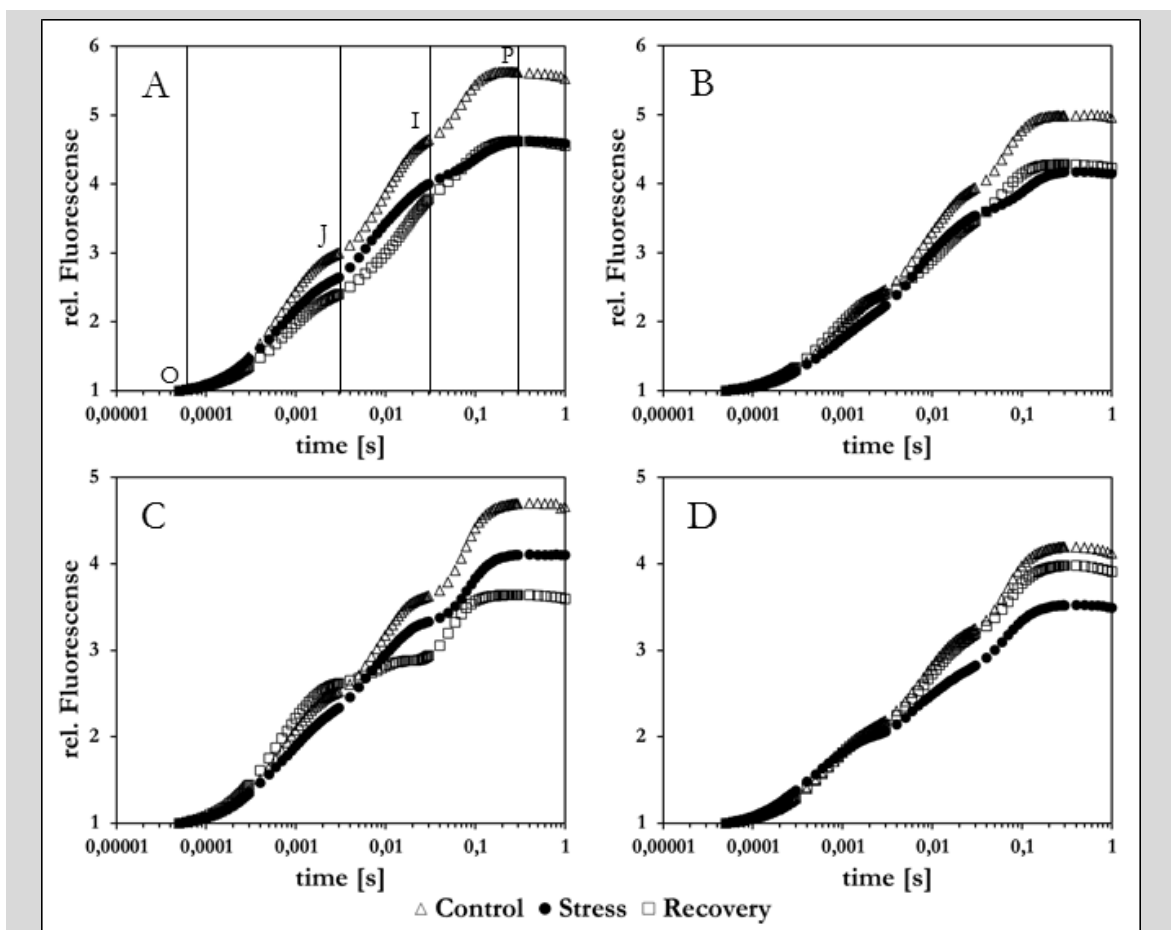


Fig. 15: Averaged polyphasic chlorophyll a fluorescence transients normalized to $F_0 = 50\mu s$ applied on a logarithmic time scale. A) *P. bisulcatum* (n = 18), B) *P. laetum* (n = 18), C) *P. miliaceum* (n = 9), D) *P. turgidum* (n = 4-6). Vertical lines in (A) mark the different steps (O, J, I and P) which occur during the polyphasic fluorescence rise at 50 μs , 2 ms, 30 ms and 300 ms.

To compare changes in the fluorescence transients independent from minimal and maximal fluorescence, transients were double normalized to $F_{50\mu s} = 0$ and $F_M = 1$ (Fig. 16 A-D) by calculating $F_V(t) = (F_t - F_0) / (F_M - F_0)$. In comparison to the transients only normalized to $F_{50\mu s}$ (Fig. 15) an F_V value of a record measured at a specific time can then be compared between control, stress and recovery samples independent from the transient's maximal and minimal fluorescence intensities F_M and $F_{50\mu s}$. The double normalized Chl a fluorescence transients give a graphical overview of their shape under the different applied water regimes in regard to $F_{50\mu s}$ and F_M . While in *P. bisulcatum*, *P. laetum* and *P. turgidum* only small changes in the fluorescence transients during drought stress and recovery could be observed (Fig. 16 A, B, D) a faster initial fluorescence rise during recovery could be shown for *P. miliaceum* (Fig. 16 C). In all species analysed in the time course of this dissertation, Chl a fluorescence rises faster under drought conditions (Fig. 16 A-D) and only in the C_3 species *P. bisulcatum* the fluorescence intensity rises slower under recovery conditions (Fig. 16 A).

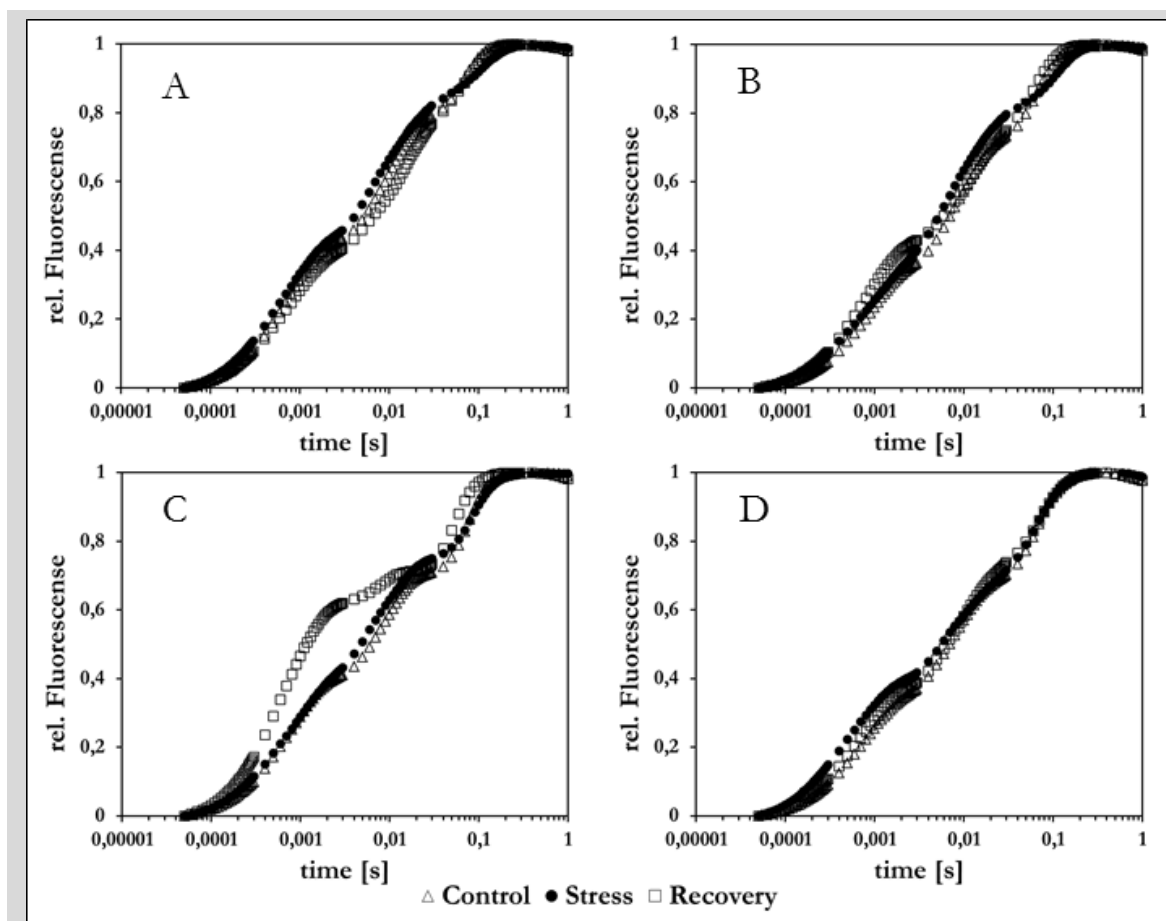


Fig. 16: Averaged chlorophyll a transients double normalized to $F_{50\mu s} = 0$ and $F_M = 1$ applied on a logarithmic time scale. A) *P. bisulcatum* (n = 18), B) *P. laetum* (n = 18), C) *P. miliaceum* (n = 9), D) *P. turgidum* (n = 4-6).

To compare control and stress and control and recovery transients with each other, ΔV curves were calculated according to the formula by YORDANOV et al. (2008, 2.2.4). Special emphasis was put on the ΔV_{OJ} curves where transients were normalized to $F_{50\mu s} = 0$ and $F_{2ms} = 1$ possibly exhibiting a K peak at ca. 150-300 μs (Fig. 17). K peaks occur, when the acceptor / donor side of PS II is inhibited, e.g. by changes to the efficiency of electron transport from the oxygen-evolving complex (OEC, STRASSER 1997). In all species the K peak was stronger expressed in drought stressed than in recovery samples. In *P. bisulcatum*, *P. laetum* and *P. miliaceum* (Fig. 17 A-C) K peaks had a relative fluorescence intensity of ca. 0.04 – 0.06, and only in *P. turgidum* relative fluorescence intensity was above 0.1 (Fig. 17 D). The OJIP transients recorded during recovery showed lower fluorescence values compared to stress values at ca. 150-300 μs where the K peak is found.

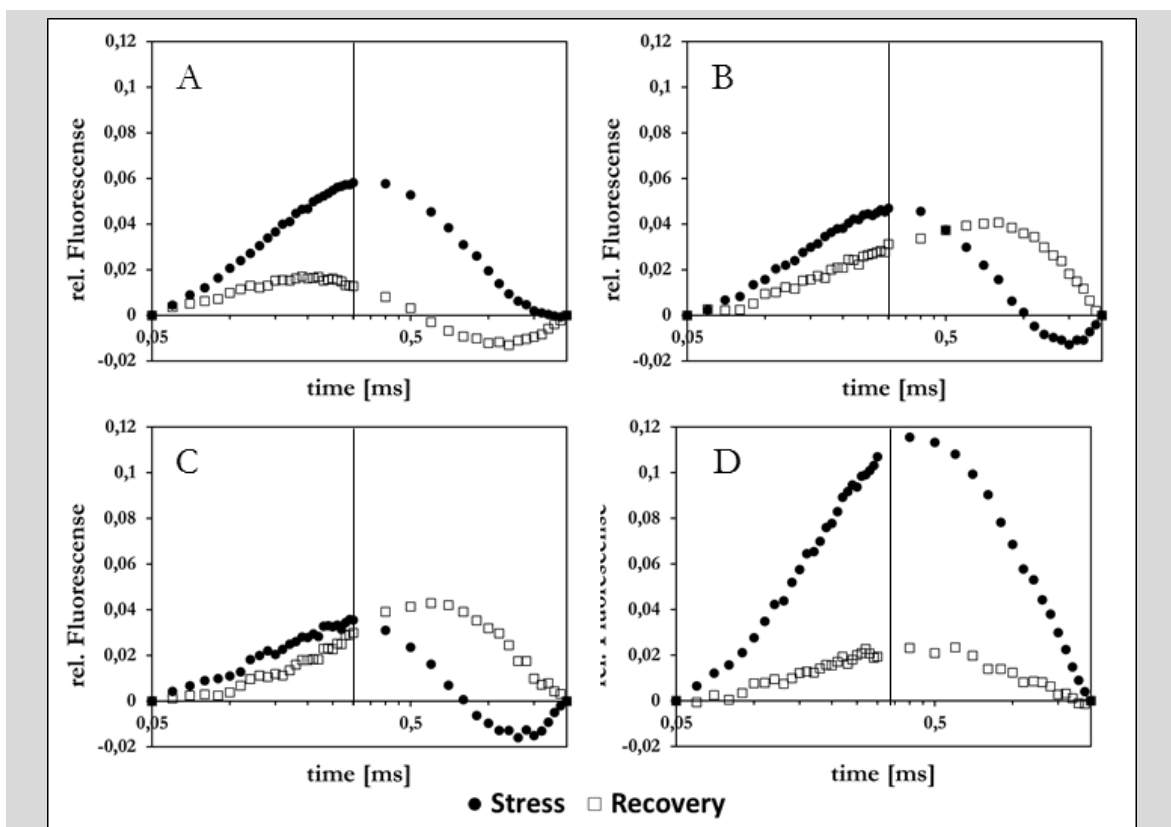


Fig. 17: ΔV_{OJ} curves applied on a logarithmic time scale. ΔV_{OJ} curves were calculated by subtraction of the normalized ($F_{50\mu s}$ and F_{2ms}) F_t values (treated measurements) from control measurements. $\Delta V_{OP} = [(F_t - F_0)_{treatment} / (F_{2ms} - F_0)_{treatment}] - [(F_t - F_0)_{control} / (F_{2ms} - F_0)_{control}]$. A) *P. bisulcatum* (n = 18), B) *P. laetum* (n = 18), C) *P. miliaceum* (n = 9), D) *P. turgidum* (n = 4-6). Vertical lines show the K peak at $\sim 300 \mu s$.

Several OJIP parameters can be calculated from single F_t - and the minimal and the maximal Chl a fluorescence values recorded. In this dissertation, only the parameters showing strong differences during drought stress and / or recovery are shown and

discussed. Table 11 outlines all calculated parameters with their appending SD and the spider plots graphically depict the parameters (Fig. 18) for each individual species (for explanation of the OJIP parameters see Table 4).

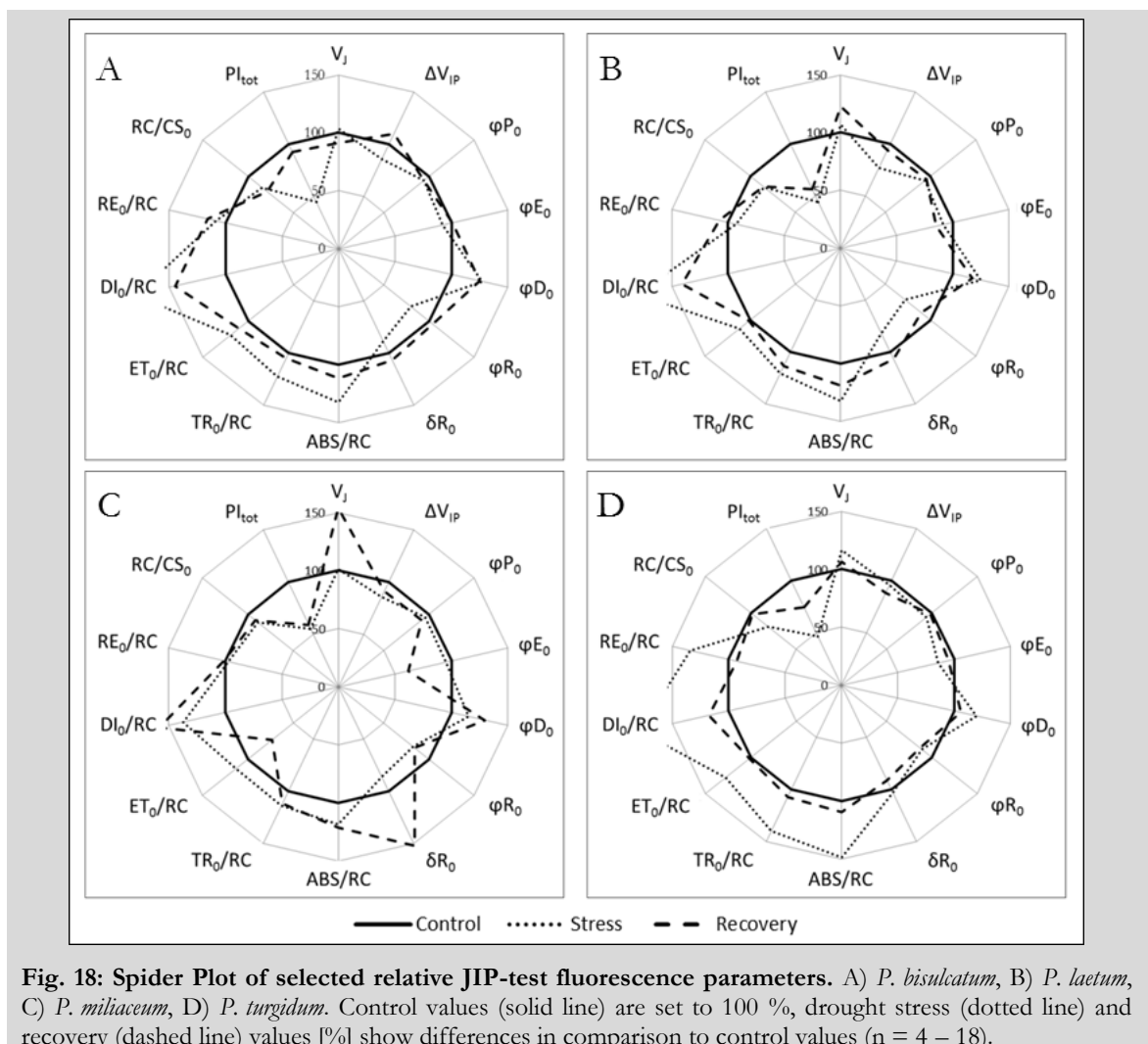
The fluorescence parameter V_J was only significantly increased in the C_4 species *P. laetum* and *P. miliaceum* under recovery conditions, φP_0 (F_V/F_M) was significantly reduced during drought stress and recovery in the species *P. bisulcatum*, *P. laetum* and *P. miliaceum*, but only during drought stress in the species *P. turgidum*. φE_0 was significantly reduced in the C_4 species *P. laetum* and *P. miliaceum* during recovery and in *P. turgidum* during drought stress. The parameter φD_0 was significantly increased in all four analysed species under drought stress and recovery conditions, except for *P. turgidum*, where a significant increase could only be shown under drought stress. φR_0 showed significant differences in the C_3 species *P. bisulcatum* where a reduction could be shown during stress, as well as in the C_4 species *P. laetum* and *P. miliaceum* where a significant reduction of the parameter was also visible during recovery.

Table 11: Relative OJIP parameters measured during control (C), stress (S) and recovery (R) in the species *P. bisulcatum*, *P. laetum*, *P. miliaceum* and *P. turgidum*. Control values were set to 100 %, OJIP parameter values of measurements taken under drought stress and recovery conditions [%] show differences in regard to relative control values. * $p < 0.05$, ** $p < 0.01$, *** $p < 0.001$ ($n = 4-18$) control vs. stress and control vs. recovery.

	V_J	ΔV_{IP}	φP_0	φE_0	φD_0	φR_0	δR_0	RC/ CS ₀	ABS /RC	TR ₀ /RC	ET ₀ /RC	DI ₀ / RC	Pi _{tot}	
<i>P. bisulcatum</i>	C	100	100	100	100	100	100	100	100	100	100	100	100	
	S	104	86*	94**	92	127**	80**	89*	84***	133**	122**	119**	180**	45***
	R	91	110	95***	101	125***	104	107	79***	112	105	110*	145**	92
<i>P. laetum</i>	C	100	100	100	100	100	100	100	100	100	100	100	100	
	S	107	77***	94**	92	125**	72***	82**	85***	132*	120*	112**	180*	44***
	R	122***	94	96***	85***	118***	90***	107	86***	119***	114***	102	141***	56***
<i>P. miliaceum</i>	C	100	100	100	100	100	100	100	100	100	100	100	100	
	S	101	86***	96**	95	115**	82***	86***	89**	119***	114***	113***	137***	55***
	R	154***	92*	92***	62***	130***	84***	152*	92	122**	111	73**	159***	59*
<i>P. turgidum</i>	C	100	100	100	100	100	100	100	100	100	100	100	100	
	S	116	96	94**	86**	120**	89	103	81***	149***	140***	128**	179***	47*
	R	107	89	98	95	106	87	91	98	110	107	102	117	75

δR_0 was only significantly decreased during stress in *P. bisulcatum*, *P. laetum* and *P. miliaceum* where it was also significantly increased under recovery conditions. The relative number of active PS II reaction centres per excited cross section (RC/CS₀) was significantly reduced in

P. bisulcatum and *P. laetum* under drought stress and recovery conditions and only during stress in *P. miliaceum* and *P. turgidum*. The absorption per reaction centre (ABS/RC) was significantly increased in all four species under drought stress conditions but was increased during recovery only in *P. laetum* and *P. miliaceum*. The values of TR₀/RC were also significantly higher in all four species under stress but were increased only in *P. laetum* under recovery conditions. The electron transport per reaction centre (ET₀/RC) was significantly increased in all four species under stress conditions and only during recovery it was significantly decreased in *P. miliaceum*. DI₀/RC was increased during drought stress and recovery treatment in all four species analysed except for *P. turgidum*, where recovery values did not significantly differ to control values. The total performance index (PI_{tot}) was significantly reduced in all four species under drought stress and stayed low under recovery conditions in the C₄ species *P. laetum* and *P. miliaceum* (see Table 11 and Fig. 18 A-D). The spider plot (Fig. 18) graphically depicts the values shown in Table 11 for better visualisation.



To also picture minor differences axes were set to a maximum of 150 % resulting in a hidden peak for the JIP-test value DI_0/RC . Parameters were arranged according to fluorescence parameters ($V_j, \Delta V_{ip}$), quantum efficiency / flux ratios ($\varphi P_0, \varphi E_0, \varphi D_0, \varphi R_0$ and δR_0), specific fluxes per active PS II reaction centre (ABS/RC, TR₀/RC, ET₀/RC and DI_0/RC), density of reaction centres (RC/CS₀) and performance index (PI_{tot}).

Furthermore a correlation between the relative values of net photosynthesis rate (P_N) and PI_{tot} values was performed to check for a correlation of those parameters (Fig. 19).

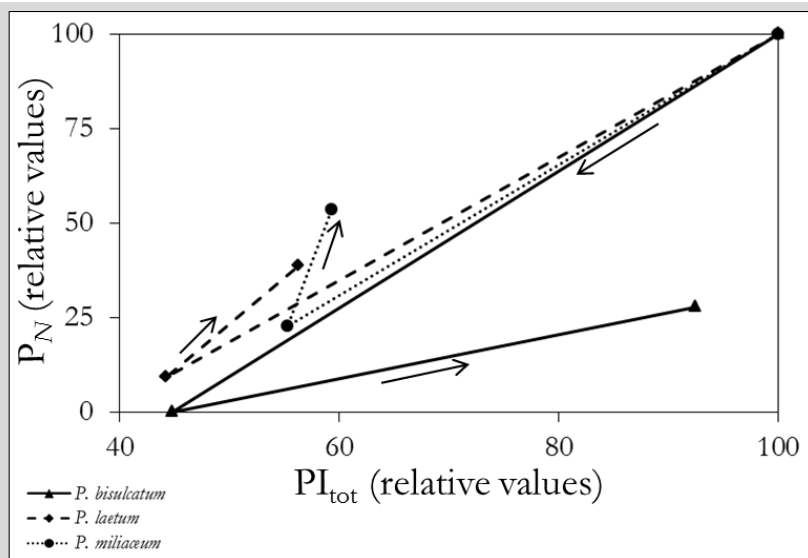


Fig. 19: Correlation of P_N and PI_{tot} (relative values as compared to control (100/100)) of *P. bisulcatum*, *P. laetum* and *P. miliaceum*. The arrow pointing to the left indicates the reduction of P_N and PI_{tot} from control to the stress condition, the arrows pointing to the right show the subsequent increases of the values from stress to recovery conditions.

3.2 Molecular analyses

Molecular analyses were conducted to obtain a picture of the molecular changes during drought stress and recovery within the different *Panicum* species and in comparison to each other. All analyses were carried out in the species *P. bisulcatum*, *P. laetum*, *P. miliaceum* and *P. turgidum*. Whole transcriptome analyses by HT-SuperSAGE (2.3.2.6) were conducted to monitor the gene expression changes under drought stress and recovery, followed by diverse molecular methods to confirm the generated results (2.3.2.7 - 2.3.2.9)

3.2.1 Protein analyses

Analyses were carried out on selected proteins playing important roles in photosynthesis. The protein content of the major CO₂ fixing enzymes RubisCO and PEPC were

investigated to check for differences in control, drought stress and recovery samples. As fluorescence measurements revealed a K peak putatively reflecting the diminished efficiency of the oxygen-evolving complex under drought stress, its content was also analysed. Finally, Dehydrin 1, a protein only expressed under drought stress (and recovery) conditions, was screened to demonstrate the severity of applied stress. Total soluble proteins were isolated according to 2.3.1.1 and run on a SDS-PAGE (2.3.1.3) to check for protein quality (Fig. 20).

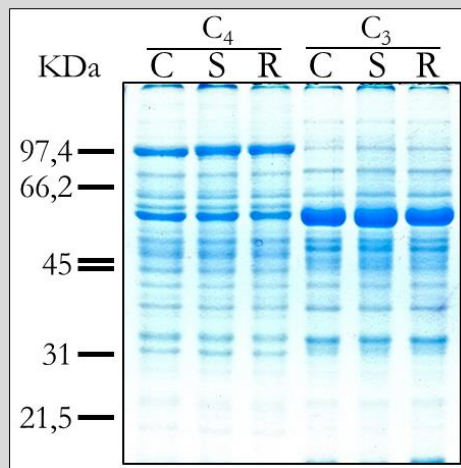


Fig. 20: SDS-PAGE with C₃ (*P. bisulcatum*) and C₄ (*P. laetum*) samples. Protein bands are clearly separated. PEPC (~100 KDa, only C₄) and RubisCO large subunit protein bands (~55 KDa, both species) are clearly visible. Control (C), stress (S), recovery (R).

The ensuing Western Blot and Immunodetection (2.3.1.4, 2.3.1.5) analyses generated the pictures depicted in Fig. 21.

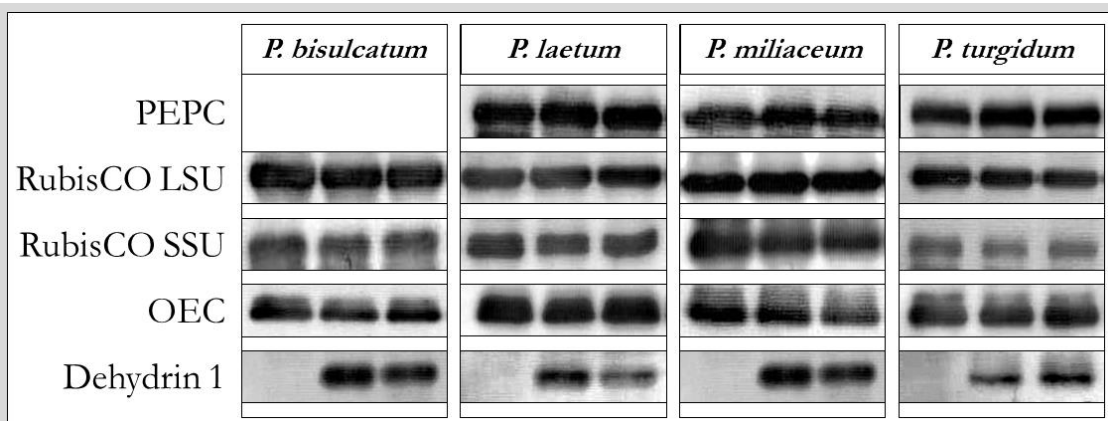


Fig. 21: Immunodetection of PEPC (100 KDa), RubisCO LSU (55 KDa) and SSU (15 KDa), OEC (33 KDa) and Dehydrin 1 (17 KDa) in the species *P. bisulcatum*, *P. laetum*, *P. miliaceum* and *P. turgidum*. Control, severe drought stress and recovery samples were analysed (from left to right per species) with polyclonal antibodies (1:5000). Only Dehydrin 1 was differentially expressed under stress and recovery conditions.

To not only visually interpret the results, blots were scanned and the single bands were analysed by ImageJ (2.3.1.6) by counting pixels. These results were used for statistical analyses, see Table 12.

Table 12: Number of counted pixels for protein bands detected by Immunodetection for each *Panicum* species. * $p < 0.05$, ** $p < 0.01$, *** $p < 0.001$ ($n = 2-3$) control vs. stress and control vs. recovery (unpaired t-test). LSU = large subunit, SSU = small subunit.

		RubisCO LSU	RubisCO SSU	PEPC	OEC	Dehydrin 1
<i>P. bisulcatum</i>	C	121.933	158.754	-	95.188	0
	S	135.558	173.368	-	89.561	119.076***
	R	119.122	163.041	-	98.617	119.484***
<i>P. laetum</i>	C	123.165	171.080	87.568	142.887	0
	S	124.312	164.377	75.212	127.534	71.962*
	R	102.201	165.733	84.364	148.351	40.932**
<i>P. miliaceum</i>	C	126.011	178.280	163.255	132.706	0
	S	127.655	170.874	185.154	142.634	167.404***
	R	115.684	152.566	166.638	143.497	127.336**
<i>P. turgidum</i>	C	119.044	164.826	135.288	116.852	0
	S	102.783	142.137	137.843	114.703	110.461*
	R	99.245	150.881	121.261	115.357	149.947*

The protein content of PEPC (100 KDa), only analysed in C_4 species, was not significantly changed under severe drought stress or recovery conditions ($n = 3$). The protein contents of RubisCO large subunit (LSU, 55 KDa) and small subunit (SSU, 15 kDa) as well as of the oxygen-evolving complex (33 KDa) neither were changed significantly under severe drought stress nor recovery conditions ($n = 3$). Only the protein content of Dehydrin 1 (17 KDa) was significantly changed under severe drought stress as well as recovery conditions ($p < 0.001$, $n = 3$), see Table 12 and Fig. 21.

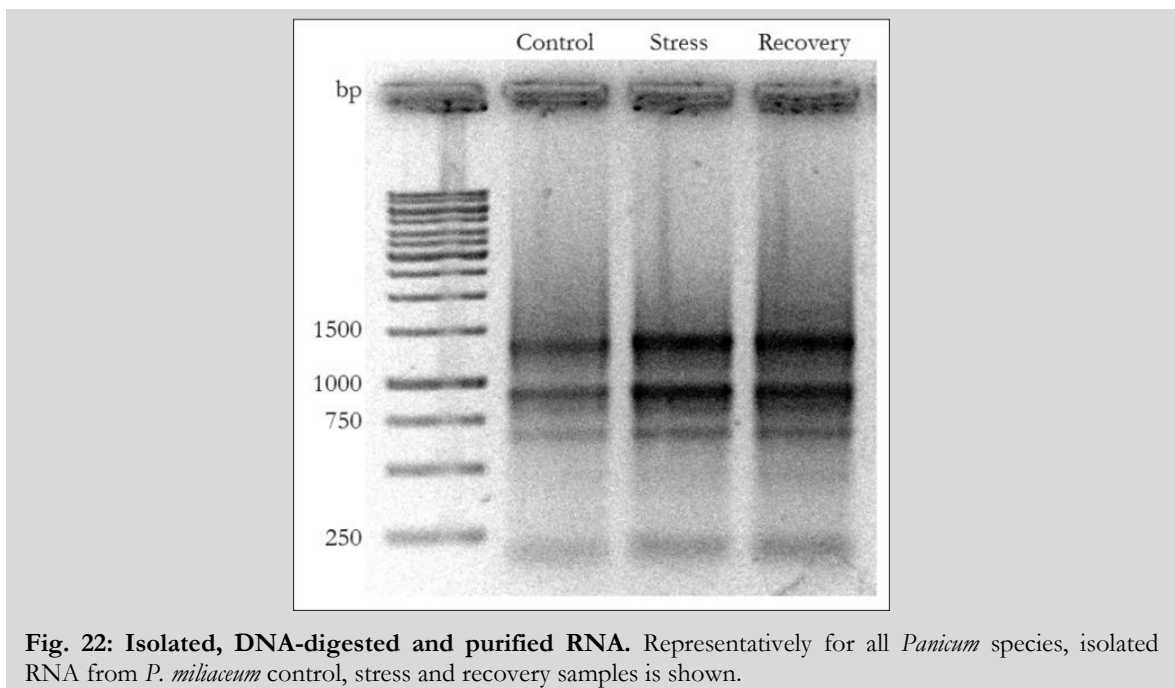
Whole proteome analyses (2D-Gels and subsequent DIGE analyses) under control, severe drought stress and recovery conditions (soluble proteins) of all four *Panicum* species investigated in this dissertation were carried out in the course of a separate Bachelor thesis (Hanna Müller, 2013).

3.2.2 Transcriptomics

In the following chapter the methods used for transcriptomic analyses are described starting from RNA isolation to validation of the HT-SuperSAGE results by qPCR.

3.2.2.1. Isolation of RNA

Total RNA from control, stress and recovery samples of *P. bisulcatum*, *P. laetum*, *P. miliaceum* and *P. turgidum* was isolated, DNA-digested and purified according to 2.3.2.1 - 2.3.2.4. 1 μ l of isolated RNA was loaded onto an agarose gel (2.3.2.5) to check for RNA quality and integrity.



There are two strong bands visible, the upper one is the 25S rRNA (between the DNA size marker bands of 1500 bp and 1000 bp), the lower one is the 18S rRNA (just below the DNA size marker band of 1000 bp) of the 80S cytosolic ribosomes. Another visible band is the 16S rRNA of the 70S plastidial ribosomes which migrates just below the 18S rRNA. The 23S rRNA (also component of the 70S ribosomes) is naturally cleaved into distinctive fragments which co-migrate with the 18S rRNAs and form another band below the 750 bp marker band in gel electrophoresis (MACHE et al. 1978). No degradation of the RNA could visually be detected nor a contamination with DNA. All RNA samples were used to conduct HT-SuperSAGE (2.3.2.6) as well as successive molecular analyses (2.3.2.7, 2.3.2.9).

3.2.2.2. HT-SuperSAGE

High throughput serial analyses of gene expression (HT-SuperSAGE) was conducted to depict the gene expression profile of the four *Panicum* species under control, severe drought stress and recovery conditions according to 2.3.2.6. Intermediary results are available only in digital files due to extensive material.

To get a first impression of the number of HT-SuperSAGE tags sequenced, a table was created listing the index sequence of the different *Panicum* samples, the number of total tags, unique tags and non-singleton tags sequenced (Table 13).

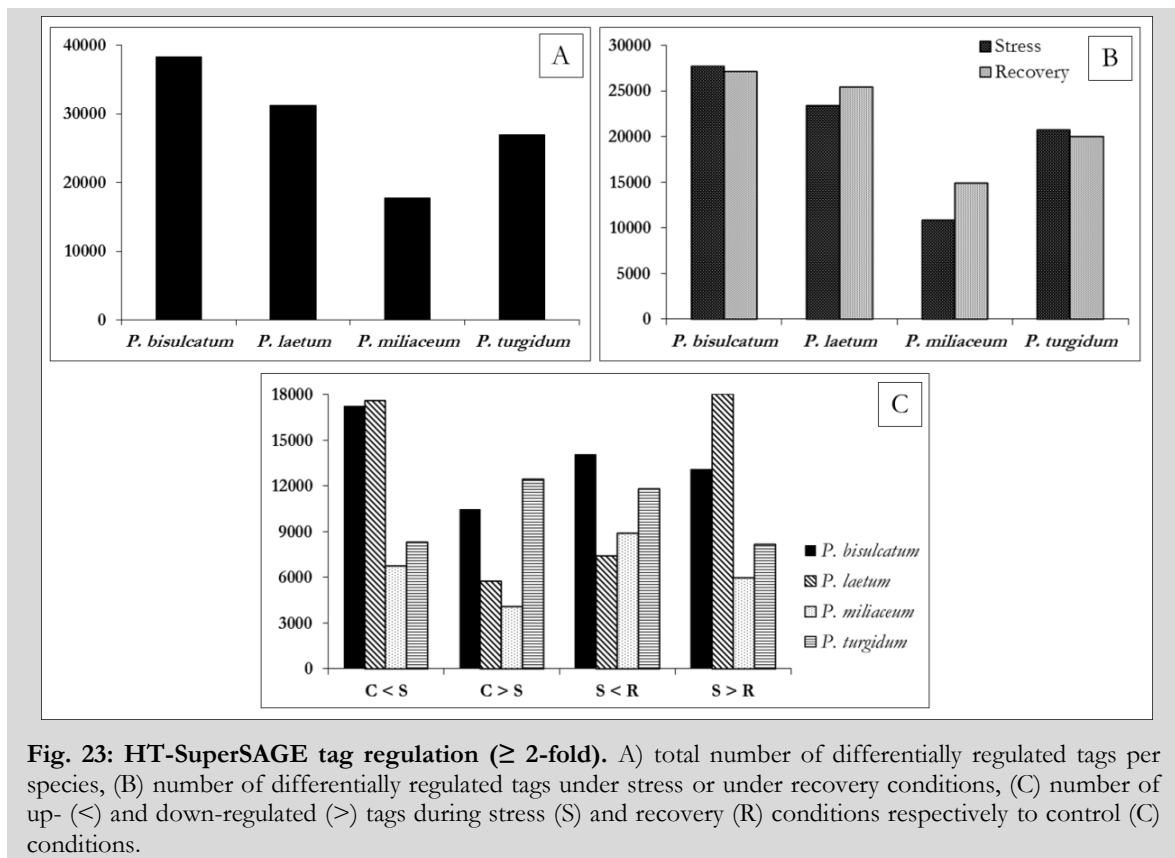
Table 13: HT-SuperSAGE results. Listed are the number of total tags (the cDNA libraries), the number of unique tags (tags showing the CATG *Nla*III RE digestion site and the index sequence) and the number of non-singleton tags (tags having an abundance of ≥ 2). Control (C), stress (S), recovery (R).

		Index sequence	N ^o of total tags	N ^o of unique tags	N ^o of non-singleton tags
<i>P. bisulcatum</i>	C	CGCATC	297677	46309	18760
	S	GACC	552131	95975	30188
	R	GACA	419728	68130	27350
<i>P. laetum</i>	C	GCGT	249293	33271	11461
	S	GCGG	396496	64274	25172
	R	GCGA	125691	22922	8159
<i>P. miliaceum</i>	C	CCAAAA	59206	13770	4083
	S	CCTAAT	97325	21416	6415
	R	GCGC	209012	41988	12871
<i>P. turgidum</i>	C	CCGAAG	238456	39985	15350
	S	CGAATA	238490	36599	13602
	R	CGTATT	212744	39643	14817

In total just over 3 million tags were sequenced, 1.2 million for *P. bisulcatum*, 770,000 for *P. laetum*, 370,000 for *P. miliaceum* and 690,000 for *P. turgidum*. Out of these only those tags were chosen for further analyses inheriting the CATG *Nla*III restriction enzyme site and the index sequence. A total number of 524,282 tags implementing these requirements were extracted, 210,000 for *P. bisulcatum*, 120,000 for *P. laetum*, 77,000 for *P. miliaceum* and 116,000 for *P. turgidum*. To exclude sequencing errors, the number of non-singleton tags, tags existing more than once, was also counted resulting in a total number of 188,228 tags, 77,000 for *P. bisulcatum*, 45,000 for *P. laetum*, 23,000 for *P. miliaceum* and 44,000 for *P. turgidum*. For each species tags were normalized to the condition exhibiting the highest

number of tags (e.g. for *P. bisulcatum*, tags expressed under control and recovery conditions were normalized to the number of tags sequenced for the stress sample).

Tags were then grouped into one data file/species to compare the differential regulation under control, drought stress and recovery conditions. To get a first impression of the number of differentially regulated tags/species, their total number was graphically displayed (Fig. 23 A) as well as the number of differentially regulated tags under drought stress as well as recovery conditions (Fig. 23 B) and the number of up- and down-regulated tags under stress and recovery respectively (Fig. 23 C).



The results showed the highest number of differentially regulated tags for the C₃ species *P. bisulcatum* (38,241 tags) followed by *P. laetum* (31,238 tags), *P. turgidum* (26,906 tags) and *P. miliaceum* (17,744 tags, see Fig. 23 A). To see if great differences between the differential regulation of HT-SuperSAGE tags expressed under stress or recovery conditions existed, their numbers were also graphically displayed (Fig. 23 B). No great differences within the same species could be uncovered with the number of differentially regulated tags fluctuating between ± 281 tags difference (*P. bisulcatum*) and ± 2022 tags difference (*P. miliaceum*). To further unravel the tag regulation, tags were separated according to their up- and down-regulation under stress and recovery conditions respectively (Fig. 23 C). In

P. bisulcatum, the highest number of tags was found being up-regulated under stress ($C < S$, 17,237 tags). In *P. laetum* most tags were down-regulated under recovery conditions ($S > R$, 18,043 tags), directly followed by the number of tags being up-regulated under stress conditions ($C < S$, 17,625 tags). In *P. miliaceum* no great differences could be detected, the highest number of tags was found being up-regulated under recovery conditions ($S < R$, 8,904 tags). *P. turgidum* exhibited the highest number of tags down-regulated under stress conditions ($C > S$, 12,432 tags) directly followed by the number of up-regulated tags under recovery conditions ($S < R$, 11,805 tags, see Fig. 23 C).

As tags were investigated under control, drought stress and recovery conditions for each species, a detailed analyses of tag expression including all treatments was conducted. Therefore 8 groups were created:

- | | | |
|----------------|----------------|----------------|
| 1. $C < S > R$ | 4. $C = S < R$ | 7. $C > S > R$ |
| 2. $C < S = R$ | 5. $C > S < R$ | 8. $C = S > R$ |
| 3. $C < S < R$ | 6. $C > S = R$ | |

The first four groups inherited all those tags up-regulated under stress and / or recovery conditions, the latter four groups inherited those tags down-regulated during stress and / or recovery. All remaining tags were not differentially regulated, neither under drought nor under recovery conditions and were not incorporated in the *in silico* analyses.

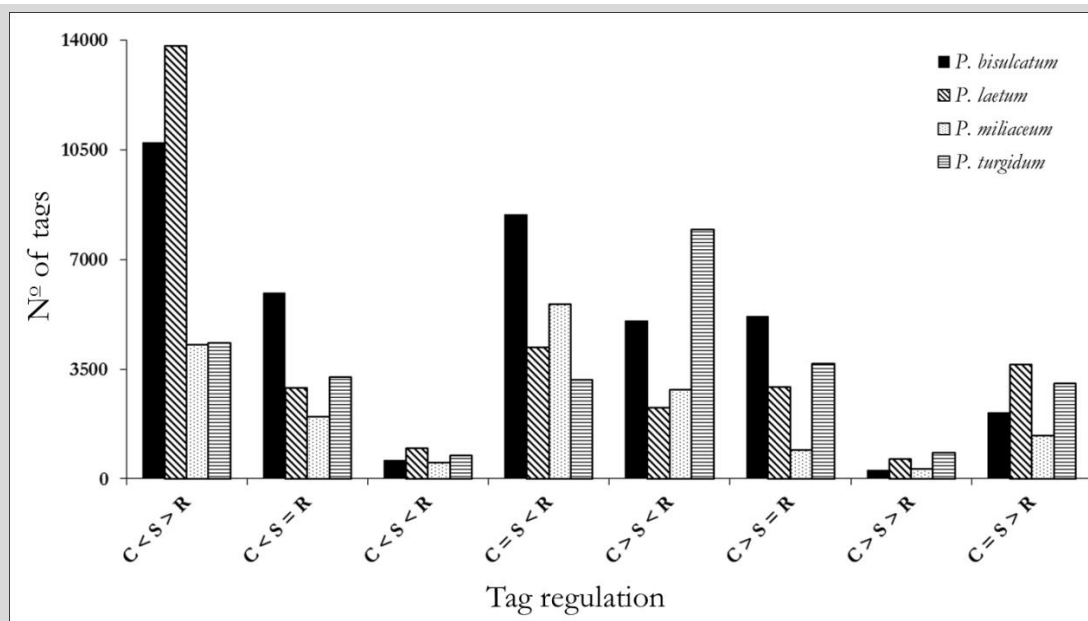


Fig. 24: Differential regulation of HT-SuperSAGE tags. Tags were grouped according to their differential regulation (≥ 2 -fold). Control (C), stress (S), recovery (R), up-regulated ($<$), down-regulated ($>$), not differentially regulated ($=$).

The species *P. bisulcatum* and *P. laetum* showed the strongest differential regulation of HT-SuperSAGE tags in group 1 (C<S>R, Fig. 24). The highest number of differentially regulated tags was up-regulated during stress and down-regulated under recovery conditions (Fig. 24). In *P. miliaceum* the up-regulation under recovery conditions (group 4, C=S<R) exhibited the highest amount of differentially regulated tags, where *P. turgidum* down-regulated the highest number of tags under stress conditions and up-regulated these tags again under recovery conditions (group 5, C>S<R). The exact numbers of tags differentially regulated in each species are listed in Table 14.

Table 14: Differentially regulated tags in the four *Panicum* species. Tags were separated into 8 groups with differential regulation and the total amount of differentially regulated tags per group is listed. Control (C), stress (S), recovery (R), up-regulated (<), down-regulated (>), not differentially regulated (=).

Species	C<S>R	C<S=R	C<S<R	C=S<R	C>S<R	C>S=R	C>S>R	C=S>R
<i>P. bisulcatum</i>	10733	5926	578	8427	5037	5172	258	2109
<i>P. laetum</i>	13786	2886	953	4191	2259	2906	609	3649
<i>P. miliaceum</i>	4281	1975	504	5567	2834	909	313	1363
<i>P. turgidum</i>	4314	3246	723	3151	7931	3672	830	3040
Total	33114	14033	2758	21336	18061	12659	2010	10161

The highest number of total differentially regulated HT-SuperSAGE tags was found for group 1 (C<S>R) with 33,114 tags followed by group 4 (C=S<R) with 21,336 tags and group 5 (C>S<R) with 18,061 tags differentially regulated in the four species (Table 14).

The subsequent analyses focused on the species-comprehensive regulation of HT-SuperSAGE tags. Therefore the total number of differentially regulated tags from all four *Panicum* species was subjected to species-comprehensive analyses (Fig. 25).

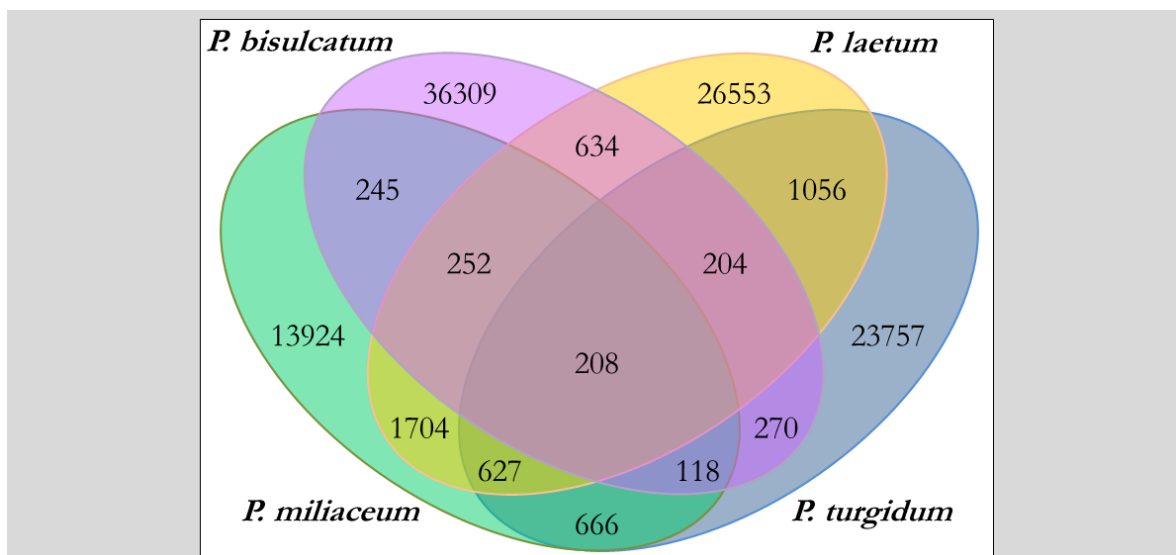


Fig. 25: Species-comprehensive comparison of the total number of differentially regulated tags. Venn diagrams show the total number of differentially regulated tags only apparent in one, two, three or all species.

The species-comprehensive analyses of the total number of differentially regulated tags / species revealed that most of the tags were species-specific. The two-species comprehensive analyses exhibited the highest number of shared tags between the species *P. laetum* and *P. turgidum*, whereas the three-species comprehensive analyses exhibited the highest number of tags for the three C_4 species *P. laetum*, *P. miliaceum* and *P. turgidum* (Fig. 25). In total 208 tags were found present in all four *Panicum* species (Fig. 25).

Additionally, the tags separated into the eight “regulation groups” were also subjected to species-comprehensive analyses as the total number of tags shared between the species (Fig. 25) does not give any information about their regulation. Therefore the 8 groups of differentially regulated tags were screened for tag-appearance in one, two, three and four *Panicum* species (Fig. 26, Fig. 27).

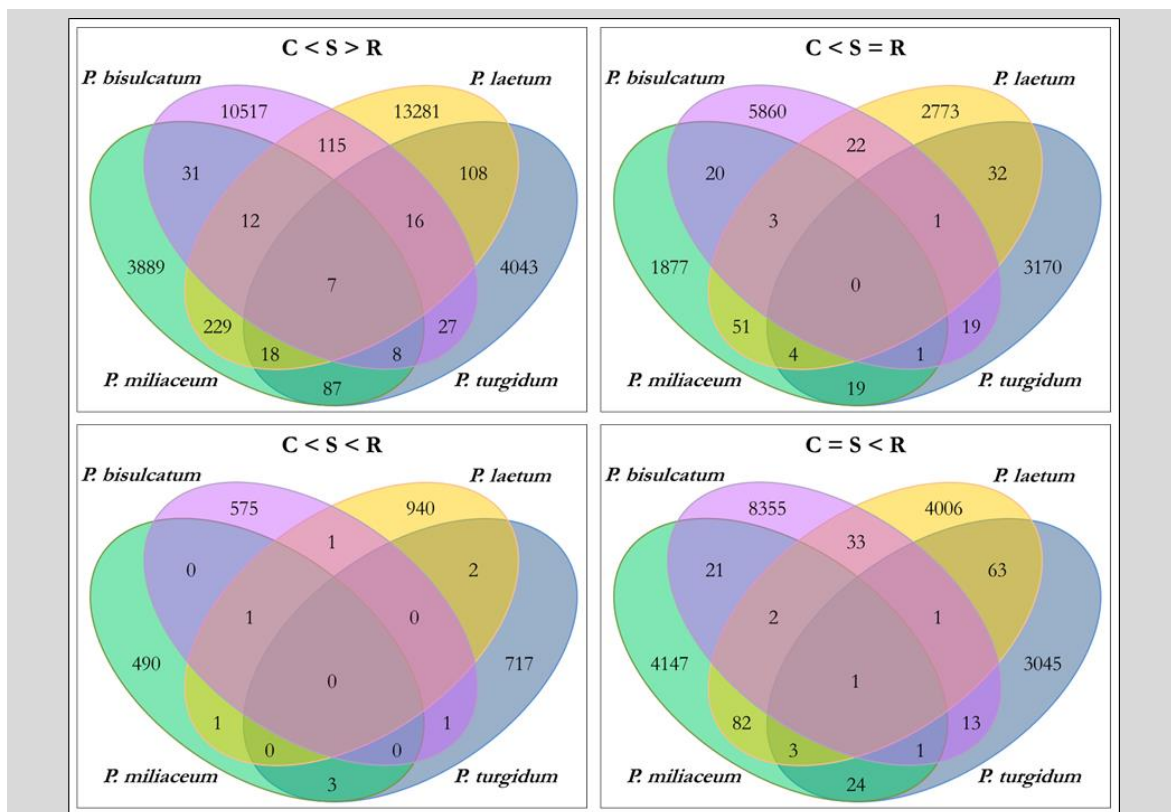


Fig. 26: Species-comprehensive comparison of the differentially regulated tags (group 1-4). Venn diagrams show the number of differentially regulated tags only apparent in one, two, three or all species. Tags of different regulation schemes (groups 1-4) were compared separately. Control (C), stress (S), recovery (R), up-regulated (<), down-regulated (>), not differentially regulated (=).

The species-comprehensive analyses revealed, that a great number of tags was species-specific and only few tags were shared between the species (Fig. 26, Fig. 27). Within the tags being up-regulated under stress and down-regulated under recovery ($C < S > R$, Fig. 26) for example only 7 tags were found present in all four species. When comparing only two

species, *P. miliaceum* and *P. laetum* shared the highest amount of tags up-regulated under stress and down-regulated under recovery conditions (229 tags, C<S>R, Fig. 26). The three-species comprehensive analyses for “group 1” tags revealed the highest number of shared tags between the C₄ species *P. laetum*, *P. miliaceum* and *P. turgidum* (18 tags, C<S>R, Fig. 26).

When looking at the “down-regulated groups 5-8” (Fig. 27) the highest number of tags shared between all four species was found for the down-regulation under stress and the subsequent up-regulation under recovery (4 tags, C>S<R, Fig. 27).

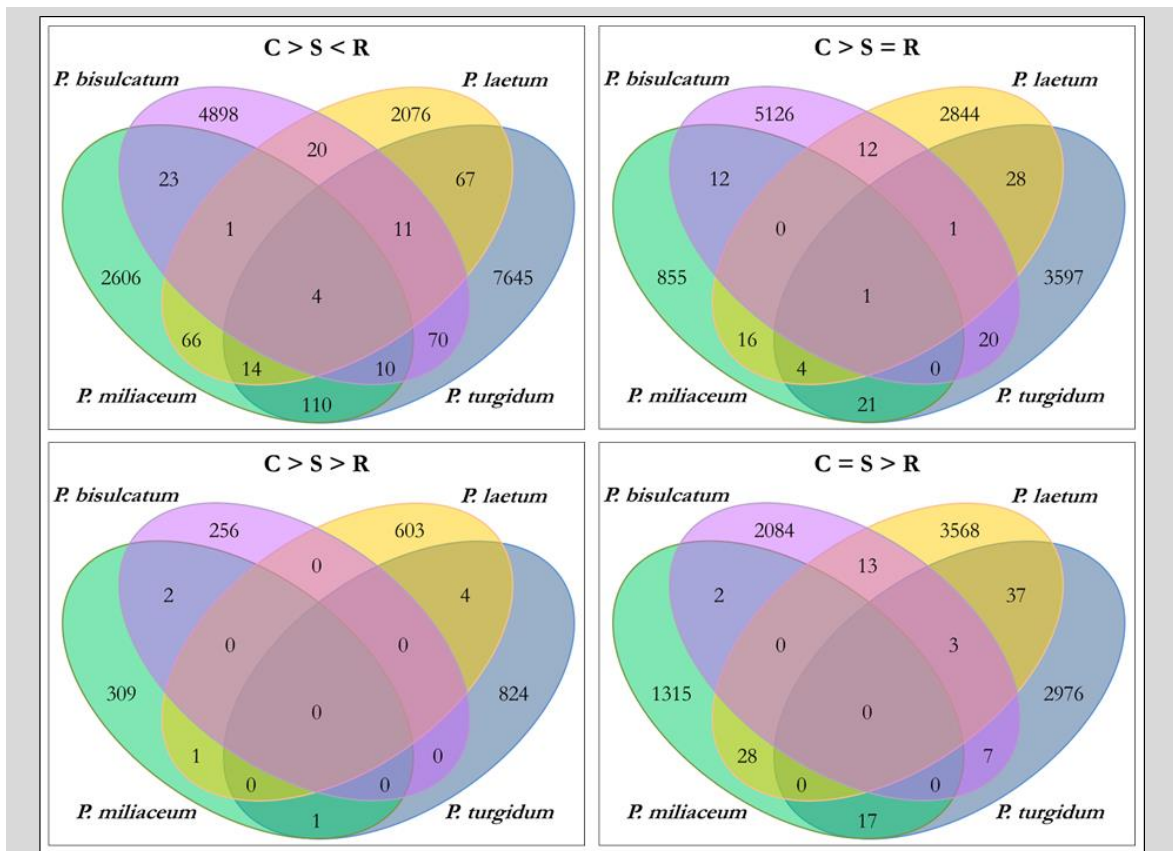


Fig. 27: Species-comprehensive comparison of the differentially regulated tags (group 5-8). Venn diagrams show the number of differentially regulated tags only apparent in one, two, three or all species. Tags of different regulation schemes (groups 5-8) were compared separately. Control (C), stress (S), recovery (R), up-regulated (<), down-regulated (>), not differentially regulated (=).

In total more tags were found to be up-regulated (group 1-4, 71,241 tags) than down-regulated (group 5-8, 42,891 tags) which is also mirrored by the fact, that in groups 1-4 only five times no tags were shared between species (0 tags, Fig. 26) whereas in groups 5-8 this number rose to 10 (Fig. 27).

Those tags shared by all four *Panicum* species in group 1 (C<S>R) were now exemplarily screened for their quantity and strength of their regulation (fold change) to see whether

they did have a great impact during drought stress (high differential regulation) or not (low differential regulation). Results of the three highest regulated tags (independent from the species) are listed in Table 15.

Table 15: Exemplary analyses of tags shared by all four *Panicum* species (C<S>R). Quantity of tags under control, stress and recovery conditions and the resulting regulation (fold change). Control (C), stress (S), recovery (R), up-regulated (<), down-regulated (>).

Species	Tag	Quantity of tags			Fold change regulation	
		C	S	R	C<S	S>R
<i>P. bisulcatum</i>	CATGAACGAGGTGA	4	33	5	8	7
<i>P. laetum</i>		4	70	4	18	18
<i>P. miliaceum</i>	AGCCGGTGCCGA	0	182	3	182	61
<i>P. turgidum</i>		23	232	42	10	6
<i>P. bisulcatum</i>	CATGGTGTGTCGAG	9	100	36	11	8
<i>P. laetum</i>		0	32	9	32	4
<i>P. miliaceum</i>	GGAGCTGGAGTT	0	130	40	130	3
<i>P. turgidum</i>		25	386	65	12	6
<i>P. bisulcatum</i>	CATGCCGGTGTGTC	2	30	11	15	3
<i>P. laetum</i>		0	29	0	29	29
<i>P. miliaceum</i>	CCTGCTGCCCGT	0	130	0	130	130
<i>P. turgidum</i>		0	7	3	7	2

It is clearly visible that the tags, although equally regulated, were differentially strong up- and down-regulated in the four species. All three tags were highly up-regulated under stress conditions in *P. miliaceum* (in C<S, up-regulation ≥ 50 -fold) whereas in the other species, the up-regulation under stress was <50-fold.

On the contrary, the abundance of the tags displayed a different result as the upper two tags in Table 15 showed the highest quantity in *P. turgidum* under stress. Due to a higher quantity under control conditions however, the fold change regulation was smaller than in *P. miliaceum*.

To monitor the expression of HT-SuperSAGE tags according to their fold change regulation, tags of the eight differentially regulated groups were divided into five schemata:

- 1) > 2-fold < 5-fold
- 2) > 5-fold < 10-fold
- 3) > 10-fold < 25-fold
- 4) > 25-fold < 50-fold
- 5) > 50-fold

These analyses were carried out to monitor the amount of tags strongly regulated (≥ 10 -fold - ≥ 50 -fold) or only weakly regulated (≥ 2 -fold < 10-fold differential regulation) under drought stress and recovery conditions. Tags were now separated according to their regulation scheme and strength of tag regulation (Table 16).

Table 16: Differential tag expression with appending tag amounts under different regulations. The amount of tags ≥ 2 -fold <5 -fold, ≥ 5 -fold <10 -fold, ≥ 10 -fold <25 -fold, ≥ 25 -fold <50 -fold or ≥ 50 -fold differentially expressed under the eight regulation schemes. Control (C), stress (S), recovery (R), up-regulated (<), down-regulated (>).

	Regul.	C<S>R	C<S=R	C<S<R	C=S<R	C>S<R	C>S=R	C>S>R	C=S>R
<i>P. bisulcatum</i>	2-fold	9286	4651	575	7172	3614	3724	257	1935
	5-fold	1084	992	3	1157	1061	1224	1	163
	10-fold	323	251	0	92	320	215	0	11
	25-fold	35	26	0	5	30	8	0	0
	50-fold	5	6	0	1	12	1	0	0
<i>P. laetum</i>	2-fold	9498	1689	898	2100	1926	1712	556	2451
	5-fold	3067	858	52	1397	210	764	43	749
	10-fold	988	297	3	539	98	322	9	381
	25-fold	168	28	0	112	20	73	0	54
	50-fold	65	14	0	43	5	35	0	14
<i>P. miliaceum</i>	2-fold	2686	271	425	360	1440	286	293	637
	5-fold	301	1064	78	4248	1103	138	19	503
	10-fold	1110	529	1	852	232	358	1	211
	25-fold	112	79	0	82	49	101	0	12
	50-fold	72	32	0	25	10	26	0	0
<i>P. turgidum</i>	2-fold	3074	2137	711	1093	6487	1176	810	2098
	5-fold	888	995	12	1822	1058	2287	20	871
	10-fold	284	96	0	221	340	182	0	68
	25-fold	54	10	0	12	31	21	0	2
	50-fold	14	8	0	3	15	6	0	1

Table 16 clearly shows, that the ≥ 2 -fold <5 -fold regulation was strongest in all species under all regulation schemata and constantly decreased with increasing fold change strength. As tendencies were very difficult to read from Table 16, results were also displayed graphically. Thereby, the ≥ 2 -fold <5 -fold expression was depicted solely (Fig. 28) as tag numbers were too high to clearly monitor the stronger fold change regulations (Fig. 29).

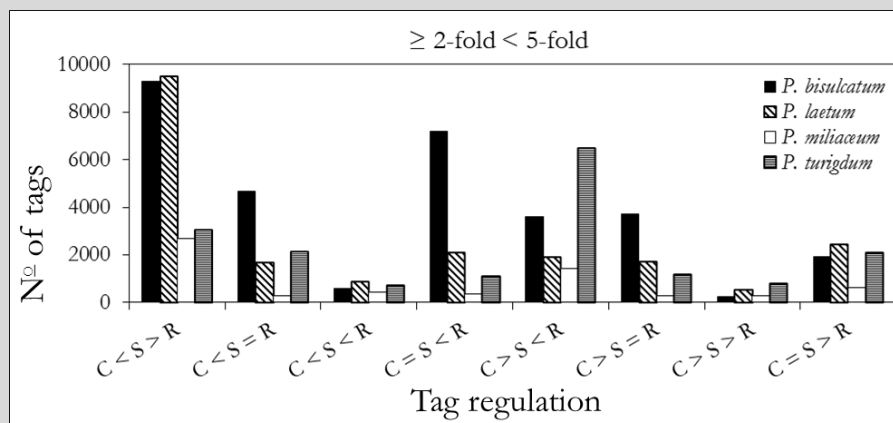
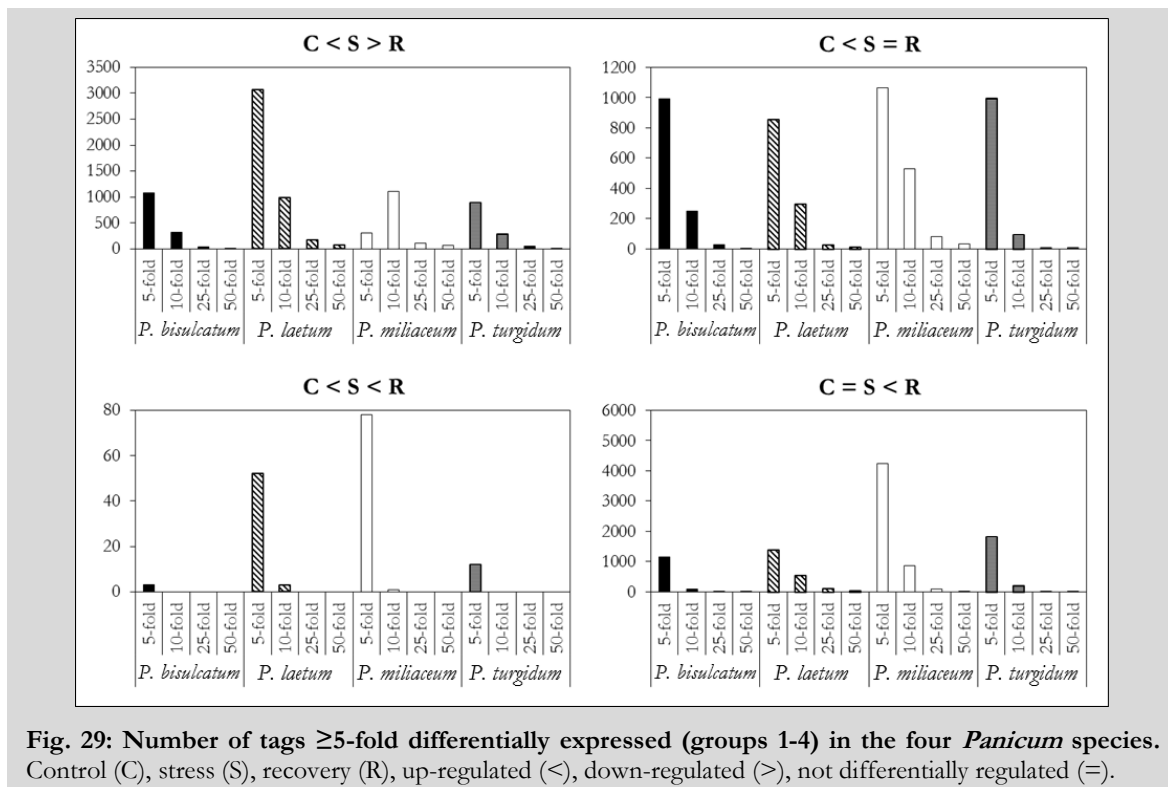


Fig. 28: Number of tags ≥ 2 -fold and < 5 -fold expressed under the different regulation schemata in the four *Panicum* species. Control (C), stress (S), recovery (R), up-regulated (<), down-regulated (>), not differentially regulated (=).

The number of tags ≥ 2 -fold and < 5 -fold differentially expressed was highest in the species *P. bisulcatum* and *P. laetum* for the regulation schemata $C < S > R$ (Fig. 28). In most groups, *P. bisulcatum* exhibited the highest (or a not much lower) number of tags except for the regulation group $C > S < R$ where *P. turgidum* showed the highest number of tags ≥ 2 -fold and < 5 -fold differentially expressed.

The number of tags equally or more than 5-fold differentially expressed under stress and recovery conditions were also graphically displayed according to the regulation groups (Fig. 29, Fig. 30).



It is clearly visible, that the species did not follow a similar gene regulation pattern under stress and recovery conditions. The 5-fold differential expression of tags up-regulated under drought and down-regulated under recovery conditions ($C < S > R$) had the highest number of tags in the species *P. laetum*, where their numbers fluctuated around 1000 tags in all four species for tags up-regulated under stress and not differentially regulated under recovery conditions ($C < S = R$, Fig. 29) for example.

The same analyses were carried out with tags regulated according to groups 5-8 (Fig. 30).

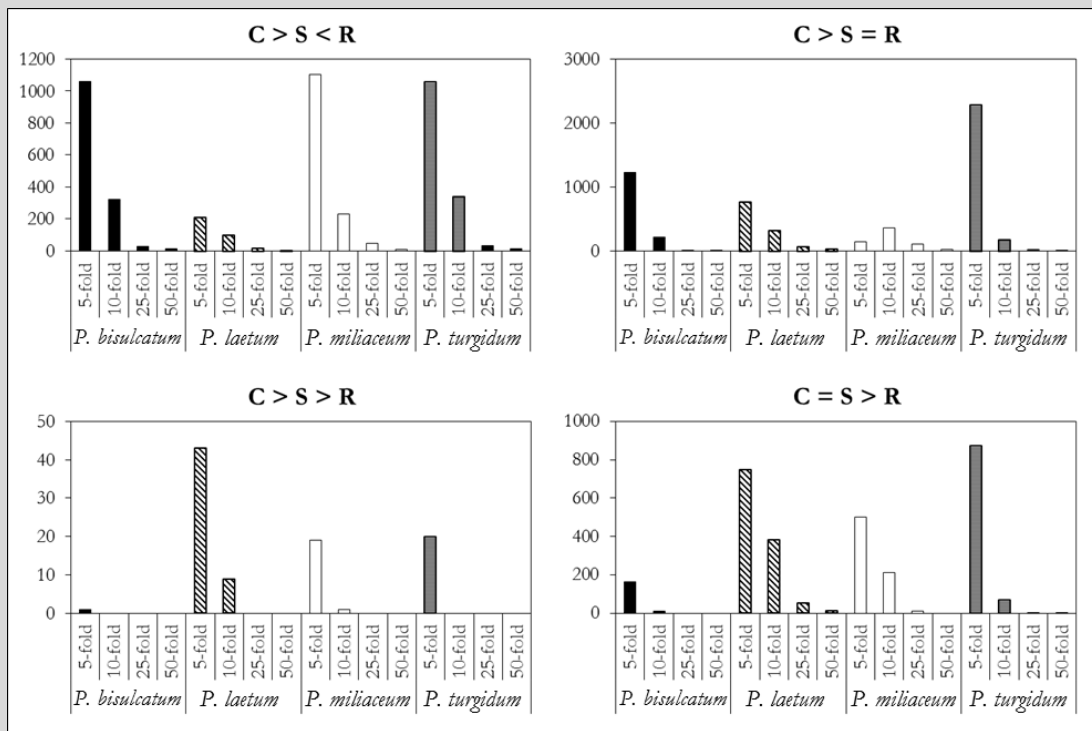


Fig. 30: Number of tags ≥ 5 -fold to ≥ 50 -fold differentially expressed (groups 5-8) in the four *Panicum* species. Control (C), stress (S), recovery (R), up-regulated (<), down-regulated (>), not differentially regulated (=).

It is clearly visible, that for groups 5-8 the species neither did follow a similar gene regulation pattern under stress nor under recovery conditions. The 5-fold differential expression of tags down-regulated under drought and up-regulated under recovery conditions ($C > S < R$) had the highest number of tags in the species *P. miliaceum*, directly followed by *P. turgidum* and *P. bisulcatum*. *P. laetum* in contrast exhibited only very low numbers. *P. turgidum* exhibited the highest numbers of 5-fold differentially expressed tags down-regulated either under stress or under recovery conditions ($C > S = R$, $C = S > R$ respectively, Fig. 30).

To get an idea about the strength of (fold change) regulation, the strongest regulated tag of each group (if ≥ 50 -fold) and species is listed in Table 17.

Table 17: Tags differentially regulated ≥ 50 -fold and the appending number of tags. The highest regulated tag in every “regulation group” was shown for every species. Numbers in bold signalise the highest regulated tag for the species.

	Regulation	C	N° of tags in		Fold change regulation	
			S	R	C / S	S / R
<i>P. bisulcatum</i>	C<S>R	0	479	34	479	14
	C<S=R	2	264	164	142	<2
	C=S<R	0	0	53	<2	53
	C>S<R	486	1	147	486	147
	C>S=R	52	0	0	52	<2
<i>P. laetum</i>	C<S>R	0	171	0	171	171
	C<S=R	2	304	325	137	<2
	C=S<R	2	1	281	<2	202
	C>S<R	454	0	97	454	97
	C>S=R	6449	11	22	579	<2
	C>S>R	1254	11	0	113	11
	C=S>R	60	116	0	<2	116
<i>P. miliaceum</i>	C<S>R	0	2059	3	2059	780
	C<S=R	0	720	391	720	<2
	C=S<R	0	0	394	<2	394
	C>S<R	289	0	119	289	119
	C>S=R	336	0	0	336	<2
<i>P. turgidum</i>	C<S>R	5	2625	13	567	202
	C<S=R	0	134	127	134	<2
	C=S<R	0	0	70	<2	70
	C>S<R	845	0	52	845	52
	C>S=R	102	0	0	102	<2
	C=S>R	51	65	0	<2	65

The highest differentially regulated tag found was 2059-fold up-regulated under stress conditions in *P. miliaceum* (C<S>R). Also in the other investigated species fold change regulation was high (e.g. *P. turgidum* C>S<R, *P. laetum* C>S=R or *P. bisulcatum* C>S<R). Tags not differentially regulated ≥ 50 -fold were not included in the table.

3.2.2.3. BLAST search

All tags from the four *Panicum* species were subjected to a BLAST search (2.3.2.8) against the EST (expressed sequence tags) database of *P. virgatum*. Unfortunately only a small number of tags could be annotated to a specific gene as displayed in Table 18. The EST database of *P. virgatum* is the only *Panicum* database available up to date, species-specific databases (EST, genome etc.) could most certainly achieve better results in numbers of tag to gene hits.

Table 18: BLAST search outcome. The total number of tags submitted to a BLAST search against the EST database of *P. virgatum*, as well as the tag to gene hits and the percentage of total tag to gene hits is shown.

Species	N ^o of tags subjected to a BLAST search	Tag to gene hits	Tag to gene hits [%]
<i>P. bisulcatum</i>	51648	1165	2.25
<i>P. laetum</i>	31238	2156	6.90
<i>P. miliaceum</i>	18895	1127	5.96
<i>P. turgidum</i>	30482	2502	8.21

The tag to gene hits [%] were highest in *P. turgidum* with 8.21 % and lowest in *P. bisulcatum* with 2.25 % coverage only.

3.2.2.4. 3' RACE

As a great number of the tags could not be annotated to a specific gene, the 3' ends of the tag-specific genes were amplified (2.3.2.7). Therefore 96 highly differentially expressed tags (24 tags / species, see 11.1, Table 26, Table 27) were selected and used to design primers.

As the up-regulation of genes plays a crucial role in stress response, in total 18 HT-SuperSAGE tags found to be strongly up-regulated during stress and / or recovery were selected to design primers for the 3' rapid amplification of cDNA ends (RACE), (C<S>R, C<S=R, C=S<R, C<S<R). The remaining 6 primers were designed out of tags found to be strongly down-regulated during stress (C>S<R, C>S=R). This was done for every *Panicum* species resulting in a total number of 96 primers to be used for the 3' RACE (11.1, Table 26, Table 27). The method was chosen as HT SuperSAGE tags were obtained from the 3' end of the genes differentially expressed (Fig. 6). Subsequently to the 3' RACE, samples were run on a 2 % agarose gel and bands with a size of 100 – 400 bp (some bigger) were cut out of the gel, diluted and sequenced (see 11.1, Fig. 39).

The 3' RACE did not work for all the primers designed (e.g. primers 17, 18 24, Fig. 39) nor did the sequencing reaction give applicable results for all sequences submitted. In total 20 sequences conforming to the requirements (sequence read length > 50 bp, clearly defined peaks etc.) could be extracted (Table 19).

Table 19: Summary of the 3' RACE outcome. The primers utilized for 3' RACE, the final length of the sequenced fragments, the total number of counted tags generated by HT-SuperSAGE for each primer and the appending regulation are shown. Control (C), stress (S), recovery (R), up-regulated (<), down-regulated (>), not differentially regulated (=), base pair (bp).

Sample	Primer	3' RACE sequence length (bp)	Tag N _s control	Tag N _s stress	Tag N _s recovery	Regulation
<i>P. bisulcatum</i>	CATGTACGTGTACGAGTGCAAGGTG (2)	142	406	1	300	C>S<R
<i>P. bisulcatum</i>	GGTGAGGAGAGTGAGGAGTGAT (3)	66	1452	4	233	C>S<R
<i>P. bisulcatum</i>	CATGGATCCTGACATCTTTGTTGGGT (5)	74	0	274	7	C<S>R
<i>P. bisulcatum</i>	GAGACACGTGTTCCGGAATCCG (9)	153	0	60	0	C<S>R
<i>P. bisulcatum</i>	CATCTCCCTCCCCCAACC (11)	108	76	1	4	C>S<R
<i>P. laetum</i>	AACGGCCTCGTGCTCGTCG (2)	106	472	0	40	C>S<R
<i>P. laetum</i>	CCACGGCGCTTGCTGCTAGCTA (14)	55	0	106	154	C<S>R
<i>P. laetum</i>	GCTCCAGGCCAGCGTATGAAGAA (17)	104	0	92	79	C<S>R
<i>P. laetum</i>	CCACCGTGTGCTCTGTGTCTCG (19)	107	0	0	198	C=S<R
<i>P. laetum</i>	AGAGCGGGCACGGCGACG (24)	211	0	15	163	C<S<R
<i>P. miliaceum</i>	CATGCGAGCAGGATTCCAAGAGAGTA (3)	134	224	0	116	C>S<R
<i>P. miliaceum</i>	GATCGGCGGCAGCACGTCC (9)	124	0	703	5	C<S>R
<i>P. miliaceum</i>	GCCGCCGACAGAGTAGAATTGT (10)	171	0	522	5	C<S>R
<i>P. miliaceum</i>	ACCGCGACGCGGAGGCTG (17)	200	0	125	87	C<S>R
<i>P. miliaceum</i>	TTCGCGTTCGCGGAGGCGG (20)	102	0	0	106	C=S<R
<i>P. miliaceum</i>	AGCGCGCCGACGGCTGAT (22)	69	0	0	100	C=S<R
<i>P. turgidum</i>	GTGCTTTGTCTCTGGCCCTTCT (2)	132	243	0	145	C>S<R
<i>P. turgidum</i>	CATGGAAATAATGTCCCCCTGCTTTG (12)	103	79	0	0	C>S=R
<i>P. turgidum</i>	CATGCGGTGTTGATTCGATGGTTTCT (14)	164	0	104	106	C<S>R
<i>P. turgidum</i>	CGCGTTAGGCGGCGGCT (17)	189	0	60	44	C<S>R

The 3' RACE elongated the 26 bp HT-SuperSAGE tag and sequences with a length of 55 bp (*P. laetum*) up to 211 bp (*P. laetum*) could be generated (for the list of sequences see 11.1). These sequences were now used to perform a BLAST search (2.3.2.8) to annotate the unknown sequences to known genes.

3.2.2.5. BLAST search for gene annotation

With the longer tag-specific sequences, a BLAST search could be carried out to annotate the 3' end cDNA sequences to a specific gene (2.3.2.8).

Table 20: Annotation of the (via 3' RACE) elongated sequences by BLAST search. Almost all sequences could be annotated to specific genes.

Sample	Primer	Annotation
<i>P. bisulcatum</i>	CATGTACGTGTACGAGTGTC AAGGTG (2)	Aquaporin
<i>P. bisulcatum</i>	GGTGAGGAGAGTGAGGAGTGAT (3)	Chlorophyll a-b binding protein 4 (lhca4)
<i>P. bisulcatum</i>	CATGGATCCTGACATCTTTGTTGGGT (5)	Hypothetical protein
<i>P. bisulcatum</i>	GAGACACGTGTTCCGGAATCCG (9)	No specific hit
<i>P. bisulcatum</i>	CATCTCCCTCCCCCAACC (11)	RubisCO small subunit
<i>P. laetum</i>	AACGGCCTCGTGCTCGTCG (2)	Photosystem II 10 kDa polypeptide
<i>P. laetum</i>	CCACGGCGCTTGCTGCTAGCTA (14)	Temperature-induced lipocalin (TIL)
<i>P. laetum</i>	GCTCCAGGCCAGCGTATGAAGAA (17)	Late embryogenesis abundant protein D-34-like
<i>P. laetum</i>	CCACCGTGTGCTCTGTGTCTCG (19)	Low-temperature induced protein
<i>P. laetum</i>	AGAGCGGGCACGGCGACG (24)	25-28S rRNA sequence / hypothetical protein
<i>P. miliaceum</i>	CATGCGAGCAGGATTCCAAGAGAGTA (3)	9-cis-epoxycarotenoid dioxygenase 1 (NCED1)
<i>P. miliaceum</i>	GATCGGCGGCAGCACGTCC (9)	ATP synthase delta chain
<i>P. miliaceum</i>	ACCGCGACGCGAGGCTG (17)	Purple acid phosphatase (PAP)
<i>P. miliaceum</i>	GCCGCCGACAGAGTAGAATTGT (10)	No specific hit
<i>P. miliaceum</i>	TTCGCGTTCGCGGAGGCGG (20)	Adenosine 5'-phosphosulfate reductase 2 (APR)
<i>P. miliaceum</i>	AGCGCGGCCGACGGCTGAT (22)	Uncharacterized protein
<i>P. turgidum</i>	GTGCTTTGTCTCTGGGCCTTCT (2)	(papain-like) cysteine proteinase (CP)
<i>P. turgidum</i>	CATGGAAATAATGTCCCCCTGCTTTG (12)	Ribonuclease precursor (RP)
<i>P. turgidum</i>	CATGCGGTGTTGATTTCGATGGTTTCT (14)	(papain-like) cysteine proteinase (CP)
<i>P. turgidum</i>	CGGCGTTAGGCGGCGGCT (17)	glycine-rich RNA-binding protein

Most sequences could be annotated to a specific gene (Table 20) except for *P. bisulcatum* (sequence 9) and *P. miliaceum* (sequence 10) where no specific hits could be found. Also *P. miliaceum* (sequence 22) did not give additional information as the BLAST search hit an uncharacterized protein. The remaining genes encoded for diverse proteins e.g. from the photosynthesis chain (*P. bisulcatum*, sequence 3, *P. laetum*, sequence 2).

To get an impression of the gene, the location of the 26 bp HT-SuperSAGE tag and the sequence generated by the 3' RACE method, a graphical overview was produced including the coding region of the gene with the appending size (in bp), the non-coding regions, the tag and the 3' RACE sequence proportional to each other (Fig. 31).

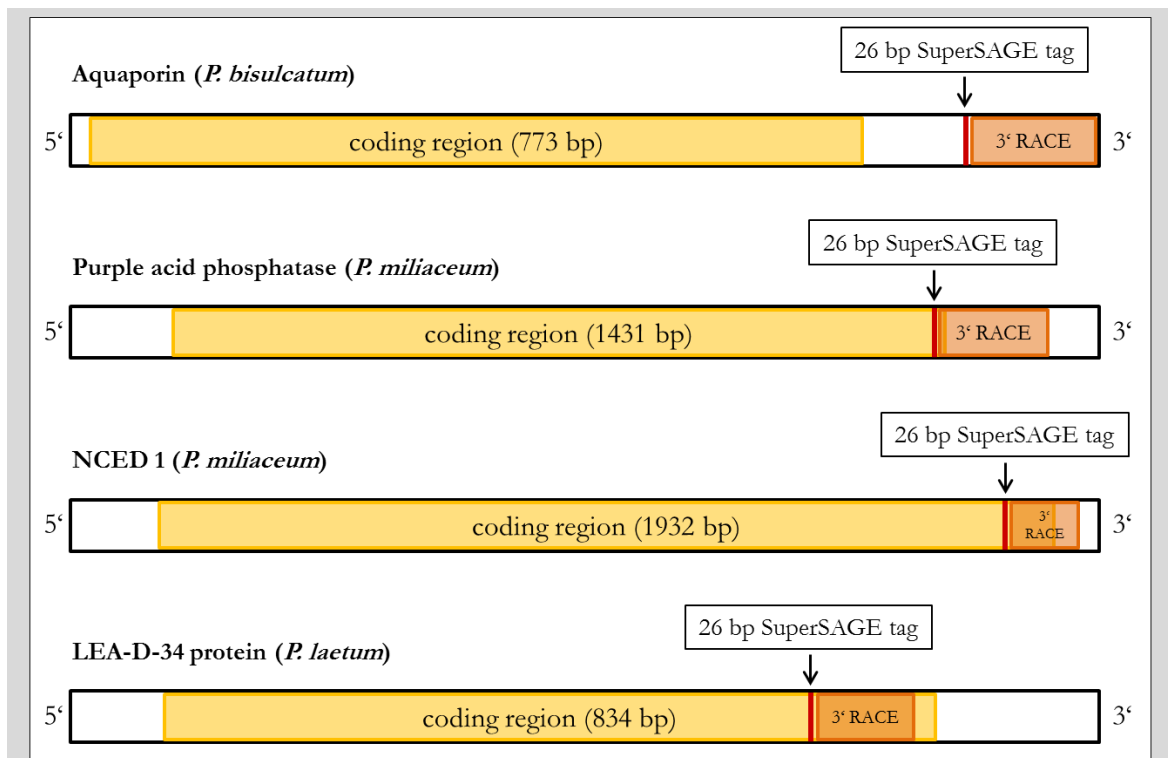


Fig. 31: Overview of elected genes concerning coding region, 26 bp tag and 3' RACE sequence. The 3' RACE sequence (orange box) as well as the tag (red vertical line) can be located within the 3' untranslated region (aquaporin), at the beginning of the coding region (yellow box, purple acid phosphatase), half within the coding- and UT region (9-cis-epoxycarotenoid dioxygenase 1 (NCED 1)) or completely in the coding region (LEA-D-34 protein).

As the 26 bp SuperSAGE tag was generated from the 3' region as well as the 3' RACE sequence they were located closer to the 3' end of the gene (Fig. 31). The tag and the 3' RACE sequence can be located completely within the non-coding as well as the coding region, or anywhere in between (Fig. 31) depending on the *Nla*III restriction enzyme site. As HT-SuperSAGE analyses were only carried out once per species ($n = 1$), further analyses had to be conducted to (partly) verify the results. The method of choice was the quantitative real-time PCR (qPCR).

3.2.2.6. Gene expression analysis by qPCR

The quantitative real-time PCR (qPCR) was conducted on reverse transcribed RNA to exemplarily verify the gene expression profile exposed by the HT-SuperSAGE analyses. Out of the listed sequences in Table 21, 5 genes were chosen to conduct qPCR analyses.

Table 21: Genes chosen for the qPCR analyses. Up-regulation (<), down-regulation (>), no differential regulation (=) in control (C), stress (S) and recovery (R) samples.

Species	Gene	Regulation as exposed by HT-SuperSAGE (C/S/R)
<i>P. laetum</i>	Temperature induced lipocalin	0 < 106 = 154
<i>P. miliaceum</i>	9-cis-epoxacarotinoid dioxygenase 1	224 > 0 < 116
<i>P. miliaceum</i>	Purple acid phosphatase	0 < 125 = 87
<i>P. turgidum</i>	Ribonuclease precursor	79 > 0 = 0
<i>P. turgidum</i>	Cysteine proteinase	0 < 104 = 106

As described in 2.3.2.9 the primer efficiency for each primer pair had to be evaluated before running the qPCR. Therefore a “standard curve” was prepared from a diluted series of a template of known concentration. It is very important, that the primer set used for the qPCR analyses is optimized to work efficiently with the gene of reference as well as with the target gene. For optimal comparison of qPCR runs, primer efficiency should be between 90 % – 110 % and the R² value (showing the linearity of the curve over the concentration range) should be ≥ 0.985 . Besides the results for the standard curves (Table 22), an amplification plot is presented (Fig. 32).

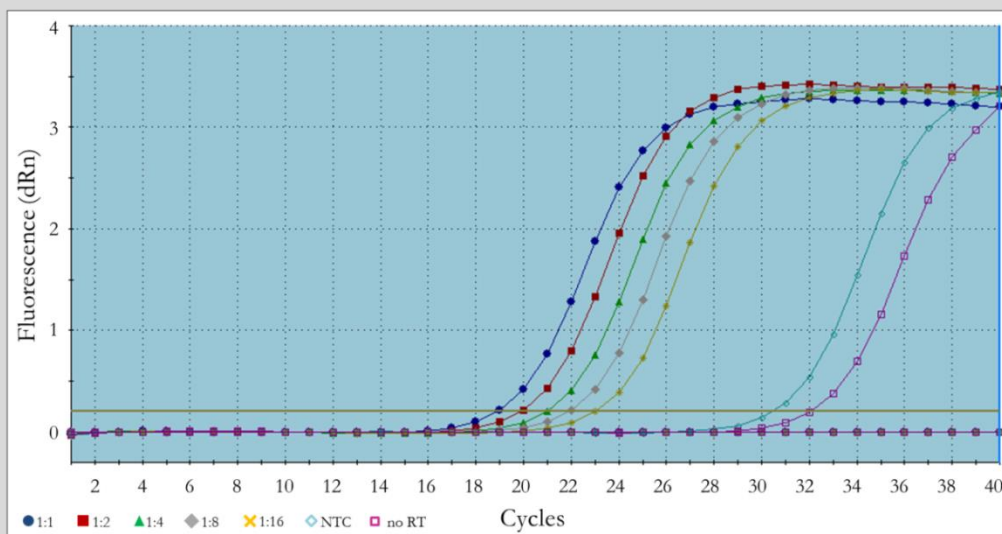


Fig. 32: Exemplary qPCR amplification plot for primer efficiency. Exemplarily the qPCR amplification plot for the evaluation of the primer efficiency of the 9-cis-epoxycarotinoid dioxygenase 1 (NCED 1) gene is shown. The undiluted sample (1:1) has a Ct (cycle threshold) value of 19, the following dilutions have Ct values +1 respectively with a Ct value of 23 for the strongest dilution (1:16). The NTC (no template control) has a Ct value of 30.5, the no RT (no real time) a Ct value of 32.

It is clearly visible that the curves for which cDNA was used as a template (in dilutions 1:1 – 1:16, filled symbols) had Ct (Cycle threshold) values between 19 and 23 and were therefore located within the range of a good Ct value between (e.g. 15 and 25). The Ct value marks the moment where fluorescence of the amplified fragment rises above ground

fluorescence. The curves where either no template was included (no template control, NTC) or RNA was used as a template instead of cDNA (no real-time, no RT) exhibited Ct values of 30.5 and 32 respectively (open symbols). The NTC was included to verify that there was no formation of primer dimers, the no RT run was included to verify that the RNA used to produce the cDNA did not contain (genomic) DNA (as amplification template) ensuring that solely gene expression on mRNA levels was measured. To verify that the NTC and no RT samples did not amplify the primer specific fragment after 30.5 and 32 cycles respectively, samples were additionally analysed on an agarose gel (2.3.2.5, Fig. 33).

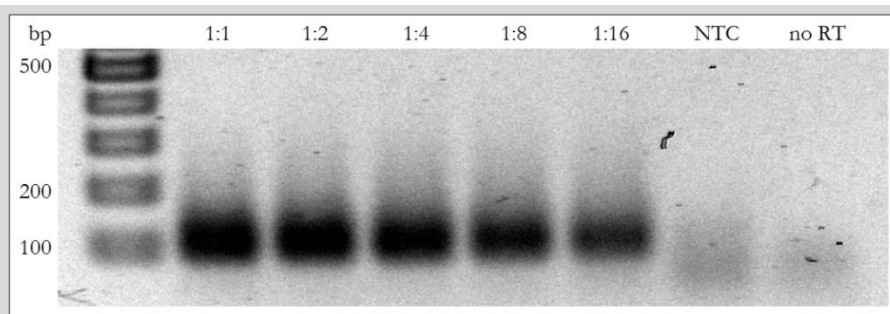


Fig. 33: Exemplary samples from the primer efficiency qPCR run on a 2 % agarose gel. Diluted samples (1:1 – 1:16), no template control (NTC) and no real-time (no RT) samples (9-cis-epoxacarotinoid dioxygenase 1) were run on a 2 % agarose gel after the primer efficiency qPCR run.

Only one fragment was amplified during the qPCR primer efficiency run with a size of just over 100 bp (expected length: 110 bp). The dilution was mirrored by the reduced thickness and intensity of the bands. Even though fragments were amplified for the NTC and no RT samples during the run after 30.5 and 32 cycles respectively (Fig. 32) this could not be visualized on the agarose gel as no bands were apparent (Fig. 33). The primer efficiency values as well as the R^2 values for the target genes are listed in Table 22.

Table 22: Standard curve results for the chosen target genes used to determine the primer efficiency by qPCR. The primers designed for the specific genes were checked for their efficiency in the appending species.

Species	Target gene	R^2 value	Efficiency (%)
<i>P. laetum</i>	Temperature induced lipocalin	0.994	103.2
<i>P. miliaceum</i>	9-cis-epoxacarotinoid dioxygenase 1	0.991	95.8
<i>P. miliaceum</i>	Purple acid phosphatase	0.994	88.4
<i>P. turgidum</i>	Ribonuclease precursor	0.982	104.2
<i>P. turgidum</i>	Cysteine proteinase	1.000	97.6

The R^2 values were all within the range of ≥ 0.985 , except for the ribonuclease precursor in *P. turgidum* (0.982). The primer efficiencies for the amplification of target genes were also in

the range of 90-110 %, except for the purple acid phosphatase in *P. miliaceum*, showing slightly lower values (88.4 %).

When performing quantitative experiments like the qPCR to measure the expression levels of target genes under different conditions (control vs. stress vs. recovery in this dissertation) a normalization of the results is required. This was done by a reference gene, a gene not differentially expressed under varying conditions. In this dissertation the cap-binding protein 20 (CPB 20) was chosen (MARTIN et al. 2007). The normalization levelled the differences in RNA isolation and efficiency of reverse transcription within the samples. The primer efficiencies for the reference gene as well as the R^2 values for each species are listed below in Table 23.

Table 23: Standard curve results for the reference gene primer efficiency qPCR run. The primers designed for the reference gene were checked for their efficiency in the appending species.

Species	Reference gene	R^2 value	Efficiency (%)
<i>P. laetum</i>	Cap-binding protein 20	0.996	114.0
<i>P. miliaceum</i>	Cap-binding protein 20	0.993	91.4
<i>P. turgidum</i>	Cap-binding protein 20	0.998	107.2

The R^2 values were all within the range of ≥ 0.985 , and the primer efficiencies for the amplification of the reference gene were also in the range of 90–110 %, except for *P. laetum* where the efficiency value was 114 %. All primers could be used for comparative analyses.

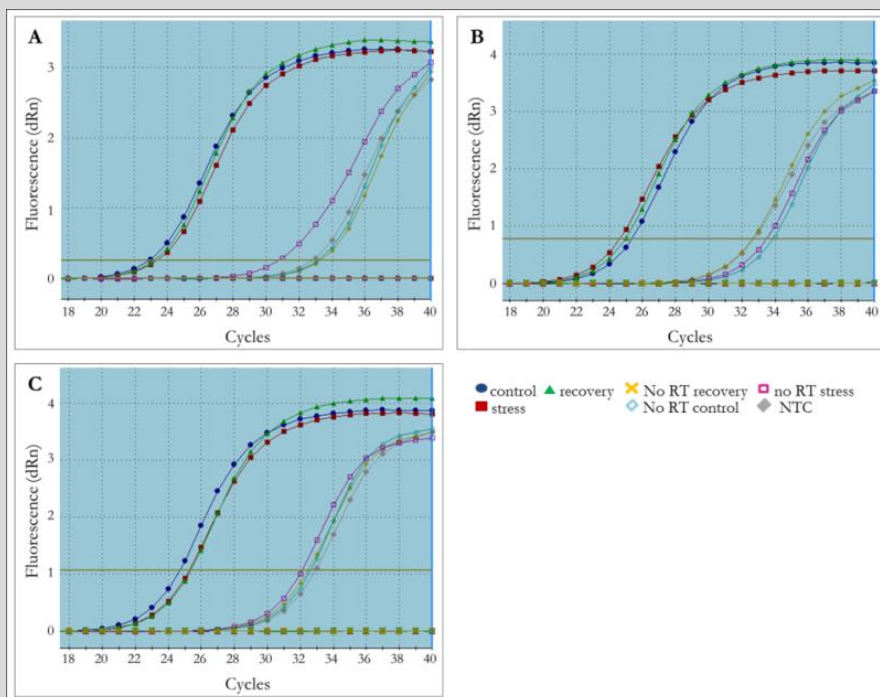


Fig. 34: qPCR amplification plots of the reference gene CPB20. A) *P. laetum*, B) *P. miliaceum*, C) *P. turgidum*. Curves have a threshold cycle (Ct) value differing by ± 0.4 - ± 0.8 cycles. The NTC (no template control) and the no RT (no real time) curves of each sample show Ct values of >31 .

Each run included the amplification of the CPB 20 reference gene, as well as the amplification of the species specific target gene. The reference gene was equally expressed in all three species under control, stress and recovery conditions (Fig. 34) as Ct values for each curve only differed between ± 0.4 cycles (*P. laetum*) - ± 0.7 cycles (*P. miliaceum*). NTC and no RT values were >31 .

The target genes were always amplified simultaneously to the reference gene in one run to exclude course-specific variations.

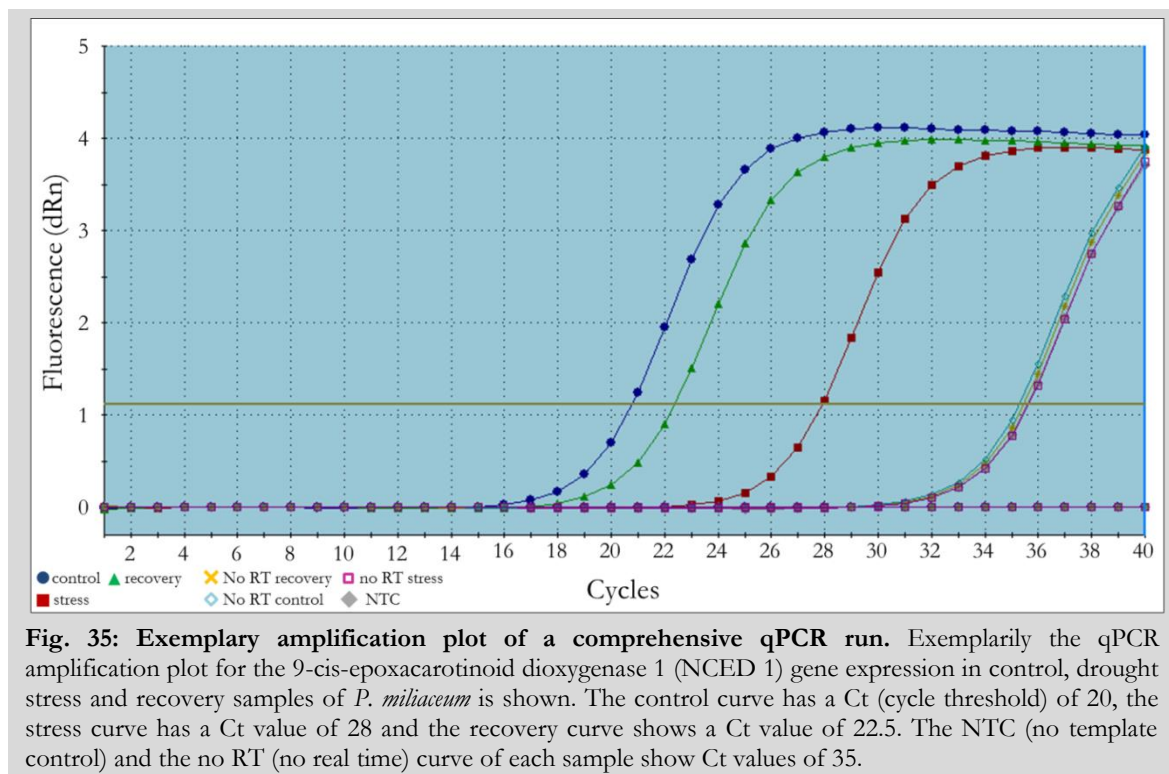


Fig. 35: Exemplary amplification plot of a comprehensive qPCR run. Exemplarily the qPCR amplification plot for the 9-cis-epoxacarotinoic dioxygenase 1 (NCED 1) gene expression in control, drought stress and recovery samples of *P. miliaceum* is shown. The control curve has a Ct (cycle threshold) of 20, the stress curve has a Ct value of 28 and the recovery curve shows a Ct value of 22.5. The NTC (no template control) and the no RT (no real time) curve of each sample show Ct values of 35.

In contrast to the CPB 20 reference gene, the target genes were all differentially amplified (Fig. 34) as curves from control, stress and recovery samples all had differing Ct values. For all species the NTC and no RT curves had Ct values >34 . Again the samples were loaded onto a 2 % agarose gel to verify the results generated by qPCR and to check if the deployed RNA was DNA-free.

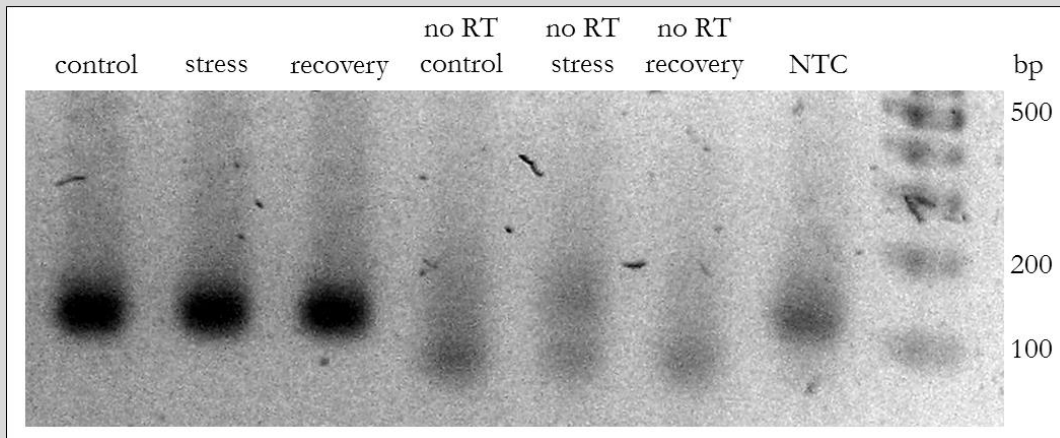


Fig. 36: Exemplary samples from the comparative qPCR run on a 2 % agarose gel. Control, stress and recovery samples, no template control (NTC) and no real-time (no RT) samples (9-cis-epoxacarotinoid dioxygenase 1) were run on a 2 % agarose gel after the comparative qPCR run.

Finally, the relative quantity chart was generated out of the Ct values and the primer efficiency values obtained by qPCR analyses for each gene, as depicted in Fig. 37. The relative quantity chart mirrors the target gene regulation in the *Panicum* species under control, drought stress and recovery conditions.

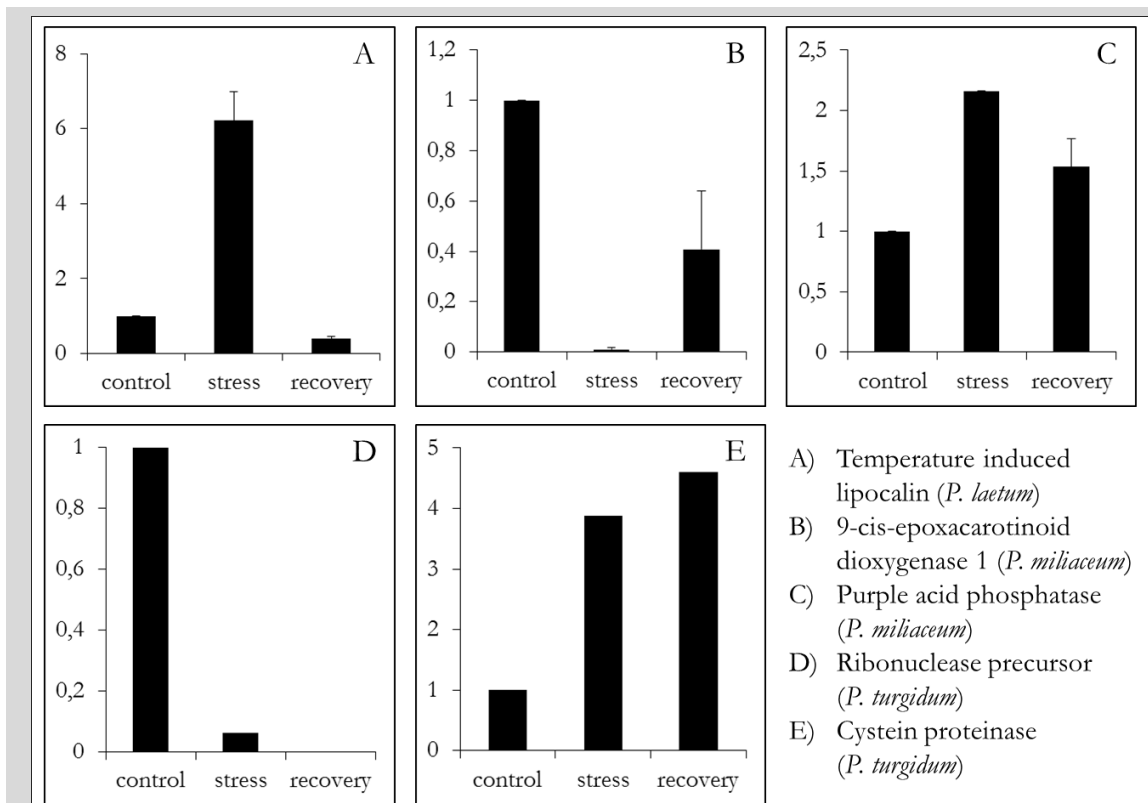


Fig. 37: Differential regulation of gene expression in A) *P. laetum*, B+C) *P. miliaceum* and D+E) *P. turgidum* detected by qPCR analyses. *P. laetum*, *P. miliaceum* (n = 3), *P. turgidum* (n = 1).

The five chosen genes in the three analysed *Panicum* species all showed differential expression under drought stress conditions. The temperature induced lipocalin in *P. laetum* was up-regulated under stress conditions (Fig. 37 A), The NCED 1 gene in *P. miliaceum* was down-regulated under stress conditions (Fig. 37 B), the purple acid phosphatase in *P. miliaceum* was up-regulated under stress conditions (Fig. 37 C), the ribonuclease precursor was down-regulated under stress as well as recovery conditions in *P. turgidum* (Fig. 37 D) and the cysteine proteinase was up-regulated under stress and recovery conditions (Fig. 37 E).

Table 24: Differential gene regulation recorded by HT-SuperSAGE and qPCR analyses. Temperature induced lipocalin (TIL), 9-cis-epoxacarotinoic dioxygenase 1 (NCED 1), purple acid phosphatase (PAP), ribonuclease precursor (RNP), cysteine proteinase (CP). Results from HT-SuperSAGE and qPCR analyses differ only in the regulation of recovery conditions in *P. laetum* (TIL) and *P. miliaceum* (PAP).

Species	Gene	Gene regulation HT-SuperSAGE	Gene regulation qPCR	Equal results?
<i>P. laetum</i>	TIL	C<S=R	C<S>R	(✓)
<i>P. miliaceum</i>	NCED 1	C>S<R	C>S<R	✓
<i>P. miliaceum</i>	PAP	C<S=R	C<S≥R	(✓)
<i>P. turgidum</i>	RNP	C<S=R	C<S=R	✓
<i>P. turgidum</i>	CP	C<S=R	C<S=R	✓

The results concerning the differential gene regulation under control, drought stress and recovery conditions generated by HT-SuperSAGE and qPCR analyses were compared (Table 24). Three out of five genes showed the same gene regulation pattern for the two methods, NCED 1 in *P. miliaceum*, RNP and CP in *P. turgidum* (Table 24). For the TIL in *P. laetum*, an up-regulation during stress condition could be shown by HT-SuperSAGE and qPCR but results differed when looking at the recovery condition. The same effect was observed for the PAP in *P. miliaceum* where an up-regulation under stress was shown by HT-SuperSAGE analyses and could be verified by qPCR but the regulation differed under recovery conditions. Never the less, qPCR could to a great extend verify the results generated by HT-SuperSAGE.

Additionally the gene-specific tags were used to conduct species-comprehensive analyses to check if their regulation was equal or not in the four *Panicum* species (Table 25).

Table 25: Species-comprehensive analyses of the genes used to conduct qPCR analyses. The regulation of the five genes was scanned in all four *Panicum* species to see if differences occurred. Genes were originally found in the species written in bold. Coloured boxed mark the regulation patten, the gene exhibited by HT-SuperSAGE analyses.

Gene	Species	C < S > R	C < S = R	C < S < R	C = S < R	C > S < R	C > S = R	C > S > R	C = S > R
Temperature induced lipocalin	<i>P. bisulcatum</i>								
	<i>P. laetum</i>								
	<i>P. miliaceum</i>								
	<i>P. turgidum</i>								
9-cis-epoxycarotenoid dioxygenase 1	<i>P. bisulcatum</i>								
	<i>P. laetum</i>								
	<i>P. miliaceum</i>								
	<i>P. turgidum</i>								
Purple acid phosphatase	<i>P. bisulcatum</i>								
	<i>P. laetum</i>								
	<i>P. miliaceum</i>								
	<i>P. turgidum</i>								
Ribonuclease precursor	<i>P. bisulcatum</i>								
	<i>P. laetum</i>								
	<i>P. miliaceum</i>								
	<i>P. turgidum</i>								
Cysteine proteinase	<i>P. bisulcatum</i>								
	<i>P. laetum</i>								
	<i>P. miliaceum</i>								
	<i>P. turgidum</i>								

For the genes temperature induced lipocalin, 9-cis-epoxycarotenoid dioxygenase 1, ribonuclease precursor and cysteine proteinase no tags were found in the other species investigated (tags with a variation of 1 b were not regarded as equal). Only the tag annotated to the gene purple acid phosphatase was found in all four *Panicum* species by scanning the total amount of tags. Even though apparent in all four *Panicum* species, the regulation altered between the species (see coloured boxes, marking the expression pattern of the tag, Table 25).

4 Discussion

The reactions of *P. bisulcatum* (C₃), *P. laetum*, *P. miliaceum* and *P. turgidum* (all C₄ NAD-ME) to drought stress were examined. Analyses were carried out on a physiological as well as on a molecular level. Below, the results will be discussed first on a broader physiological scale up to the point of specific gene expression analyses on a precise molecular level.

4.1 Physiological analyses

Physiological analyses were carried out to obtain a general overview of the plants behaviour under control, drought stress and recovery conditions in reference to photosynthesis rate (P_N), stomatal conductance to water vapour (g_{H_2O}) and water use efficiency (WUE). Furthermore profound analyses on the photosynthetic apparatus under drought conditions were compiled (chlorophyll a measurements) showing a precise picture of the reaction of its compartments. Analyses were carried out on the bases of the leaf's relative water content to ensure an equally strong desiccation stress when comparing plant species.

4.1.1 Relative leaf water content

The investigation of the impact of drought stress on plants has been subject of research for over 80 years (KRAMER 1974). There are several approaches to induce drought stress starting with the detachment of leaves (LONGXING et al. 2010), the reduction of water availability in hydro-cultures by applying PEG (Polyethylene glycol, a polymer with water binding abilities, XU & HUANG 2010), the maintenance of a low soil water status by constantly low irrigation (ALFONSO & BRÜGGEMANN 2012) or the complete desiccation of soil and plant (VICRÉ et al. 2004) just to name a few. In this dissertation the plant's reactions to drought were investigated on the bases of the relative leaf water content (RWC) by withholding irrigation for a species-specific time span. Advantages of a soil imposed drought stress are the similarity to natural drought stress as water only slowly becomes a limiting factor (not suddenly as it is the case for PEG treatments or leaf detachment). The time for attaining a specific RWC was not predetermined (in contrast to investigations where drought stress was applied for a specific number of days only) resulting in a large time span for the different *Panicum* species until attaining a RWC of 50 % (5 days for *P. bisulcatum* up to 11 days for *P. turgidum*, see Table 3, Fig. 11). During drought stress the amount of water within the plant decreases. GHANNOUM (2009) distinguishes between an early phase of water stress where the RWC is still above 70 %

(stomatal phase) and a phase where the RWC falls below 70 % (metabolic phase). In these two phases samples were collected for analyses (Fig. 11). A comparison between species of extreme tolerance to drought (*P. turgidum*) and species less tolerant or very sensitive to drought (*P. miliaceum*, *P. laetum*, *P. bisulcatum*) having the same leaf RWC (and therefore the same leaf desiccation status) and photosynthetic subtype (except *P. bisulcatum*) can reveal important mechanisms responsible for a better adaptation to drought.

4.1.2 Photosynthesis rate, stomatal conductance and transpiration rate

Gas exchange measurements give information about the plant's photosynthetic performance under any condition – be it biotic or abiotic stress or seasonal variations just to name a few examples. Under optimal conditions, CO₂ enters the plants intercellular space through the stomata and is then fixed in the chloroplast to be converted to sugar. This process involves a complex machinery of enzymes and substrates starting with the allocation of reducing equivalents (NADPH+H⁺, ATP) by the light reaction to supply the energy consuming fixation of CO₂ by RubisCO – the dark reaction. Two different photosynthetic pathways exist, named according to the first metabolite synthesised by CO₂/HCO₃⁻ fixation – C₃ and C₄ photosynthesis. Whilst in plants using the C₃ photosynthetic pathway, CO₂ is directly fixed by RubisCO and converted to 3-phosphoglycerate (PGA) – a C₃ metabolite, CO₂ is prefixed by PEPC, forming a C₄ metabolite – malate – in plants using the C₄ photosynthetic pathway. The morphologically most important attribute of C₄ photosynthesis is the spatial separation of photosynthetic active cells in mesophyll (MC)- and bundle sheath cells (BSC) where HCO₃⁻ pre-fixation by PEPC (MC) and the final CO₂ fixation by RubisCO (BSC) take place separately. Due to the spatial separation of carbon dioxide pre- and final fixation in C₄ plants, a high CO₂ partial pressure around RubisCO is provided, suppressing its oxygenic function and therefore photorespiration.

The photosynthesis- or carbon assimilation rate mirrors the efficiency of final carbon dioxide fixation by RubisCO. This fixation is dependent on a multitude of factors, be it water availability and the relying transpiration rate and stomatal conductance, light, temperature or many more. Under optimal conditions (control conditions) the C₃ and C₄ *Panicum* species analysed in this dissertation confirmed the P_N values measured by PINTO et al. (2011) who showed P_N values of ~20 μmol m⁻²s⁻¹ for a C₃ grass and ~30 μmol m⁻²s⁻¹ for a C₄ grass. During moderate drought stress photosynthesis rates significantly declined in all three species (Fig. 12) due to a reduction of the CO₂ concentration in the chloroplast by a

rapid decline of stomatal conductance (Fig. 13, BRESTIC et al. 1995). RubisCO activity is not limiting net CO₂ uptake of leaves submitted to a moderate drought stress (HOLADAY et al. 1992) so that the reduction of chloroplastial CO₂ concentration by stomatal closure must be a major limiting factor of P_N . This has also been shown by CORNIC et al. (1989) for C₃ species and CORRÊA DE SOUZA et al. (2013) for C₄ species. The so called “stomatal phase” (GHANNOUM 2009) occurs when drought stress leads to a RWC not less than 70 % and CO₂ influx is limited by closed stomata. Under severe drought stress (RWC < 70 %) stomatal conductance declined even further but limited photosynthetic rates can also be a result of metabolic inhibition – the “metabolic phase” (GHANNOUM 2009) including declining RubisCO activity (BOTA et al. 2004). When re-watered, plants showed an increase in P_N to values comparable to moderate drought stress showing the regeneration capability of all three species (Fig. 12 A-C). The CO₂ exchange rate of *P. bisulcatum* under severe drought stress showed values slightly negative which accounted for the sum of mitochondrial- and photorespiration.

When comparing the species with each other, C₄ grasses showed significantly higher P_N than the C₃ species (Fig. 12 D). These results confirm the measurements undertaken by NIPPERT et al. (2007) where C₄ grasses had higher photosynthesis rates than C₃ species under control conditions. This is due to the fact, that the CO₂ concentration mechanism conducted in C₄ leaves allows RubisCO to operate at high partial CO₂ pressure ($p\text{CO}_2$), leading to the CO₂-saturation of P_N in normal air (GHANNOUM et al. 2011). Under moderate drought P_N was much stronger reduced in *P. bisulcatum* (C₃) than in its C₄ sister species (Fig. 12 D). Even though net CO₂ uptake was equally reduced by stomatal closure in C₃ and C₄ grasses submitted to a moderate desiccation, CO₂ concentration around RubisCO declined much faster in C₃ than in C₄ grasses due to the pre-fixation of HCO₃⁻ by PEPC resulting in a high $p\text{CO}_2$ around RubisCO even at low intracellular $p\text{CO}_2$ values. During severe drought stress and recovery, photosynthesis rates were still higher in the C₄ species as could also be shown by RIPLEY et al. (2010).

The stomatal conductance to water vapour ($g_{\text{H}_2\text{O}}$) is a parameter used to monitor the aperture of the stomata at a given time under environmental conditions. Under control conditions (high water availability) stomatal conductance in grasses analysed in this dissertation showed values of averaged 180 $\mu\text{mol m}^{-2}\text{s}^{-1}$ (Fig. 13) confirming the values measured by several groups (FAY et al. 2012, GHANNOUM et al. 2001). During drought stress, stomatal conductance decreased to counteract excess loss of water through transpiration. Stomatal closure is either initiated by abscisic acid – ABA – (SHINOZAKI &

YAMAGUCHI-SHINOZAKI 2007), a phytohormone with great importance in drought stress response or by direct evaporation of water from the guard cells (MAHAJAN & TUTEJA 2005). Former process is referred to as hydroactive closure as it involves ions and metabolites; latter is referred to as hydropassive closure without metabolic involvement. Even before a reduction in mesophyll turgor pressure due to water shortage, stomata close as a response to soil desiccation by an ABA mediated efflux of K^+ ions from the guard cells. The reduction of K^+ ions in the guard cells leads to a loss of turgor pressure inducing stomatal closure (MAHAJAN & TUTEJA, 2005). In all three species analysed in this dissertation stomatal closure was initiated by drought stress and g_{H_2O} was significantly reduced during moderate and severe drought stress (Fig. 13 A-C) and did not increase until rehydration as could also be shown by DE CARVALHO et al. (2011). When comparing the species amongst each other (Fig. 13 D) no significant differences in the measured values occurred, supporting data from the literature where KÖRNER et al. (1979) investigated the stomatal conductance of 246 plant species finding no differences between C_3 and C_4 grasses. Also BOLTON & BROWN (1980) found no differences in stomatal behaviour for *Panicum* species of C_3 and C_4 photosynthesis type. Even though relative reduction [%] of g_{H_2O} was significantly higher ($p < 0.05$) in *P. bisulcatum* (93 % during stress) – reflecting the sensitivity of the C_3 species to drought – compared to *P. laetum* (88 % during stress) and *P. miliaceum* (75 % during stress) – reflecting the better adaptation of C_4 grasses to drought – absolute values did not significantly differ during control and drought stress.

4.1.3 Leaf Water use efficiency

There are two different approaches to determine the relative water use efficiency of plants. One parameter assessed is the whole plant water use efficiency, calculated as the produced biomass per water used, describing crop productivity. It is usually used as a key indicator for plant fitness and distribution (LONG 1999). The second parameter is the leaf water use efficiency (WUE) which was applied in this dissertation. Leaf water use efficiency is determined by the aperture of the plant's stomata, the resultant transpiration rate and the final fixation of carbon dioxide by RubisCO (P_N/T , 2.2.3). An increase in WUE can hence be achieved when stomatal conductance and consequently the transpiration rate decrease and photosynthesis rates stay more or less constant or when photosynthesis rates increase with constant transpiration rates. The former is the case in C_4 species when applying moderate drought, the latter is responsible for the higher WUE of C_4 grasses compared to their C_3 sister species. Increased WUE of C_4 - compared to C_3 species is due to a higher P_N

per leaf area which is attained by the C_4 specific CO_2 concentration mechanism (GHANNOUM et al. 2011).

As mentioned above, C_4 plants have a competitive advantage over C_3 species when water is limited and stomata are closed due to the CO_2 concentration mechanism by PEPC resulting in a CO_2 saturated environment around RubisCO. In C_3 plants however, the decrease of stomatal conductance and transpiration rate directly results in a decline of chloroplastidial CO_2 concentration around RubisCO facilitating photorespiration. Therefore, photosynthesis rates decline faster during the initial phase of water stress (the stomatal phase, GHANNOUM 2009) when comparing C_3 and C_4 plants (see also Fig. 12 D). If photosynthesis rates are not (or only slightly) limited by a moderate drought stress but transpiration decreases, WUE increases. A significant increase in WUE due to moderate drought stress was only visible in *P. miliaceum* (Table 10) supporting data from the literature, where the same effect was observed for *Panicum* species of the NAD-ME photosynthesis subtype (GHANNOUM et al. 2002, ALFONSO & BRÜGGEMANN 2012). Nevertheless there could also be an increase in leaf WUE detected (even if not significant) in *P. laetum* under moderate drought stress (Table 10). During severe drought stress, WUE values decreased (ns) compared to control conditions for *P. laetum* and *P. miliaceum*. The C_3 species *P. bisulcatum* showed negative values (with $p < 0.001$, control vs. stress) due to a negative P_N value (Table 10, see also Fig. 12). Under control, drought stress and recovery conditions, results showed that WUE was generally higher in C_4 - than in C_3 plants due to their (above mentioned) CO_2 concentration mechanism around RubisCO in the bundle sheath cells (OSMOND et al. 1982) and the resultant higher P_N . This is also reflected by the values for *P. bisulcatum* (C_3), *P. laetum* and *P. miliaceum* (both C_4) where *P. bisulcatum* had a significantly lower WUE than *P. laetum* and *P. miliaceum* under control, as well as under drought stress and recovery conditions (Fig. 14). These results underline the findings by PINTO et al. (2011) and ALFONSO & BRÜGGEMANN (2012) where a significantly higher WUE of C_4 grasses compared to C_3 grasses under control and drought stress conditions was found.

4.1.4 Chlorophyll a fluorescence transients and JIP-test parameter

When light is exhibited on a photosynthetic sample, part of it is used for chemical work. Excess light energy is either dissipated as heat or chlorophyll a fluorescence, where the redox state of Q_A is the major determinant of the variable fluorescence yield (LAZAR & SCHANSKER 2009). It has been summarized by STRASSER et al. 2000 (and references therein) that, “at a given moment, the shape of the fluorescence transient of any sample is

determined by the physiological state of the sample at that moment and the physical and chemical environmental conditions around the sample. It must also be pointed out that the actual physiological state of a sample at a given moment is a function of all the states the sample went through in the past". Based on this, recorded Chl a transients were analysed starting with the normalization of the polyphasic Chl a transients.

When normalizing the polyphasic fluorescence transient to $F_{50\mu s}$ changes in the maximal fluorescence F_M can be made visible. The maximal fluorescence depicts the functionality of primary photochemistry in PS II, a reduction in yonder therefore represents the diminished functionality. STRASSER & STRASSER (1995) could show that F_M in DCMU (3-(3,4-dichlorophenyl)-1,1-dimethylurea) inhibited samples appeared at 2ms – the J step of Strasser's OJIP polyphasic fluorescence transient – reflecting the single turn-over of Q_A to Q_A^- . The species investigated in this dissertation exhibited "normal" OJIP polyphasic fluorescence transients under control conditions (Fig. 15) with the O, J, I and P steps clearly visible. Interestingly, the fluorescence intensity decreased with drought tolerance in *P. bisulcatum* exhibiting the highest F_M , and *P. turgidum* exhibiting the lowest relative maximal fluorescence value. Chl a transients recorded under severe drought stress did not as clearly show the OJIP steps as under control conditions due to changes in the photosynthetic apparatus (Fig. 15) which will in detail be discussed in the following. The recovery transients were still different from control transients, except for the transient of *P. turgidum* which was very similar to the control transient (Fig. 15 D).

To calculate differences between the transients concerning F_t values, curves were normalized to $F_{50\mu s}$ and F_M . No great differences in the transients could be revealed except for the recovery transient of *P. miliaceum* reflecting the inability to recover from severe drought stress within a short period of time (Fig. 16). Even though double normalization did not reveal major differences, selected JIP-test parameter still showed significant differences as discussed below (Table 11).

ΔV_{OJ} curves were generated according to the formula in Table 4 to depict the K peak. The K peak at around 300 μs gives information about the electron transport between the oxygen-evolving complex (OEC) and the first electron acceptor in PS II – tyrosinZ (TyrZ) and therefore the OEC's efficiency (JIANG et al. 2006). A clearly defined K peak can indicate the inhibition of the oxygen-evolving complex which has been shown for heat stress several times (GUISSE' et al. 1995, JIANG et al. 2006). Another reason for the appearance of a K peak can be the reduction of electron donation independent from the inhibition of the OEC. In this dissertation a clearly defined K peak was exhibited by

P. turgidum under severe drought stress, followed by *P. bisulcatum*, *P. laetum* and *P. miliaceum* showing K peaks three times smaller than *P. turgidum* (Fig. 17). It can be suggested, that also drought stress (besides heat stress) may have an effect on the electron transport through the OEC, accounting for the down-regulation of PS II function. An appearing K peak results from a steeper rise of the induction curve. The down-regulation of the oxygen-evolving complex and PS II seems to play a major role to drought stress adaptation in *P. turgidum* as the JIP-test parameters describing PS II functions are also strongest inhibited in this species (for discussion see below, Table 11). It seems, that the ability to strongly down-regulate photosynthesis is a major adaptation to drought in this desert species, especially when focussing on the strong up-regulation of photosynthetic functionality shortly after re-watering (Fig. 17, Fig. 18).

The JIP-test fluorescence parameter V_j reflects the relative variable fluorescence intensity at 2 ms normalized to $F_{50\mu s}$ and F_M . At the time point of 2 ms, the first event of Q_A reduction – the single turnover from Q_A to Q_A^- – has taken place. In *P. laetum* and *P. miliaceum* this parameter was only significantly increased during the recovery measurements, leading to the conclusion, that the single turn-over event was inhibited during the early hours of recovery.

The JIP-test fluorescence parameter φP_0 ($TR_0/ABS = 1 - (F_0/F_M) = F_V/F_M$) denotes the quantum yield of primary photochemistry and expresses the probability that an absorbed photon leads to the event of the first reduction of Q_A – the single turnover. φP_0 is used as an indicator for the maximum efficiency of PS II photochemistry (BAKER 1991, KRAUSE & WEIS 1991). BJÖRKMANN & DEMMING (1987) could show that F_V/F_M values in leaves of C_3 and C_4 plants under control conditions were remarkably uniform. Photoinhibition of PS II could then easily be detected by means of persistently reduced F_V/F_M values. In the 4 *Panicum* species analysed in this dissertation, φP_0 values were only slightly – but significantly – affected by drought stress. A reduction of 6 % during drought stress in *P. bisulcatum*, *P. laetum* and *P. turgidum* and of 4 % in *P. miliaceum* compared to control values reflects the inferior probability that an absorbed photon leads to the single reduction of Q_A (Table 11). Even though analysed plants differed in their drought tolerance as measured by the time to reach a RWC of 50 %, no inter-specific changes could be observed in the behaviour of the maximum yield of primary PS II photochemistry at a RWC of 50 %. The only minor reduction of φP_0 during drought in all four *Panicum* species confirmed the stability of the potential efficiency of PS II photochemistry. OUKARROUM et al. (2007) could also show a reduction of φP_0 under severe drought stress in barley, as well as VAN HERDEN et al. (2007)

and GOMES et al. (2012). After re-watering the maximum efficiency of PS II photochemistry only recovered in the most drought tolerant species *P. turgidum*, reflecting the plants ability to not only withstand severe water loss for a long period but also to recover from yonder within a very short period of time (2 h), (Table 11, Fig. 18). In *P. bisulcatum*, *P. laetum* and *P. miliaceum* φP_0 values still differed significantly from control values, reflecting the inferior ability to quickly recover from severe water loss regarding the quantum yield of primary PS II photochemistry. This effect could also be shown by OUKARROUM et al. (2007) where some of the investigated species exhibited φP_0 values close to control values after re-watering and some did not. It is possible that a membrane-related damage occurred, affecting thylakoid functionality (SOUZA et al. 2004) which is likely to happen upon rehydration (KAISER 1987). According to the results obtained in this dissertation, φP_0 could be used as an indicator of the plants ability to quickly recover from severe drought stress even though the parameter is generally considered as a very robust, unaffected parameter as it arithmetically only includes F_0 and F_M fluorescence values and no values from the Chl a transient (F_t).

ΔV_{IP} ($= 1 - V_I$) significantly decreased in *P. bisulcatum*, *P. laetum* and *P. miliaceum*, expressing the diminished amplitude of the I-P phase and therefore the diminished ability of electron transport beyond Q_A . Parameters also related to the electron transport beyond Q_A are φR_0 and δR_0 . φR_0 expresses the probability that an absorbed photon leads to a reduction of the PS I end acceptor. φR_0 ($= RE_0/ABS = 1 - F_t/F_M$) is therefore a parameter reflecting quantum efficiency changes in the multiple turnover phase of Q_A . The parameter δR_0 relates to PS I quantum efficiency by expressing the probability that an electron from the intersystem electron carriers is transported to the PS I end acceptor. δR_0 is thereby dependent on the variable fluorescence at 30 ms (F_t) and 2 ms (F_j), ($\delta R_0 = RE_0/RT_0 = (F_M - F_t)/(F_M - F_j)$). Like for ΔV_{IP} , these values were significantly decreased under drought stress in *P. bisulcatum*, *P. laetum* and *P. miliaceum* but not in *P. turgidum*. A reduction of ΔV_{IP} could also be shown by OUKARROUM et al. (2009) suggesting changes in PS I content. Accordingly, drought stress may lead to an inactivation of PS I as it acts as a source for ROS. Furthermore, SCHANSKER et al. (2005) demonstrated the dependency of the I-P phase on the electron flow through PS I and the electron flow on the acceptor site of PS I which were down-regulated under drought stress. JEDMOWSKI et al. (2012) could also show a significant decrease in δR_0 and φR_0 under drought stress due to an increase in V_I (for φR_0 , data not shown in this dissertation). The C_4 species *P. laetum* and *P. miliaceum* also had a significantly decreased efficiency of PS I end acceptor reduction by an absorbed photon

(φR_0) during recovery, in contrast to *P. bisulcatum*. Interestingly, the C_3 species could recover better from severe drought stress concerning PS I than its C_4 sister species *P. laetum* and *P. miliaceum*. From the results obtained in this dissertation, the JIP-test parameters ΔV_{IP} , φR_0 and δR_0 can also be used to screen for drought tolerance as the most drought tolerant species was not significantly affected (Table 11).

The JIP-test parameter $\varphi E_0 (= (F_v/F_m)(1-V_j) = ET_0/ABS)$ describes the quantum yield of electron transport and expresses the probability that an absorbed photon leads to an electron transport further than Q_A^- . It describes – so to say – the following step of electron transport in the electron transport chain of PS II after φP_0 . φE_0 was not changed in the C_3 species *P. bisulcatum*, leading to the conclusion, that the electron transport was not inhibited in this step. In the C_4 species *P. laetum* and *P. miliaceum*, the quantum yield of electron transport was only significantly reduced during recovery whereas in *P. turgidum* φE_0 was only significantly reduced during stress. This effect was mainly caused by the strong changes in V_j for *P. laetum* and *P. miliaceum* (Table 11) and φP_0 for *P. turgidum*. Surprisingly, the significant changes in φP_0 (F_v/F_m) did not have any influence on the JIP-test parameter φE_0 in *P. bisulcatum* (Table 11). It seems that in the most drought tolerant species *P. turgidum*, the photosynthetic apparatus was inhibited (or its activity was reduced) in all “stages” of electron transport (concerning PS II), while in the other species investigated this was not the case during stress. Nevertheless, the recovery ability of *P. turgidum* was greater than in its C_4 sister species which showed inhibition of φE_0 under recovery conditions (Table 11, Fig. 18). A decrease in φE_0 during drought stress could also be shown by CHRISTEN et al. (2007).

Another JIP-test parameter also describing quantum efficiencies or flux ratios is φD_0 . φD_0 ($1 - \varphi P_0$) expresses the probability than the energy of an absorbed photon is not used to accomplish chemical work but is dissipated as heat. During drought stress φD_0 was significantly increased in all four analysed *Panicum* species reflecting the efficiency reduction of the photosynthetic apparatus. Interestingly, only *P. turgidum*, the C_4 species having the strongest drought tolerance showed φD_0 values under recovery conditions similar to control values. All other *Panicum* species still showed significantly increased φD_0 values during recovery. This reflects the extremely good ability of *P. turgidum* to recover from severe drought stress as soon as water is available again and also showed the diminished capability of *P. bisulcatum*, *P. laetum* and *P. miliaceum* to quickly recover from severe drought stress (Table 11, Fig. 18). The increase of φD_0 during stress (and recovery) could also be shown for *Sorghum* and *Hordeum* by JEDMOWSKI et al. (2012), indicating that the absorbed

energy could not be used adequately in the electron transport chain. As the parameter is dependent on the values of φP_0 ($\varphi D_0 = 1 - \varphi P_0$) it is not surprising, that the plants show the same pattern of significant values (e.g. a significant differences between control and stress measurements only for *P. turgidum* in φD_0 and φP_0).

Another very important parameter is the relative number of active PS II reaction centres per excited cross-section RC/CS_0 ($= \varphi P_0(V_J/M_0)F_0$) as all parameters describing the specific fluxes per active PS II reaction centre arithmetically include RC/CS_0 (as described below). In all four species analysed in this dissertation, RC/CS_0 was significantly reduces under severe water stress, reflecting the down-regulation of PS II function as could already be shown by the appearance of a K peak, and the reduced parameters φP_0 and φE_0 . A decrease of active PS II reaction centres per excited cross-section under drought stress could also be shown by JEDMOWSKI et al. (2012) and VAN HEERDEN et al. (2007). IVANOV et al. (2006) could additionally show that the decline of active PS II reaction centre density contributes to PS II photoprotection under drought stress. Surprisingly, RC/CS_0 almost returned to control values in *P. miliaceum* and *P. turgidum* 2 h after re-watering, which indicates, that especially in *P. miliaceum* the reduced number of PS II reaction centres did not account for the bad appearance of the Chl a transient under recovery conditions. As already discussed for the parameters above, *P. turgidum* exhibits great recovery abilities also when it comes to up-regulation of RC/CS_0 after re-watering.

Concerning the specific fluxes per active PS II reaction centre (x/RC), significant changes could be shown for each parameter (Table 11). The absorption flux ABS/RC ($= M_0(1/V_J)(1/\varphi P_0)$) expresses the effective antenna size of an active PS II reaction centre. The significant increase in all four *Panicum* species under severe drought stress can be ascribed to the reduced relative number of active PS II reaction centres per excited cross section (RC/CS_0) which has been discussed above. Another effect which leads to an increase of ABS/RC could be the regrouping of antenna from inactive to active PS II reaction centres (STRASSER et al. 1995, VAN HEERDEN et al. 2003). Under recovery conditions however, *P. miliaceum* still showed increased ABS/RC values contrary to RC/CS_0 values and *P. bisulcatum* vice versa whereas *P. turgidum* did not show any significant changes at all. Again this accounts for the good adaptation of *P. turgidum* to drought and also the good ability of *P. bisulcatum* to recover from drought stress (Table 11, Fig. 18). An increase in the ABS/RC value under drought stress could also be shown by JEDMOWSKI et al. (2012), GOMES et al. (2012) and GUHA et al. (2013) supporting the data collected in this dissertation.

The values TR_0/RC , ET_0/RC and DI_0/RC were increased during drought stress in all four species just like ABS/RC . $TR_0/RC (= M_0(1/V_j))$ expresses the trapped energy flux leading to a reduction of Q_A , $ET_0/RC (= M_0(1/V_j)(1-V_j))$ expresses the electron transport flux further than Q_A and $DI_0/RC (= ABS/RC-TR_0/RC)$ expresses the dissipation flux, are all greater under drought due to reduced active PS II reaction centres. GUHA et al. (2013) could show an increase of TR_0/RC under drought conditions supporting the data collected. Like the dissipation probability (φD_0), the dissipation flux (DI_0/RC) was greatly enhanced under drought as well as under recovery conditions (except for *P. turgidum*) expressing the release of excess light energy which could not be used for chemical work as could also be shown by GUHA et al. (2013). For all the specific fluxes per active PS II reaction centre, *P. turgidum* showed the highest relative values during drought but no significant changes during recovery, leading to the conclusion that the drought tolerance of this species is caused by a strong down-regulation of the photosynthetic apparatus under drought stress (reduced active PS II reaction centres), but a similarly strong up-regulation of yonder under recovery conditions (Table 11, Fig. 18 D).

$PI_{tot} = [(RC/ABS) [(F_V/F_M)/1-(F_V/F_M)] [(1-V_j)/(1-(1-V_j))]] (\delta R_0/(1-\delta R_0))$ expresses the efficiency of energy conservation from absorbed photons to the reduction of the PS I end acceptor. It is significantly reduced during drought in all four *Panicum* species and only completely recovers in *P. bisulcatum* and *P. turgidum* (Table 11, Fig. 18) suggesting that drought stress did not irreversibly damage the photosynthetic apparatus. Similar results generated by VAN HEERDEN et al. (2007) indicated that PS II function was not damaged by drought but was instead down-regulated to provide a balance between the activity of the electron transport chain and the Calvin cycle. The performance index is used as a tool to screen for overall plant performance under different conditions (ZIVCAK et al. 2008, STRASSER et al. 2010). Due to limitations concerning PS II (decreased φP_0 , φE_0) and PS I (decreased δR_0 , φR_0) the total performance index was reduced during drought. This effect was also observed by JEDMOWSKI et al. (2012) and OUKARROUM et al. (2009) proposed that the inactivation of PS I under drought occurred due to PS I acting as an alternative source for oxygen radicals resulting in declined PI_{tot} values. The results generated in this dissertation support the parameter PI_{tot} as a tool for screening drought tolerance in regard to recovery abilities.

It can be concluded, that *P. turgidum* shows the strongest ability to withstand severe damage of the photosynthetic apparatus under drought stress by a strong down-regulation of PS II

(ΔV_{OJ} , φP_0 , φE_0) but no significant changes in PS I (ΔV_{IP} , φR_0 , δR_0). Its fast recovery ability (no significant differences in control vs. recovery analyses) in its natural environment, where drought periods are common (1.3.4), is highly useful as scarce water can be directly used to perform photosynthesis and growth for rapid seed production.

Surprisingly, *P. turgidum* is followed by *P. bisulcatum* when it comes to photosynthetic adaptation to drought stress. This is interesting, as *P. bisulcatum* is a C₃ plant and not very well adapted to drought (1.3.1) as could also be shown by the physiological analyses (Fig. 12 A - Fig. 14 A). The photosynthetic apparatus however showed a better adaptation to drought as well as during recovery than the apparatus of its C₄ sister species *P. laetum* and *P. miliaceum* (e.g. for the parameters φR_0 , φE_0 , ΔV_{IP} , V_J , ABS/RC , TR_0/RC and PI_{tot}). It has been suggested by GHANNOUM (2009) that the C₃ photosynthetic apparatus is less prone to drought stress than the C₄ photosynthetic apparatus as “there is a limited capacity for photorespiration or the Mehler reaction to act as significant alternative electron sinks under water stress in C₄ photosynthesis. This may explain why C₄ photosynthesis is equally or even more sensitive to water stress than its C₃ counterpart in spite of the greater capacity and water use efficiency of the C₄ photosynthetic pathway” (GHANNOUM 2009). The resistance to desiccation and the capacity for osmotic adjustment differ in hygro-, meso- and xerophytes of C₃ photosynthesis type but the sensitivity of photosynthetic mechanisms to water loss is similar in all three types of plants (CORNIC & MASSACCI 1996). Interestingly this is not the case for C₄ plants showing a strong interconnection to precipitation amounts in regard to the different subtypes. In this dissertation it could be shown, that even within the same subtype of C₄ photosynthesis (NAD-ME) there can appear great differences in drought tolerance. Especially the photosynthetic apparatus of *P. miliaceum* does not seem to quickly recover after re-watering as fluorescence transients and OJIP parameters exhibit worse values under recovery conditions even though *P. miliaceum* showed best recovery rates concerning the photosynthesis rate (Fig. 12). It seems that gas exchange measurements cannot be directly interconnected with single fluorescence values. The correlation of the net photosynthesis rate P_N with the performance index PI_{tot} revealed different behaviours concerning C₃ and C₄ *Panicum* species (Fig. 19). While the reaction to drought stress was similar in all three species (*P. bisulcatum*, *P. laetum* and *P. miliaceum*) - with a stronger reduction in the P_N then in the PI_{tot} values - the reactions during the recovery period were different. During recovery, the C₄ species *P. laetum* and *P. miliaceum* showed similar relative recovery values concerning PI_{tot} and P_N values where for *P. bisulcatum* the P_N recovery value was over 60 % lower than the PI_{tot} value. It seems that the photosynthetic

inhibition two hours after re-irrigation is still stronger in the C_4 species, on the contrary, the recovery of the carbon assimilation rate is much stronger inhibited in the C_3 species even though, Chl a fluorescence values (PI_{tot}) almost recovered to control values. The balance between the generation of reduction equivalents and their uptake is therefore better in the C_4 species. It seems that limitations in enzyme activity could play a greater part in photosynthetic inhibition than down-regulation of the photosynthetic apparatus.

Nevertheless, these investigations suggest that the OJIP measurements can be a valuable, non-invasive tool to screen for the different reactions to drought stress in species of the same subtype.

4.2 Molecular analyses

Molecular analyses were carried out to obtain a picture of the plants behaviour under control, drought stress and recovery conditions on a protein and gene expression (transcriptional) level. The results generated by the transcriptomic approach (HT-SuperSAGE) were verified by qPCR analyses supporting elected gene regulation pattern. Analyses were carried out on the bases of the leaf's relative water content to ensure an equally strong desiccation stress when comparing plant species.

4.2.1 Analyses of the content of selected proteins

The protein content of RubisCO (LSU and SSU), PEPC, OEC and Dehydrin 1 was investigated to illustrate potential differences under control, severe drought stress and recovery conditions.

The protein RubisCO is a hetero-16-mer consisting of 8 large subunits and 8 small subunits. It is a major photosynthetic enzyme and catalyses the carboxylation of ribulose-1,5-bisphosphate (RuBP) to 3-phosphoglycerate. In all species investigated in this dissertation RubisCO (LSU and SSU) content did not significantly differ between control, stress and recovery samples (Fig. 21). It has been shown before (ALFONSO & BRÜGGEMANN 2012 for *P. miliaceum*) that the protein content of the subunits is very robust to water stress application. Even though, gas exchange measurements reveal a significant decrease in photosynthetic activity under severe drought stress, it is not the protein content of the CO_2 fixing enzyme RubisCO responsible for the decline. An explanation would be the enzyme's activity, which has been shown to decline during drought stress several times (ALFONSO & BRÜGGEMANN 2012, LAWLOR & TEZARA 2009, HU et al. 2010 a). An

inhibition in the enzyme's activity would account for the diminished photosynthesis rate in all four species (Fig. 12). Furthermore it has been suggested that a decreased capacity for RuBP regeneration resulting from diminished ATP synthesis or impaired Calvin cycle activity could contribute to metabolic limitations under severe drought stress (LAWLOR 2002). The inactivation of RubisCO activase and therefore the inhibition of RubisCO itself could also contribute to the diminished P_N rates. Due to the increasing values of net photosynthesis rate under recovery conditions (Fig. 12) the irreversible inhibition of RubisCO through oxidation by reactive oxygen species (ROS) was regarded as a minor inhibitory factor.

The PEP-Carboxylase is only present in C_4 species and responsible for the pre-fixation of HCO_3^- in the mesophyll cells. The homotetramere's protein content was not significantly decreased during drought stress and recovery in all three C_4 *Panicum* species investigated in this dissertation (Fig. 21). It has been shown by ALFONSO & BRÜGGEMANN (2012), that PEPC content stayed unchanged in *P. miliaceum* during drought stress supporting the results in this dissertation. CARMO-SILVA et al. (2008) could show that PEPC activity was increased in NAD-ME species under drought stress due to an increased phosphorylation state of PEPC. They suggested that an increased activity may be a strategy to retain high CO_2 levels in the mesophyll cells to antagonise decreasing CO_2 contents due to closed stomata supporting the results obtained in this dissertation (Fig. 13). In contrast, ALFONSO & BRÜGGEMANN (2012) considered a PEPC feedback inhibition by increased mesophyll cell aspartate concentrations and a resultant decline in photosynthetic rates. Further investigations have to be performed to clarify the role of PEPC in photosynthetic inhibition.

The oxygen-evolving complex feeds electrons into PS II to fill the electron gap produced by photochemical reactions. For that matter water is split into oxygen and protons ($2H_2O \rightarrow O_2 + 4H^+ + 4e^-$) which are then subsequently released to TyrZ in PS II. In this dissertation the protein content of the OEC was not significantly affected in all four *Panicum* species under drought and recovery conditions (Fig. 21) even though a clearly defined K peak appeared in the chlorophyll fluorescence studies suggesting the diminished efficiency of the oxygen-evolving complex (Fig. 17). PAWŁOWICZ et al. (2012) could show a decrease in OEC activity by destabilization which would explain the decreased activity and the resultant K peak at constant protein contents.

Dehydrin 1 is a protein only expressed under drought stress as could be shown by western analyses in this dissertation (Fig. 21). Dehydrins (or group 2 LEA proteins, 4.2.2.4) have a

protective function by stabilizing proteins and macromolecular complexes like membranes under drought stress (CLOSE 1996). They show a conserved consensus sequence (DEYGNP) close to the N-terminus of the protein and usually have a lysine-rich sequence called the K-segment (EKKGIMDIKEKLGP) near the carboxy terminus (INGRAM & BARTELS 1996). Their up-regulation reflects the drought stress plants were exposed to and also shows that even though the RWC returned to control values 2 h after irrigation (Fig. 11) protein and membrane stabilization is still important as the recovery status on a molecular level has not returned to control conditions.

In summary it could be shown that the proteins RubisCO (LSU and SSU), PEPC and OEC were not reduced under neither drought stress nor recovery conditions reflecting the robustness of these proteins. Nevertheless it was suggested that they could play crucial roles in non-stomatal photosynthetic inhibition due to reduced activity.

4.2.2 Transcriptomics

Transcriptomics, or gene expression analyses, are based on the investigation of mRNA levels in a given sample. Changes in the constellation of these mRNA levels can appear when biotic or abiotic conditions alter and conditions deviate from optimum to stress. In this dissertation, the influence of drought stress on four different *Panicum* species (1.3) was investigated by transcriptomic approaches to identify differences in gene expression levels under severe drought stress and recovery in comparison to control conditions (2.1.4). The up- and down-regulation of transcripts helps the plant to maintain essential conditions to survive the impact of stress and revert to initial conditions once the stress is overcome. The identification of up-regulated and therefore putatively protective genes is of high interest to understand how and why certain plants can adapt to drought stress better than others.

In the following part the methods used for gene expression profiling, the results generated and the molecular mechanisms functioning under drought stress will be discussed.

4.2.2.1. Gene expression profiling by HT-SuperSAGE

High throughput serial analyses of gene expression (HT-SuperSAGE) was developed by MATSUMURA et al. (2010) on the bases of SuperSAGE (MATSUMURA et al. 2003), LongSAGE (SAHA et al. 2002) and SAGE (VELCULESCU et al. 1995) and allows genome-wide quantitative transcript profiling. In contrast to analogue microarray technologies, the method uses the next generation sequencing (NGS) platforms (in this case the Illumina

platform) to monitor gene expression by sequencing-based analyses. In contrast to former methods, HT-SuperSAGE produces a tag-based gene expression profile with tag fragments of a length of 26-27 bp, long enough to unambiguously annotate the tags to their specific genes (MATSUMURA et al. 2010). By using different index sequences (Fig. 6, step 9), the multiplexing of samples (libraries) in a single sequence run (Illumina Genome Analyzer) also minimizes costs and maximises the sample throughput per run which can be more than 100 libraries in a single run (MATSUMURA et al. 2010). *In silico* analyses (scripts written in Perl) reliably separated the 12 libraries generated in this dissertation (Table 13) according to their 4-6 bp long unique index sequences (Table 8). To exclude single-base errors in the index sequences and therefore a contamination of the libraries, MATSUMURA et al. (2010) applied the 5000 most abundant tags to a BLAST search with the outcome of less than 0.2 % contamination by single-base errors in the index sequence. They could furthermore show, that using the restriction enzyme *NlaIII*, only 7-8 % of the transcripts were missing in the total amount of tags generated, in contrast to ~20 % missing tags when using the restriction enzyme *BfaI*. HT-SuperSAGE was mostly applied on organisms with known genomes so that tag-to-gene annotation was high. As this premise was not the case for the *Panicum* species studied in this dissertation, the EST database of *P. virgatum* was used to annotate the tags. Gene expression profile studies have been carried out in non-model organisms without a fully sequenced genome or EST database before (*Nicotiana benthamiana*, see MATSUMURA et al. 2003). As tag-to-gene annotation was difficult, the 3' RACE method was deducted to generate longer sequences downstream of the generated tags equally to the approach in this dissertation.

Nowadays transcriptomic approaches usually use the “whole transcriptome shotgun sequencing” (short RNA-Seq) method as it does not necessarily need a reference genome for the annotation of sequenced tags and is therefore an adequate alternative when investigating non-model organisms without fully sequenced genomes.

The HT-SuperSAGE outcome (Table 13) exhibited a total number of sequenced tags just over three million for the 12 libraries. Included in these three million tags were also tags with partial index sequences or tags longer than 27 bp or further “mistakes”. To identify the tags with a complete and correct index sequence and a length of maximum 27 bp, data were run *in silico* with scripts written in Perl. Those tags were then called “unique” tags in the sense of tags correctly sequenced to the expectations. These tags inherited all tags with an abundance of ≥ 1 tag. In total 524,282 of these unique tags were generated for the 12 libraries – 17 % of the number of total tags. In addition, the number of “non-singleton”

tags (tags existing more than once) was also calculated to furthermore exclude sequencing errors in singlet tags. KIDO et al. (2012) established in their work the $n < 2$ frequency as cut-off threshold for “non-singleton” tags which was also applied in this dissertation. The number of “non-singleton” tags was 188,228 tags for all 12 libraries - 6.1 % from the total number of sequenced tags. For further analysis, those tags present in the “unique” tags libraries were used as comparative analysis on the base of fold change (≥ 2) were carried out also excluding sequencing errors.

When separating the libraries according to the species, *P. bisulcatum* with just over 1,2 million unique tags (control, stress and recovery) showed the highest number of tags, followed by *P. laetum* with just over 770 thousand tags and *P. turgidum* with almost 690 thousand tags. For *P. miliaceum* only just over 365 thousand were found (Table 13). The most representative library considering the number of tags was found for *P. bisulcatum* (stress) with 95975 “unique” tags. The least representative library was found for *P. miliaceum* (control) with 13770 tags only. To estimate the coverage of the transcriptome by the tags, the total number of tags per genotype was considered in relation to the number of expected transcripts per cell (KIDO et al. 2012). Numbers of transcripts can range from 100,000 (KIPER et al. 1979) to 500,000 (KAMALAY & GOLDBERG 1980) per plant cell. Except for *P. miliaceum* with fewer than 100,000 tags, all investigated *Panicum* species range between 100,000 – 500,000 tags and showed the diversity of possibly expressed genes.

The molecular mechanisms underlying the differential gene expression under drought stress as well as recovery conditions play an important part in response and tolerance to environmental stresses such as dehydration. As genes from diverse pathways like signal perception and first reactions to drought (mostly transcription factors) to “classical” drought induced genes are expressed under drought stress, their roles will be discussed below.

4.2.2.2. ABA-dependent and ABA-independent gene expression

Stress response and tolerance are inalienable for plants to survive drought - and other environmental stresses. Drought stress induces the expression of a variety of genes whose products do not only function in stress tolerance by producing metabolic proteins but also in stress response by regulating gene expression and signal transduction (YAMAGUCHI-SHINOZAKI & SHINOZAKI 2006 and references therein). This is also monitored by the high up-regulation of tags under stress conditions in the *Panicum* species investigated (Fig. 23 C, Fig. 24) where just over 6000 (*P. miliaceum*) to 18000 (*P. laetum*) tags were found to be ≥ 2 -

fold up-regulated under drought stress conditions. The expression of genes is regulated by a precise signal transduction network that transfers the information from the perception of stress signals to stress-responsive gene expression (YAMAGUCHI-SHINOZAKI & SHINOZAKI 2006). Two groups of proteins have been elucidated regulating signal transduction and gene expression in response to drought stress. The first group includes chaperones, late embryogenesis abundant (LEA) proteins, mRNA-binding proteins, key enzymes for osmolyte biosynthesis such as proline, water channel proteins, sugar and proline transporters, detoxification enzymes, enzymes for fatty acid metabolism, proteinase inhibitors and lipid-transfer proteins (YAMAGUCHI-SHINOZAKI & SHINOZAKI 2006). The second group includes transcription factors, protein kinases, protein phosphatases and enzymes involved in phospholipid metabolism and abscisic acid (ABA) biosynthesis, just to name a few. ABA is a very important plant hormone produced under drought stress, regulating the closure of stomata in guard cells and gene-expression (HIMMELBACH et al. 2003). Two signal transduction cascades have been elucidated, an ABA-independent as well as an ABA-dependent cascade transferring the initial stress signal to affect gene expression. In this process, various transcription factors and *cis*-acting elements in the stress-responsive promoters function for plant adaptation to drought stress (YAMAGUCHI-SHINOZAKI & SHINOZAKI 2006).

To study the molecular mechanisms of gene expression under drought stress, the major *cis*- and *trans*-acting elements in the stress-inducible promoters as well as transcription factors are mostly investigated (SHINOZAKI et al. 2003, YAMAGUCHI-SHINOZAKI & SHINOZAKI 2005). As the stress-responsive mechanism is found to be up-regulated in a great variety of species including dicots and monocots (CHOI et al. 2002, GAO et al. 2002, DUBOUZET et al. 2003), it is assumed that also in the *Panicum* species these genes were up-regulated and HT-SuperSAGE tags could in future be annotated (when complete genomes of the species are available). Therefore their function will be discussed in detail below.

As mentioned above, an ABA-dependent and an ABA-independent signal transduction pathway exist. In the ABA-independent pathway, the promoter regions of many drought-inducible genes inherit a conserved 9 bp long sequence called the drought-responsive element (DRE) - TACCGACAT, an essential *cis*-element (SHINOZAKI & YAMAGUCHI-SHINOZAKI 2000). A similar *cis*-acting element is the C-repeat (CRT) induced by cold-stress (BAKER et al. 1994). The DRE/CRT element is essential for the DRE binding proteins 1 and 2 (DREB1/C-repeat binding factor CBF, DREB2) which bind to the sequence and induce gene transcription. Eight DREB2-type proteins could be identified until now, but

only the expression of the *DREB2* genes encoding for DREB2A and DREB2B is initiated by drought stress (SAKUMA et al. 2002, QIN et al. 2004). As the DREB1/CBF transcription factors induced by cold stress also bind to the DRE/CRT *cis*-acting element, genes involved in drought stress tolerance are also transcribed (cross-talk between cold- and drought stress regulatory networks, Fig. 38).

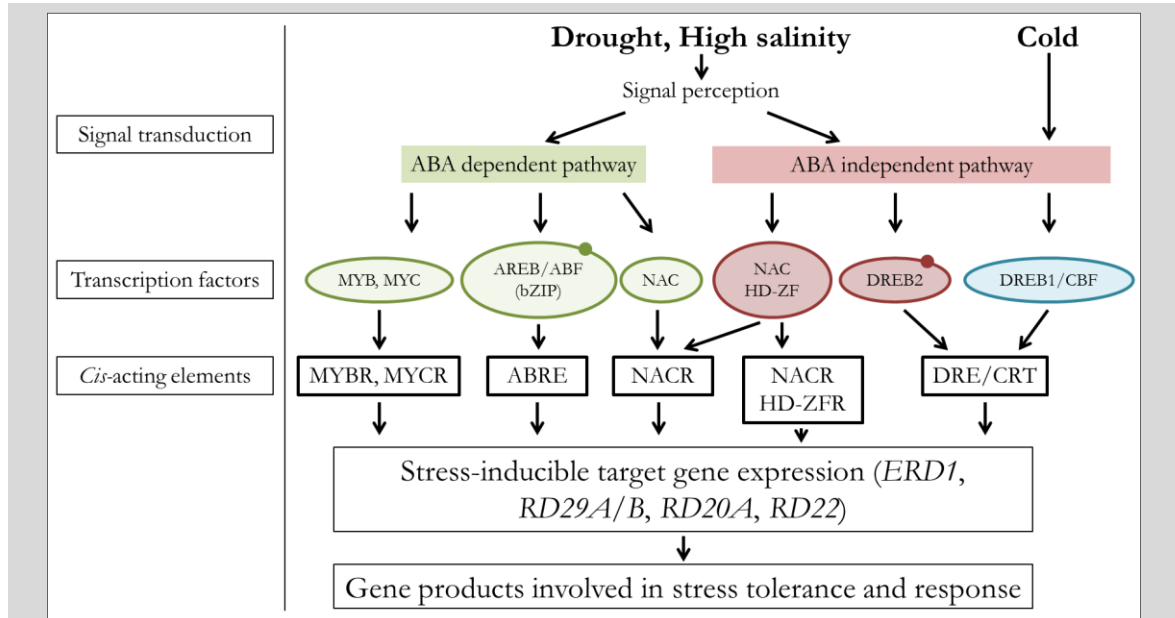


Fig. 38: Transcriptional regulatory networks of abiotic stress signals and gene expression (according to YAMAGUCHI-SHINOZAKI & SHINOZAKI 2006). Three ABA dependent and three ABA independent pathways are known. Transcription factors are shown in coloured ellipses, filled circles mark posttranscriptional modifications (AREB/ABF and DREB2). The *cis*-acting elements are black-rimmed (fat line).

Over 40 genes downstream of DREB1/CBF have been identified encoding for RNA-binding proteins, sugar transport proteins, desaturases, carbohydrate metabolism-related proteins, LEA proteins, osmoprotectant biosynthesis proteins and proteases (YAMAGUCHI-SHINOZAKI & SHINOZAKI 2006 and references therein). These results suggest that the overexpression of the DREB/DRE regulon can improve drought stress tolerance in crops. There are further *cis*-acting elements and transcription factors up- and downstream of the DREB/DRE regulon which will not be discussed in detail. For further information see YAMAGUCHI-SHINOZAKI & SHINOZAKI (2006).

Other transcription factors found to be expressed under drought stress independent from ABA belong to the family of NAC and homeo domain-zink finger (HD-ZF) transcription factors (TRAN et al. 2004). Over 100 *NAC* genes have been identified up to date (NAKASHIMA et al. 2012) and the over-expression of stress-responsive *NAC* (SNAC) genes has led to improved drought tolerance in the transgenic plants (NAKASHIMA et al. 2012).

The ABA responsive pathway also leads to major gene expression under drought stress. Many of the ABA-inducible genes inherit a conserved, ABA-responsive, major *cis*-acting element, the ABA-responsive element called ABRE (PyACGTGGC), in their promoter regions (Fig. 38). However, this element in the promoter region alone is not sufficient for stress-induced gene expression but additional copies of the ABRE or coupling elements are necessary for ABA-responsive gene expression (YAMAGUCHI-SHINOZAKI & SHINOZAKI 2006). The ABRE elements are recognized by a group of bZIP transcription factors, the ABRE-binding proteins (AREB) or ABRE-binding factors (ABFs, CHOI et al. 2000) and some of them function as *trans*-acting activators up-regulated by ABA and dehydration like AREB1/ABF2, AREB2/ABF4 and ABF3 (UNO et al. 2000). In *Arabidopsis*, 75 bZIP transcription factors were found, 13 of them belonging to the AREB/ABF subfamily (JAKOBY et al. 2002). Their posttranscriptional modification by protein kinases (SnRK2) and phosphatases (their function will be discussed later, 4.2.2.4) through phosphorylation or dephosphorylation is a very important factor in ABA-mediated gene expression (FURIHATA et al. 2006, NAKASHIMA & YAMAGUCHI-SHINOZAKI 2013).

A different group of ABA-responsive transcription factors are the MYC and MYB transcription factors binding to the MYCR and MYBR *cis*-acting elements of stress-inducible target genes. The accumulation of endogenous ABA leads to the production of MYC and MYB transcription factors indicating, that they play a role in the later stages of drought stress response (ABE et al. 2003). The possibility to find a high number of these transcription factors in the investigated *Panicum* species is therefore high as leaf samples were collected after a long exposure to drought. For a detailed review and image of ABA dependent signal transduction see LINDEMOSE et al. (2013).

As a great number of genes is transcribed through ABA-mediated signal transduction, the synthesis of ABA also plays an important role in the plant's stress response. ABA is synthesized *de novo* upon dehydration, a major gene in this process is *NCED3*, encoding for the 9-cis-epoxycarotenoid dioxygenase 3 (NCED3) which is the rate-limiting enzyme in ABA synthesis. Overexpression of *NCED3* in transgenic plants revealed a strong resistance to drought, whereas knockout mutants were very susceptible to drought (TUCHI et al. 2001). Upon rehydration, a great number of metabolites and proteins are catabolized to an inactive form, among them ABA. The differential gene expression during rehydration therefore is great, also indicated by the high number of genes differentially regulated in the *Panicum* species under recovery (Fig. 23 B and C, Fig. 24). More than 14,000 tags (*P. miliaceum*) up to almost 26,000 tags (*P. bisulcatum*) were differentially regulated under

recovery- compared to stress conditions. Many of these rehydration-inducible genes function in the recovery process from drought stress and their promoters contain a *cis*-acting element (the ACTCAT' motive, OH et al. 2005) where special bZIP transcription factors bind to (SATOY et al. 2004).

In the first hours of drought stress induction a different group of genes is up-regulated in comparison to gene expression responses under longer lasting drought application. These slowly expressed genes usually encode for LEA proteins, detoxification enzymes and osmoprotectants. The timing is thereby regulated by the combination of transcription factors and the *cis*-acting elements in the promoter regions of stress-inducible genes (YAMAGUCHI-SHINOZAKI &SHINOZAKI 2006) with the ABA-dependent transcription factors playing a major role in the late response to drought stress. Also these transcription factors and mRNAs encoding the diverse proteins could be among the differentially regulated *Panicum* tags.

It has been shown that besides the positive regulation of gene expression under dehydration, also the negative regulation of genes plays a very important role. RNA interference as well as mRNA degradation seem to play crucial roles in stress responsive gene expression (JONES-ROHADES & BARTELS 2004, SUNKAR & ZHU 2004). When looking at the differential gene expression profiles of the four *Panicum* species their reaction to drought stress significantly differ when it comes to positive (up-regulation) or negative (down-regulation) gene regulation (Fig. 23 C, Fig. 24). Where in the more drought susceptible species *P. bisulcatum*, *P. laetum* and *P. miliaceum* the up-regulation of genes played a greater part during drought stress, the down-regulation of gene expression was greater in the drought tolerant species *P. turgidum*. Under recovery conditions however, the up-regulation of genes (compared to the number of genes down-regulated under recovery conditions) was greater in the species *P. bisulcatum*, *P. miliaceum* and *P. turgidum* but not in *P. laetum* where more tags were down- than up-regulated (Fig. 23 C). When looking at the detailed profile of differential gene expression in the *Panicum* species (Fig. 24) it is clearly visible, that the up-regulation under drought stress and the subsequent down-regulation of tags (C<S>R) is more important in the drought susceptible species *P. bisulcatum* and *P. laetum*. The contrary gene regulation (C>S<R) is however most important in the drought tolerant species *P. turgidum*. These results suggest the different adaptation mechanisms of plants where the drought sensitive species up-regulate “protective” genes and the drought tolerant species shuts down a great amount of processes. This result support the results

generated by chl a fluorescence measurements, where *P. turgidum* down-regulated parts of PS II under drought stress and up-regulated these under recovery conditions.

Nevertheless it should be taken into account, that in the sum of tags (across the four species) the up-regulation of tags under stress and the subsequent down-regulation (C<S>R) excels the number of tags down-regulated under stress and up-regulated under recovery (Table 14). Additionally, the number of tags only up-regulated under recovery conditions is also high in the sum of tags suggesting the importance of genes being only expressed to regenerate the original conditions (Table 14).

4.2.2.3. The MAPKinase pathways

One of the major mechanisms to control cellular functions in plants under stress conditions is the phosphorylation of proteins. Special protein kinase cascades, the so called mitogen-activated protein kinase (MAPK) cascades, function as signalling modules in plant cells. Three of those protein kinases are functionally linked starting with the MAPK kinase kinase (MAPKKK) which phosphorylates a MAPK kinase (MAPKK) which itself phosphorylates a MAPK. The MAPKKK activates the MAPKK by phosphorylation of a single conserved threonine and/or serine residue in the amino acid sequence. The MAPKK however activates the MAPK by phosphorylation of two conserved amino acids, a threonine and a tyrosine residue in the TEY activation loop (Thr, Glu, Tyr). Once the MAPK is phosphorylated it is mostly translocated into the nucleus where it can in turn phosphorylate transcription factors needed for gene expression (as described above, TRIESMANN 1996). MAPK cascades consequently play an important role in the transduction of stress signals from the membrane to the nucleus, other enzymes or cytoskeleton components in the cytoplasm. In this context MAPK cascades can also interact with upstream kinases or G proteins. G proteins (guanosine nucleotide-binding proteins, GTP-binding proteins) belong to a protein family involved in transmitting external signals into the cell. They directly bind to receptors in the plasma membrane and transmit signals by functioning as molecular switches (“on” when binding GTP, “off” when binding GDP). KYRIAKIS & AVRUCH (2001) could show that these G proteins regulate MAPKKKs. In *Arabidopsis* at least 20 MAPK, 10 MAPKK and 60 MAPKKK genes have been identified (ICHIMURA et al. 2002) controlling gene expression; more than 100 genes have been identified to be regulated by MAPK cascades and it is assumed that also in the *Panicum* species these genes (and most certainly also the HT-SuperSAGE tags) can be found. Another family of protein kinases are the SNF1/AMP activated protein

kinases which sense the ATP/AMP ratio in the cell (BARTELS & SUNKAR 2005) and control gene-expression in carbohydrate metabolism. They are regulated by dehydration and ABA and it is possible that they were also differentially regulated in the *Panicum* species under stress conditions as some of them are also activated by osmotic stress and ABA in rice (KOBAYASHI et al. 2004).

4.2.2.4. Calcium signals and protective proteins

Ca²⁺ ions function as second messenger in the calcium signalling pathways responding to different environmental stresses. They interconnect external stimuli to intracellular responses (BARTELS & SUNKAR 2005). Three different Ca²⁺ sensor classes have been identified – calmodulin, calcium-dependent protein kinases (CDPKs) and calcineurin B-like proteins (CBLs) involved in drought- (and salt) stress response (YANG & POOVAJAH 2003, KONOPKA-POSTUPOLSKA et al. 2009). Ca²⁺ sensors and the ca²⁺ signals induce gene expression of a great variety of genes (SEKI et al. 2002) and it is possible that also genes differentially regulated in the *Panicum* species were controlled by calcium signals. SAIJO et al. (2001) could show that a CDPK from rice – OsCDPK7 – is a positive regulator when it comes to tolerance against drought and other abiotic stresses and knockout mutants of a CBL – ScaBP5/CBL1 – showed hypersensitivity to drought (ALBRECHT et al. 2003).

The family of protective proteins plays a major part when it comes to adaptation against drought stress. An important group of protective proteins are the late embryogenesis-abundant (LEA) proteins which accumulate under drought stress in the vegetative tissue. Usually *LEA* genes are expressed in the maturing embryo and account for a great amount of mRNA and protein content in yonder (GALAU et al. 1986). They support the cell to withstand severe water loss (INGRAM & BARTELS 1996). In the vegetative tissue, *LEA* genes are expressed by ABA which is a major signal during drought stress (4.2.2.2) and it is likely that *LEA* genes were also expressed in the studied *Panicum* species. It is the case for *P. laetum*, were a HT-SuperSAGE tag could be annotated to a gene encoding a LEA protein (Table 19). The results support the general knowledge about LEA protein accumulation, as the tag was found to be 129-fold up-regulated under drought stress conditions and also stayed up-regulated under recovery conditions. LEA proteins are separated into four different groups (DURE et al. 1989). Group 2 LEA proteins are also called dehydrins and their genes (or at least the gene encoding dehydrin 1) were expressed in the *Panicum* species as the protein dehydrin 1 could be detected by western analyses (4.2.1).

Heat shock proteins (HSPs) also belong to the family of protective proteins and enclose chaperones which stabilize assembling proteins. SUN et al. (2001) could show that *Arabidopsis* mutants overexpressing a HSP (AtHSP17) had a greater drought stress tolerance compared to the wild type plants. It is therefore possible that the - under stress and recovery - differently regulated HT-SuperSAGE tags derived from the *Panicum* species could also be annotated to HSPs in the future. HSPs also play a great part in removal of damaged proteins, so that genes encoding for the HSPs could also be found under recovery conditions.

Aquaporins also belong to the family of protective proteins and allow the plant to control water fluxes across the membrane. They form a group of major intrinsic proteins (MIPs) and their genes are either induced by drought stress to distribute water in the tissue (YAMAGUCHI-SHINOZAKI et al. 1992) or down-regulated under limited water resources to reduce the loss of water out of the cell (YAMADA et al. 1997). It is therefore conceivable that genes encoding aquaporins were differentially regulated in the *Panicum* species under droughts tress and could be identified in the future. The annotation of the HT-SuperSAGE tags delivered an aquaporin hit for *P. bisulcatum* (Table 20, 4.2.2.7) confirming that these proteins play an important part in plant water status regulation. In the case of *P. bisulcatum* the aquaporin was highly down-regulated under stress conditions and highly up-regulated under recovery conditions supporting the results from YAMADA et al. (1997).

Furthermore the regulation of the amount of proteases and proteinase inhibitors as well as polyamines in the drought stressed plants is important as these also help to maintain protein homeostasis and cellular functions under stress conditions.

4.2.2.5. Species-comprehensive analyses

Species-comprehensive analyses were conducted to reveal tags differentially regulated in all four *Panicum* species. The comparison of all differentially regulated HT-SuperSAGE tags (independent from the type of regulation) is depicted by a Venn diagram (Fig. 25). Out of the ca. 106,000 differentially regulated tags only 208 tags were found apparent in all four species. It is likely that these tags take over important functions in maintaining plant homeostasis during drought stress and recovery; future tag to gene annotation has to reveal their functions. It is also possible that these tags can be found in a great variety of (at least) grasses as they can already be found in the four *Panicum* species. When looking at the tags only apparent in three out of four species, the C₄ *Panicum* grasses *P. laetum*, *P. miliaceum* and *P. turgidum* share the greatest number of tags (627 tags, Fig. 25). This is not surprising as

ZIMMERMANN et al. (2013) could show the phylogenetic integration of the before mentioned C_4 species into a single clade – the Panicinae clade. They are closer related to each other than to *P. bisulcatum* which could be an explanation for the greater number of tags they share. When running two species-comprehensive analyses, *P. miliaceum* and *P. laetum* share the highest number of differentially regulated tags (1704 tags, Fig. 25). Regarding their phylogenetic relationship (ZIMMERMANN et al. 2013) they are the closest related species out of the four *Panicum* grasses and it is not remarkable that the highest amount of shared tags could be found for them. As mentioned above *P. miliaceum* and *P. laetum* are closest related to each other. Following those, *P. laetum* and *P. turgidum* and then *P. miliaceum* and *P. turgidum* are phylogenetically closest related to each other (ZIMMERMANN et al. 2013). This systematic relationship is also mirrored in the number of differentially regulated HT-SuperSAGE tags as *P. laetum* and *P. turgidum* shared 1056 tags and *P. miliaceum* and *P. turgidum* shared 666 tags (Fig. 25).

The species-comprehensive analyses conducted for the different “regulation groups” (Fig. 26, Fig. 27) showed only few tags present in all four species. For group 1 (C<S>R, Fig. 26) seven tags were found existent in four species, group 4 (C=S<R, Fig. 26) only had 1 tag apparent in all analysed species and groups 2 and 3 (C<S=R, C<S<R, Fig. 26) shared no tags between the four *Panicum* grasses. Those seven tags up-regulated under stress conditions and down-regulated under recovery conditions (group 1) found in all four grasses could play a constitutive part in plant protection; future tag to gene annotation has to reveal their function. It can be assumed that they take over protective roles and the fold-change regulation of the tags underlines their importance. Except for one tag in *P. laetum* all tags are up-regulated ≥ 5 -fold, the highest up-regulation is found in *P. miliaceum* where a 182-fold up-regulation under stress conditions could be monitored (Table 15). The tag in group 4 was highest up-regulated (40-fold) in *P. miliaceum* (data not shown) and the gene might play an important role in restoring control conditions. The three species-comprehensive analyses of groups 1 – 4 show that most tags were shared between the C_4 species which again is ascribed to their closer phylogenetic relationship as explained above. When looking at the species-comprehensive analyses from groups 5 – 8 even less tags could be found existent in all four species (Fig. 27). In group 5 (C>S<R) only four tags were apparent in all species, in group 6 the number dropped to one tag and in groups 7 and 8 no tags could be found apparent in all four species (Fig. 26). The down-regulation of genes is a way to protect the plant during drought stress as “normal” functions are closed

down to save energy. It seems thought, that every species down-regulates its “own” set of genes.

Overall it can be resumed that the species-comprehensive analyses revealed the greatest amounts of tags for the individual *Panicum* species, only few tags were found in two-, three- or all species. The tags found in all four species might in future be annotated to genes important in a great variety of grasses with basic functions concerning adaptation to drought stress. Tags found in three species were higher for the C₄ grasses and could in future reveal C₄-specific mechanisms relevant to protect the plants from damage caused by drought. Nevertheless the grasses have their very own specific “way” to cope with drought stress and no “comprehensive” reaction (on a tag expression level) could be observed.

4.2.2.6. Fold-change regulation of HT-SuperSAGE tags

The fold-change regulation of tags was analysed to mirror the strength of up- or down-regulation in the different *Panicum* grasses. A high up-regulation shows the importance of the tag in the species under stress or recovery conditions, a strong down-regulation of tags in contrast can mirror the protection of a specific system not being used under stress- or recovery condition. Tags were separated into different groups according to the strength of fold-change (Table 16, Fig. 28, Fig. 29, Fig. 30, Table 17). Fold-change regulation was set to very low ($\geq 2 - < 5$), low ($\geq 5 - < 10$), medium ($\geq 10 - < 25$), high ($\geq 25 - < 50$) and very high (≥ 50) to see if there were parallels in the strength of the grasses’ reactions to drought stress. Table 16 clearly shows that most tags were only regulated in a low manner. Drought stress exerted for a long time to the plants evoked mostly only little reactions (on a tag-specific level). This might be due to the fact that first reactions during the onset of drought stress already passed and the adaptation process begun. The number of tags correlates negatively with rising fold-change, the higher the fold-change, the lower the tag numbers. Interestingly there are two exceptions, *P. miliaceum* shows higher numbers of tags 5-fold and 10-fold differentially expressed in the C<S=R group and *P. turgidum* shows higher numbers of tags 5-fold regulated in the C>S<R group (Table 16). The stronger regulation of tags in these groups reflects their importance under long-lasting drought stress and also reflects the importance of the regulation schemata for the species.

When looking at the different regulation schemata (Fig. 28 - Fig. 30) low tag regulation (<5-fold) was most important in the drought susceptible species *P. bisulcatum* and *P. laetum*. Under drought stress conditions these species exhibited most tags up-regulated under stress- or recovery conditions. Interestingly, *P. turgidum* had the highest amount of low-

regulated tags in the group C>S<R reflecting the opposite adaptation mechanism. The drought susceptible species up-regulate genes whereas the drought resistant species down-regulates a great amount of genes (and therefore processes). This could be one of the mechanisms making plants more resistant to drought.

Some tags were differentially regulated with a very high fold change ≥ 50 under drought stress or recovery – 25 in *P. bisulcatum*, 176 in *P. laetum*, 165 in *P. miliaceum* and 47 in *P. turgidum*. These tags (and the appending genes) play crucial roles in the adaptation to drought stress and their (future) annotation will reveal their functions. In Table 17 the highest regulated tag in each regulation group is represented, in *P. miliaceum* an up-regulation of 2059-fold could be shown under drought stress. In *P. turgidum* the highest differentially regulated tag in contrast was down-regulated 845-fold under drought stress conditions. The future annotation of these tags will reveal important gene candidates with crucial functions in drought stress adaptation – maybe completely new to the research community.

4.2.2.7. BLAST and qPCR results

The BLAST search was carried out to annotate selected HT-SuperSAGE tags to their appending genes. The only *Panicum* genome (or EST database) available at the time was the EST database of *P. virgatum*, leading to very low numbers of tag to gene annotations (Table 18). The highest annotation could be generated for *P. turgidum* (8.2 %), followed by *P. laetum* (6.9 %), *P. miliaceum* (5.7 %) and *P. bisulcatum* (2.3 %). The percentage of annotated tags correlates with the phylogenetic relationship of the species to *P. virgatum*. *P. turgidum* is closest related to *P. virgatum*, followed by *P. laetum*, *P. miliaceum* and last *P. bisulcatum* (ZIMMERMANN et al. 2013).

The tags successfully elongated via the 3' RACE method (Table 19) could almost all be annotated to genes encoding diverse proteins (Table 20). For the five *P. bisulcatum* sequences, one “no specific hit” and one “hypothetical protein” were found, two proteins associated with photosynthesis and one aquaporin (for discussion see 4.2.2.4). Both proteins associated with photosynthesis were down-regulated under stress supporting the physiological measurements undertaken, where *P. bisulcatum* also down-regulated its photosynthetic functions under stress (3.1.2, 4.1.2).

For *P. laetum*, many of the annotated genes translate unknown (98), putative (334) or hypothetical proteins (972) or no hits were found at all (27, data not shown). The highest regulated and annotated tag for *P. laetum* was found in the C>S<R group. This tag was also

subjected to the 3' RACE method to verify the results (*P. laetum* 2, Table 19). The BLAST search with the 26 bp HT-SuperSAGE tag delivered a putatively expressed cytochrome b₆f complex subunit (*Oryza sativa*) where the elongated 3' RACE sequence (106 bp, Table 20) delivered a predicted PS II 10 KDa polypeptide (*Setaria italica*). Both proteins belong to the photosynthesis chain. Nevertheless the results suggest different proteins and further investigations would be necessary to verify the correct expression even though it is more likely that the annotation of the 106 bp long sequence is correct. However, the result does correlate with the physiological measurements undertaken (PEA measurements) where a reduction in PS II efficiency or beyond (intersystem carriers) could be shown for *P. laetum* (3.1.4, 4.1.4). Further proteins like the temperature-induced lipocalin (TIL) and a LEA protein (for discussion see 4.2.2.4) were up-regulated under drought stress conditions and stayed up-regulated also under recovery (S=R). In contrast to the results generated by HT-SuperSAGE, the qPCR analysis on the TIL suggested a down-regulation (S>R) from stress to recovery conditions. These deviations could be attributed to differing leaf material used for the diverse methods, as leaf material was collected in 2011 and 2012. Lipocalins are proteins transporting hydrophobic molecules like lipids, their function under drought stress however must be clarified in the future.

For *P. miliaceum* six sequences were used for the BLAST analyses. Two sequences delivered a “no specific hit” and an “uncharacterized protein” (Table 20). The only annotated protein down-regulated under stress and up-regulated under recovery conditions was the 9-cis-epoxycarotenoid dioxygenase 1 (NCED 1). The NCED 1 catalyses the cleavage of cis-epoxycarotenoids and is considered to be the key rate-limiting enzyme in ABA biosynthesis. HU et al. (2010 b) could show a strong expression of the AhNCED 1 mRNA in peanut leaves and roots under water stress. An up-regulation of the *NCED* gene in the first hours after drought stress induction could also be shown by HUH et al. (2010) and several others. At least seven homologous *NCED* genes are known in *Arabidopsis* but their individual function is still hardly understood. Nevertheless the role of *NCED* genes is of high importance as “modulation of endogenous ABA levels is possible via engineering *NCED* expression, which subsequently changes drought tolerance and most likely other responses to osmotic stress” (BARTELS & SUNKAR 2005). In contrast to the published results, the HT-SuperSAGE tag annotated to the NCED 1 was strongly down-regulated in eight day-drought stressed leaves of *P. miliaceum* (Table 19). It is assumed that the duration of imposed drought stress (eight days) was too long and ABA biosynthesis was down-regulated. The qPCR analysis carried out on NCED1 supported the results generated by

HT-SuperSAGE (Fig. 37, Table 24). Additional qPCR analysis also showed a down-regulation of the gene four days after drought stress induction where the RWC was still above 70 % (data not shown). Further investigations must confirm the assumption stated above but the results generated in this dissertation show how important it is to also focus on long-lasting drought stress to understand the full range of *NCED* gene regulation.

For the purple acid phosphatase (PAP) in *P. miliaceum* HT-SuperSAGE results suggested an up-regulation under drought stress (C<S) followed by a constant regulation under stress and recovery (S=R). The qPCR results suggested a minimal down-regulation (S≥R) very similar to the HT-SuperSAGE results. These deviations could be attributed to differing leaf material used for the diverse methods, as leaf material was collected in 2011 and 2012. Phosphatases regulate e.g. the phosphoregulatory mechanisms of MAPK cascades by forming a counterpart to these (4.2.2.3). Two major families of phosphatases exist, the phosphoprotein (serine/threonine) phosphatases (PPases) and the phosphotyrosine phosphatases (protein tyrosine phosphatases, PTPases, BARTELS & SUNKAR, 2005). Especially the PTPases play a major role in the regulation of MAPK cascades by forming a negative feedback loop (JACOBY et al. 1997). PPases in contrast play a role in dehydration adaptation (MIYAZAKI et al. 1999) and their protein family consists of more than 100 genes also regulating the ABA pathway and stomatal closure under drought stress (MACROBBIE, 2002). The purple acid phosphatases belong to the family of PTPases and their sequences are highly conserved with >70 % sequence homology in plant species (LORD et al. 1990). It is therefore not surprising that a purple acid phosphatase was found in every *Panicum* species when carrying out species-comprehensive analyses (Table 25). Due to their diverse functions, their regulation in the individual species differed (Table 25) and future investigations would have to reveal the function and the exact gene in each species.

An adenosine 5'-phosphosulfat reductase was only up-regulated under recovery conditions in *P. miliaceum* (Table 20). The enzyme mostly participates in sulphur metabolism where the amino acid cysteine is the first stable product of sulphur assimilation. As sulphur assimilation is very cost-intensive, the sulphur assimilation could be an explanation for the up-regulation of the protein only under recovery conditions, where more energy is available. Also the necessity of cysteine for protein formation could explain the strong up-regulation (106-fold) as damaged proteins have to be newly built. Surprisingly the adenosine 5'-phosphosulfat reductase was not reduced under stress conditions although the photosynthesis rate was diminished and assimilation is linked to photosynthesis. Further

investigations have to clarify the importance of the adenosine 5'-phosphosulfat reductase under stress and recovery conditions.

For *P. turgidum* four sequences underwent BLAST analyses and interestingly two sequences hit the same protein family, the (papain-like) cysteine proteinase (*P. turgidum* 2 and *P. turgidum* 14, Table 20). The family of cysteine proteases degrades proteins and the enzymes are involved in abiotic stress response via signalling pathways (GRUDKOWSKA & ZAGDAŃSKA 2004). This could explain the different regulations of the HT-SuperSAGE tags (*P. turgidum* 2: C>S<R and *P. turgidum* 14: C<S=R, Table 19) as damaged proteins have to be disintegrated immediately independent from the plant's condition (e.g. the cysteine proteinase found in *P. turgidum* 2 disintegrates proteins under control conditions whereas the cysteine proteinase found in *P. turgidum* 14 only disintegrates proteins under stress conditions). As the cysteine protease family is big, further investigations have to reveal the exact enzymes with their appending functions. The qPCR analysis carried out on the CP of *P. turgidum* 14 and the RNP (*P. turgidum* 17) supported the results generated by HT-SuperSAGE (Table 24, Fig. 37).

Just like one of the (papain-like) cysteine proteinases, a glycine-rich RNA-binding protein was up-regulated under drought stress and stayed up-regulated under recovery conditions (Table 19, Table 20). RNA-binding proteins bind to dsRNA or ssRNA and form ribonucleoprotein complexes. They play important roles in diverse processes like cellular function, transport, localization, RNA-splicing, mRNA stabilization and many more. More than 500 genes encoding for RNA-binding proteins are currently known and a great number of researches work on this important group of proteins (STEFEL et al. 2005). It is not surprising that the RNA-binding protein was up-regulated under stress and recovery conditions helping the plant to maintain functional.

Out of the 20 HT-Super SAGE tags four annotated genes were chosen to show the diversity of the localization of the 26 bp HT-Super SAGE tag and 3' RACE sequence (Fig. 31). Tag and sequence were located completely in the 3' untranslated region (UTR) for the aquaporin in *P. bisulcatum* where in the LEA-D-34 protein in *P. laetum* the tag and 3' RACE were completely located in the coding region of the mRNA (Fig. 31). The results show that independent from the location of the HT-SuperSAGE tag, the 3' RACE method and all following analysis work well and can be conducted without further adjustment. It has to be mentioned, that due to high costs, the HT-SuperSAGE analyses were only conducted once where it would have been better to conduct the run several times for more powerful data (n=3). Nevertheless, the qPCR results mostly confirm the HT-SuperSAGE results (Table

24) and the data generated can be used for further investigations helping biotechnological or breeding approaches.

5 Summary

Drought stress is one of the major abiotic factors diminishing crop productivity world wide. In the course of climate change, regions which already experience dry seasons nowadays will suffer from elongated drought periods and water shortage. These climatic changes will not only have an impact on the regional flora and fauna but also on the people inhabiting these areas. It is therefore of great importance to understand the reactions of plants to drought stress to help breeding and biotechnological approaches for the benefit of new robust cereal cultures growing under low water regimes.

In this dissertation four grasses of the genus *Panicum*, *P. bisulcatum* (C₃), *P. laetum*, *P. miliaceum* and *P. turgidum* (all C₄ NAD-ME) were subjected to drought stress. The plants diverse reactions were investigated on a physiological as well as on a molecular level to deepen the understanding of drought stress responses. Drought stress was imposed for a species-specific period until a relative leaf water content (RWC) of ~50 % was reached in each grass. Physiological measurements were conducted on leaves with a RWC of ~50 % investigating chlorophyll a fluorescence parameters with a Plant Efficiency Analyzer (PEA) and gas exchange parameters like the photosynthesis rate and stomatal conductance with a Gas Fluorescence Chamber (GFS-3000). Subsequent molecular analysis were conducted on leaf samples taken (RWC = 50 %) analysing different proteins and the transcriptome of the *Panicum* species.

The physiological measurements revealed a higher photosynthesis rate for the C₄ grasses under drought stress with no significant differences between the C₄ species. Also the water use efficiency was significantly higher in the C₄ species in comparison to the C₃ species independent from the water regime supporting results from the literature. The chlorophyll a measurements revealed the strongest adaptation to water shortage in the C₄ species *P. turgidum* followed by the C₃ species *P. bisulcatum*. It has been shown before (GHANNOUM 2009) that the C₄ photosynthesis apparatus is more prone to drought stress than the C₃ apparatus – despite the higher water use efficiency. Results also suggested that the great adaptation of *P. turgidum* to drought stress arose from its ability to recover from drought stress (all JIP test parameters showed no significant differences between control and recovery samples). The additional down-regulation of PS II but not of PS I under drought stress also helped the plant to endure times of water shortage and facilitated the recovery when water was available again.

Protein analyses on the content of PEPC, OEC and RubisCO (LSU and SSU) revealed no changes. Dehydrin 1 in contrast was strongly up-regulated under drought stress and

recovery in all four *Panicum* species. The stable content of the OEC protein was therefore not the catalyst of rising K peaks measured by chlorophyll a fluorescence and a reduced OEC activity was supposed.

Transcriptomic analyses revealed a myriad of differentially regulated tags. Due to unsequenced genomes, tags could only be partially (8 % maximum for *P. turgidum*) annotated to their specific genes. Diverse methods were therefore used to annotate the most highly regulated tags to their genes and their products. Special emphasis was put on the regulation of five gene products confirming the regulation schemata from the HT-SuperSAGE analyses. Interestingly one protein – the NCED1 – was down-regulated under stress conditions, in contrast to results from the literature. It is therefore of great importance to investigate longer lasting drought to understand the full range of drought stress adaptation. Future genome sequencing projects might also include the *Panicum* species investigated in this dissertation and important gene candidates with no hits (maybe completely new to the research community) might help breeding and biotechnology approaches to produce more drought resistant crop species.

6 Zusammenfassung

Im Zuge des prognostizierten Klimawandels werden die Analysen der pflanzlichen Reaktionen auf Trockenheit immer wichtiger. Eine stetig zunehmende Anzahl an Menschen, die in schon trockenen Gebieten der Welt leben, müssen auch in Zukunft ernährt werden. So müssen sowohl biotechnologische- als auch Zuchtansätze neue pflanzliche Genotypen finden, die auch unter geringer Wasserverfügbarkeit Ernteerträge liefern. Zusätzlich kann die Untersuchung der pflanzlichen Antworten auf Trockenheit Einblicke in eine zukünftige Artenverteilung geben. Es ist daher von großer Bedeutung zu verstehen, warum einige Arte unter geringer Wasserverfügbarkeit überleben, während andere Arten sterben.

Laut dem „Intergovernmental Panel on Climate Change“ (IPCC) wird es in den kommenden 100 Jahren zu einem Temperaturanstieg von bis zu 7°C in weiten Teilen der Welt kommen. Auch die Niederschlagsmengen werden sich verändern, sodass vor allem Südeuropa, weite Teile Afrikas und Teile Mittelamerikas mit einer geringeren Menge an Regen auskommen müssen. Konsequenzen dieser klimatischen Veränderungen sind neben einer Verminderung der Biodiversität auch eine Neuverteilung von Flora und Fauna, was sich letzten Endes auch auf die Bevölkerung in den betroffenen Gebieten auswirkt.

Da Pflanzen sessil leben, sind sie den Umweltbedingungen um sich herum ausgesetzt. Wenn sich klimatische Bedingungen vom Normalzustand ändern erfahren Pflanzen daher eine Stress-Situation. Um diesem Stress entgegen zu wirken, haben Pflanzen Schutz- und Anpassungsmechanismen entwickelt welche von zellulärer bis molekularer Ebene reichen. Eine große Rolle bei der Anpassung an warme und trockene Standorte spielt vor allem der Photosynthesetyp, der genutzt wird. Im Laufe der Evolution haben sich verschiedene Typen entwickelt, benannt nach dem ersten Metabolit welches während der CO₂-Fixierung gebildet wird – C₃ und C₄ Photosynthese. Obwohl nur ca. 3 % aller Angiospermen den C₄ Photosyntheseweg nutzen beträgt der Beitrag zur weltweiten Primärproduktion dieser Arten 25 % und bis zu 30 % des terrestrischen CO₂ wird von ihnen fixiert. In trockenen und warmen Regionen haben C₄ Arten zudem einen kompetitiven Vorteil gegenüber C₃ Pflanzen, da sie eine höhere Wassernutzungseffizienz aufweisen. Diese entsteht sowohl durch morphologische als auch durch physiologische Besonderheiten. C₄ Pflanzen besitzen zwei photosynthetisch aktive Zelltypen, die Mesophyll (MZ)- und die Bündelscheidenzellen (BSZ). Diese Gewebearrangung wird auch als „Kranz“ Anatomie bezeichnet. Die RubisCO, die in Pflanzen für die CO₂ Fixierung zuständig ist, liegt in C₄ Pflanzen hauptsächlich in den BSZ vor. Die initiale CO₂ Fixierung wird in C₄ Pflanzen von der

PEPC durchgeführt, welche in den MZ zu finden ist. Das vorfixierte CO₂ wird aus den MZ in die BSZ transportiert und liegt dort für RubisCO verfügbar vor wodurch die oxygene Funktion der RubisCO (Photorespiration) unterdrückt wird. Die Photosynthesekapazität ist demnach in C₄ Pflanzen höher als in C₃ Pflanzen wenn Außentemperaturen 30°C – 45°C erreichen. Im Gegensatz zu C₃ Arten erfahren C₄ Arten deshalb keinen CO₂ Mangel wenn die Stomata an heißen und trockenen Tagen geschlossen werden, um dem Wasserverlust durch Transpiration vorzubeugen. Diese Charakteristika führen zu einer zwei – drei Mal so hohen Wassernutzungseffizienz der C₄ Arten und ermöglichen es diesen, wärmere und trockenere Regionen dieser Welt zu dominieren. Die C₄ Photosynthese umschließt verschiedene Subtypen, wobei in dieser Arbeit nur Arten untersucht wurden, die den NAD-Malat Enzym (NAD-ME) Subtyp nutzen.

Die Ordnung der Gräser (Poales) umfasst den größten Teil der C₄ Photosynthese betreibenden Pflanzen. In dieser Arbeit wurden Gräser der Gattung *Panicum* untersucht, welche wichtige Getreide wie zum Beispiel die Rispenhirse (*P. miliaceum*) umfasst. Die in dieser Arbeit untersuchten Gräser *P. bisulcatum* (C₃), *P. laetum*, *P. miliaceum*, und *P. turgidum* (alle C₄ NAD-ME) wurden sowohl auf Grund ihrer ökologischen- als auch ökonomischen Relevanz, der Anpassung an Wassermangel (Trockenstress) und der Anzuchtmöglichkeit gewählt. Vor allem *P. miliaceum* hat einen hohen ökonomischen Wert, wohingegen *P. laetum* und *P. turgidum* als so genannte „lost crops of Africa“ einen eher geringeren ökonomischen Wert haben. Diese Arten wachsen auch in extrem trockenen Zeiten und wilde Bestände werden oft von der Bevölkerung geerntet. *P. turgidum* hat zusätzlich einen hohen ökologischen Wert, da es als Sandbinder der fortschreitenden Wüstenausbreitung entgegenwirkt. Die Anpassung an Trockenstress nimmt von *P. turgidum* über *P. miliaceum* und *P. laetum* hin zu *P. bisulcatum* ab. So sollen Unterschiede der Trockenstressanpassung (trotz gleichem C₄ Photosynthese-Subtyp) sowohl auf physiologischer als auch molekularer Ebene aufgezeigt werden.

Trockenstress trägt zu einem weltweiten Ernteverlust von bis zu 50 % bei. Es ist daher enorm wichtig die pflanzlichen Reaktionen (Anpassung an Trockenheit und Vermeidung von Schäden) zu verstehen um dem Verlust entgegen zu wirken. Trockenstress beeinträchtigt die Pflanzen auf allen Ebenen, von der Physiologie bis hin zu Genexpression. Auf der physiologischen Ebene wird die C₃ Photosynthese sowohl stomatär als auch nicht-stomatär gehemmt. Sinkt der Blattwassergehalt, schließen sich die Stomata und der sinkende CO₂-Gehalt wird zum Photosynthese-limitierenden Faktor. Bei C₄ Arten wird die Photosynthese in den Schluss der Stomata nicht limitiert, erst nicht-

stomatäre, metabolische Effekte (ab einem relativen Blattwassergehalt von <70 %) limitieren die Photosyntheserate. Die molekularen Antworten der Pflanzen auf Trockenstress sind divers. Osmotischer Stress löst über so genannte ABA-abhängige oder ABA-unabhängige Signalwege in der Zelle ein Netzwerk an die Transkription regulierenden Faktoren aus. Transkriptionsfaktoren, die stress-induzierbare Gene kontrollieren, werden durch die Signalwege angeschaltet, diese wiederum aktivieren Gene, die Produkte (z. Bsp. Proteine und Metabolite) zum Schutz und zur Anpassung an Trockenstress transkribieren. Alle diese Mechanismen zusammen – physiologische, metabolische, proteomische und molekulare – ermöglichen es der Pflanze unter Wassermangel zu überleben.

In dieser Dissertation wurden die vier Gräser der Gattung *Panicum* Trockenstressexperimenten unterzogen. Dabei wurden die Gräser für eine artspezifische Zeitspanne Trockenstress ausgesetzt, indem kein Wasser gegeben wurde. Nachdem Blattproben vom Kontrollzeitpunkt genommen wurden (an Tag 1 nach Bewässerungsstopp) wurden bei einem relativen Blattwassergehalt (RWC) von ca. 70 % weiter Blattproben genommen (geringer Stress). Bei einem RWC von ca. 50 % wurden Blattproben genommen (Stress) und die Pflanzen danach wieder bewässert. Zwei Stunden nach Wiederbewässerung wurden erneut Proben genommen um den Erholungszustand zu überprüfen. Jede Art hatte dabei einen unterschiedlich langen Zeitraum der Trockenphase – *P. bisulcatum* wurde nur für 5 Tage nicht gegossen bis es einen RWC von 50 % erreichte, bei *P. turgidum* belief sich dieser Zeitraum auf 11 Tage.

Die physiologischen Messungen zur Bestimmung der Photosyntheserate, stomatären Leitfähigkeit, Wassernutzungseffizienz und Chlorophyll a (Chl a) Fluoreszenz wurden jeweils vor den Blattprobenahmen durchgeführt. Dabei wurde für die Chl a Fluoreszenzmessungen der „Plant Efficiency Analyser“ (PEA) genutzt, für alle anderen Messungen die „Gasfluoreszenzklammer GFS 3000“. Für die molekularen Analysen wurden die gesammelten und in Stickstoff gefrorenen Blattproben in einer Kugelmühle zermahlen um für Protein- und Transkriptomanalysen zur Verfügung zu stehen. Zur Untersuchung ausgewählter Proteine (RubisCO LSU und SSU, OEC, PEPC und Dehydrin 1) wurde die „SDS-PAGE“ mit anschließendem „Western Blot“ und „Immunodetektion“ gewählt. Die Transkriptome der einzelnen Arten wurden mit Hilfe der Methode „SuperSAGE“ isoliert. Weitere Methoden, um die Ergebnisse der SuperSAGE zu untermauern und weiterzuführen waren die 3' RACE, gefolgt von einer BLAST Suche und qPCR Analysen an ausgewählten Genen. Alle gesammelten Daten wurden am Ende statistischen Analysen unterzogen um ihre Signifikanzen zu testen.

Die Messungen der Photosyntheserate bestätigten Werte aus der Literatur, wo signifikant höhere Photosyntheseraten in C_4 Pflanzen sowohl unter Kontroll- als auch Stress-Bedingungen gemessen wurden. Dies liegt an der oben beschriebenen Anatomie der C_4 Pflanzen, die neben einer erhöhten Wassernutzungseffizienz auch die Photosynthese bei geringer CO_2 Zufuhr ermöglicht. Zusätzliche Untersuchungen des RubisCO Gehalts zeigten keine Veränderung in der Proteinmenge unter Trockenstressbedingungen in den untersuchten Arten. Dies schließt eine metabolische Limitierung der Photosyntheserate unter Stress jedoch nicht aus, da auch bei gleichbleibendem Proteingehalt eine verminderte Aktivität vorliegen kann. Weitere Messungen müssten bestätigen, dass es sich bei der Abnahme der Photosyntheserate unter Stress um eine erst stomatäre- und dann zusätzlich metabolische Limitierung handelt (wie es in der Literatur beschreiben ist). Die Messungen des stomatären Widerstands zeigten ein ähnliches Bild im Vergleich zur Photosyntheserate. Mit abnehmendem relativem Blattwassergehalt sanken auch die Werte des stomatären Widerstands signifikant in den untersuchten Arten. Bei einem Vergleich der Arten konnten jedoch keine signifikanten Unterschiede aufgezeigt werden. Der stomatäre Widerstand ist somit nicht artspezifischen Unterschieden unterlegen und liefert keine Hinweise auf die Trockenstresstoleranz der jeweiligen Art. Messungen der Wassernutzungseffizienz konnten die Werte aus der Literatur bestätigen, da die C_4 Arten unter Kontroll-, Stress- und Erholungsbedingungen signifikant höhere Werte aufzeigten als die C_3 Art.

Chlorophyll a Fluoreszenzanalysen zeigten eine Limitierung des Photosyntheseapparates unter Trockenstressbedingungen in allen untersuchten Arten, wobei sich die Limitierung bei *P. turgidum* als einzige Art nur auf Photosystem II (PS II) bezog. Zusätzlich waren die Werte der Erholungsproben bei *P. turgidum* die einzigen, die keine signifikanten Unterschiede zu Kontrollwerten aufwiesen. Dies zeigt die extreme Anpassung dieser Art an Trockenstress, wo verfügbares Wasser sofort zu einer „Widerbelebungs“ des Photosyntheseapparates führt um Biomasse und Samen zu produzieren. Alle weiteren untersuchten *Panicum* Arten zeigten auch nach der Wiederbewässerung noch signifikant geringere Werte für PS I und II im Vergleich zur Kontrolle. Vor allem *P. miliaceum* (welches eine relativ gute Trockenstresstoleranz aufweist) zeigte schlechte Werte unter Erholungsbedingungen. Für eine gute Adaptation spielt folglich nicht nur die Trockenstresstoleranz eine wichtige Rolle, sondern auch die Fähigkeit sich bei wieder verfügbarem Wasser schnell zu regenerieren. Die Messung des *Performance Index* (PI_{tot}) zeigten sehr ähnliche Werte für alle Arten unter Stressbedingungen. Unter Erholungsbedingungen zeigte nach *P. turgidum* (C_4) erstaunlicherweise die C_3 Art

P. bisulcatum den besten Wert. Es konnte schon früher gezeigt werden, dass der C_3 Photosyntheseapparat an sich besser an Trockenheit angepasst ist als der C_4 Photosyntheseapparat. Die Ergebnisse dieser Dissertation untermauern dies. Die Analysen des sogenannten „*K peaks*“, der den Sauerstoffkomplex (OEC) widerspiegelt, zeigten die größte Abweichung vom Kontrollwert in *P. turgidum*. Proteinanalysen des OEC zeigten jedoch keine Abnahme des Proteingehalts, was eine enzymatische Limitierung allerdings nicht ausschließt. Die Chl a Fluoreszenzanalysen konnten zeigen, dass die gute Anpassung an Trockenstress in *P. turgidum* auf Ebene des Photosyntheseapparates vor allem durch die Runterregulierung des PS II unter Stressbedingungen entsteht. Die Regeneration des Apparats unter Erholungsbedingungen ist ein weiteres wichtiges Merkmal. Die Ergebnisse dieser Dissertation zeigen, wie wichtig auch die Messung des Erholungszustands ist. Die Transkriptomanalysen zeigten, dass die Anzahl der unter Stress heraufregulierten „*tags*“ höher war, als die Anzahl an herunterregulierten *tags*. Interessanterweise war das Verhältnis in der Art *P. turgidum* umgekehrt, wo die Herunterregulierung von Genen unter Stress eine wichtigere Rolle spielte. Bei artübergreifenden Analysen konnte gezeigt werden, dass es nur eine marginale Anzahl an *tags* gab, die in allen untersuchten Arten gleich reguliert waren (13 Stück). Das zeigt die enorme Diversität der Trockenstressanpassung in den Gräsern. Die Anzahl gleicher *tags*, die in den C_4 Arten differentiell exprimiert wurden lag immer über der Zahl an *tags*, die auch in der C_3 Art gefunden wurden. Dies spiegelt die Verwandtschaftsverhältnisse der Gräser gut wieder und zeigt, dass sich mit abnehmendem Verwandtschaftsgrad die Genregulierung zunehmend ändert. Da nur eine sehr geringe Anzahl an *tags* ihren zugehörigen Genen zugeordnet werden konnte (max. 8 % in *P. turgidum*) wurden bestimmte, hoch differentiell regulierte *tags*, für weiterführende Analysen ausgewählt. Unter diesen befanden sich *tags*, die Genen des Photosyntheseapparates zugeordnet werden konnte. Weiter Zuordnungen gab es für Aquaporine, die eine wichtige Rolle bei der Verteilung des Wassers in der Zelle spielen, „*late embryogenesis abundant*“ Proteinen, die bei der Trockenstressantwort eine schützende Funktion übernehmen oder Cystein Proteinase, die Proteine degradieren und über Signalwege eine Rolle bei der Trockenstressanpassung spielen. Neben diesen Genprodukten wurde ein *tag* der 9-cis-epoxycarotinoid Dioxygenase 1 (NCED 1) zugeordnet, welche das Eingangsenzym der ABA Biosynthese ist. Interessanterweise widersprachen die Ergebnisse (der *tag* war stark herunterreguliert während der Stressphase) bisherigen Ergebnissen in der Literatur, wo das Enzym nach kurzer Zeit des Trockenstresses hochreguliert wurde. Das Ergebnis in dieser Dissertation zeigt, wie wichtig

es ist, auch lange anhaltenden Trockenstress (5 – 11 Tage) zu untersuchen. Um die Ergebnisse der HT-SuperSAGE Methode zu untermauern, wurde mit ausgewählten *tags* eine qPCR Analyse durchgeführt. Die Ergebnisse dieser Analyse bestätigten die *tag* Regulation von Kontrolle zu Stress zu 100 %, die *tag* Regulation von Stress zu Erholung zu 60 %. Die qPCR Ergebnisse konnten folglich die HT-SuperSAGE Ergebnisse bestätigen und die generierten Daten könnten in Zukunft genutzt werden, um biotechnologische- oder Zuchtprogramme bei der Herstellung trockenstressresistenterer Arten zu unterstützen.

7 References

- Abe H, Urao T, Ito T, Seki M, Shinozaki K, Yamaguchi-Shinozaki K (2003) *Arabidopsis* AtMYC2 (bHLH) and AtMYB2 (MYB) function as transcriptional activators in abscisic acid signalling. *Plant Cell* 15:63–78
- Abideen Z, Ansari R, Khan MA (2011) Halophytes: Potential source of ligno-cellulosic biomass for ethanol production. *Biomass Bioenerg* 35:1818–1822
- Adam JG (1966) La végétation de l'Aftout es Saheli (Mauritanie occidentale). *Bull IFAN, Série A* 28:1292–1319
- Albrecht V, Wein S, Blazevic D, D'Angelo C, Batistic O, Kolukisaoglu U, Bock R, Schulz B, Harter K, Kudla J (2003) The calcium sensor CBL1 integrates plant responses to abiotic stresses. *Plant J* 36: 457–470
- Alfonso SU, Brüggemann W (2012) Photosynthetic responses of a C₃ and three C₄ species of the genus *Panicum* (s.l.) with different metabolic subtypes to drought stress. *Photosynth Res* 112:175-191
- Aliscioni SS, Giussani LM, Zuloaga FO, Kellogg EA (2003) A molecular phylogeny of *Panicum* (Poaceae: Paniceae): tests of monophyly and phylogenetic placement within the Panicoideae. *Am J Bot* 90:796–821
- Altschul SF, Gish W, Miller W, Myers EW, Lipman DJ (1990) Basic Local Alignment Search Tool. *J Mol Biol* 215:403–410
- Ashoub A, Berberich T, Beckhaus T, Brüggemann W (2011) A competent extraction method of plant proteins for 2-D gel electrophoresis. *Electrophoresis* 32:2975–2978
- Ashraf M, Yasmin N (1995) Responses of four arid zone grass species from varying habitats to drought stress. *Biol Plant* 37:567–575
- Baker NR (1991) A possible role for photosystem II in environmental perturbation of photosynthesis. *Plant Physiol* 81:563–570
- Baker NR, Webber AN (1987) Interactions between photosystems. *Adv Bot Res* 13:1–66
- Baker SS, Wilhelm KS, Thomashow MF (1994) The 5'-region of *Arabidopsis thaliana* cor15a has *cis*-acting elements that confer cold-, drought- and ABA-regulated gene expression. *Plant Mol Biol* 24:701–13
- Barrs HD, Weatherley PE (1962) A re-examination of relative turgidity technique for estimating water deficits in leaves. *Aust J Biol Sci* 3:413
- Bartels D, Sunkar R (2005) Drought and salt tolerance in plants. *Cr Rev Plant Sci* 24:23–58

- Björkman O, Badger MR, Armond P (1980) Response and adaptation of photosynthesis to high temperatures. In: Turner NC, Kramer PJ (Eds) Adaptation of plants to water and high temperature stress. John Wiley and Sons, New York. 233–250
- Bolton JK, Brown RH (1980) Photosynthesis of grass species differing in carbon dioxide fixation pathways. V. Response of *Panicum maximum*, *Panicum milioides*, and tall fescue (*Festuca arundinacea*) to nitrogen nutrition. Plant Physiol 66: 97–100
- Bota J, Medrano H, Flexas J (2004) Is photosynthesis limited by decreased Rubisco activity and RuBP content under progressive water stress? New Phytol 162:671–681
- Bradford MM (1976) A rapid and sensitive method for the quantitation of microgram quantities of protein utilizing the principle of protein-dye binding. Anal Biochem 72:248–254
- Bray EA, Bailey-Serres J, Weretilnyk E (2000) Responses to abiotic stresses. In: Gruissem W, Buchanan B, Jones R (Eds) Biochemistry and molecular biology of plants. American Society of Plant Biologists, Rockville, MD. 158–1249
- Brestic M, Cornic G, Fryer MJ, Baker NR (1995) Does photorespiration protect the photosynthetic apparatus in French bean leaves from photoinhibition during drought stress? Planta 197: 450–457
- Brink M (2006) Cereals and pulses. PROTA. 1–297
- Brown ME, Hintermann B, Higgins N (2009) Markets, climate change, and food security in West Africa. Environ Sci Technol 43:8016–8020
- Caemmerer S, Farquhar GD (1981) Some relationships between the biochemistry of photosynthesis and the gas exchange of leaves. Planta 153:376–387
- Carmo-Silva AE, Bernardes da Silva A, Keys AJ, Parry MAJ, Arrabaça MC (2008) The activities of PEP carboxylase and the C₄ acid decarboxylases are little changed by drought stress in three C₄ grasses of different subtypes. Photosynth Res 97:223–233
- Choi DW, Rodriguez EM, Close TJ (2002) Barley *Cbf3* gene identification, expression pattern, and map location. Plant Physiol 129:1781–87
- Choi H, Hong J, Ha J, Kang J, Kim SY (2000) ABFs, a family of ABA-responsive element binding factors. J Biol Chem 275:1723–30
- Christen D, Schönmann S, Jermini M, Strasser RJ, Défago G (2007) Characterization and early detection of grapevine (*Vitis vinifera*) stress responses to esca disease by *in situ* chlorophyll fluorescence and comparison with drought stress. Environ Exp Bot 60:504–514

- Christin P-A, Salamin N, Kellogg EA, Vicentini A, Besnard G (2009) Integrating phylogeny into studies of C₄ variation in the grasses. *Plant Physiol* 149:82–87
- Clayton WD, Vorontsova MS, Harman KT, Williamson H (2006 onwards) GrassBase - The Online World Grass Flora. <http://www.kew.org/data/grasses-db.html>. [accessed 08 November 2006; 15:30 GMT]
- Close T (1996) Dehydrins: Emergence of a biochemical role of a family of plant dehydration proteins. *Physiol Plantarum* 97:795–803
- Cornic G, Le Gouallec J-L, Briantais J-M, Hodges M (1989) Effect of dehydration and high light on photosynthesis of two C₃ plants (*Phaseolus vulgaris* L. and *Elatostema repens* (Lour.) Hall f.). *Planta* 177:84–90
- Cornic G, Massaci A (1996) Leaf photosynthesis under drought stress. In Baker NR (Ed) *Photosynthesis and the environment*. Kluwer Academic Publishers, NL 347–366
- Corrêa de Souza T, Magalhães PC, Mauro de Castro E, Pereira de Albuquerque PE, Marabesi MA (2013) The influence of ABA on water relation, photosynthesis parameters, and chlorophyll fluorescence under drought conditions in two maize hybrids with contrasting drought resistance. *Acta Physiol Plant* 35:515–527
- De Carvalho CR, Cunha A, Marques da Silva J (2011) Photosynthesis by six Portuguese maize cultivars during drought stress and recovery. *Acta Physiol Plant* 33:359–374
- Dubouzet JG, Sakuma Y, Ito Y, Kasuga M, Dubouzet EG, Miura S, Seki M, Shinozaki K, Yamaguchi-Shinozaki K (2003) OsDREB genes in rice, *Oryza sativa* L., encode transcription activators that function in drought-, high- salt- and cold-responsive gene expression. *Plant J* 33:751–63
- Dure III, Crouch M, Harada J, Ho THD, Mundy J, Quatrano RS, Thomas T, Sung ZR (1989) Common amino acid sequence domains among the LEA proteins of higher plants. *Plant Mol Biol* 12:475–486
- El-Keblawy A, Al-Ansari F, Al-Shamsi N (2011) Effects of temperature and light on salinity tolerance during germination in two desert glycophytic grasses, *Lasiurus scindicus* and *Panicum turgidum*. *Grass Forage Sci* 66:173–182
- Emendack Y, Herzog H, Götz K-P, Malinowski DP (2011) Mid-season water stress on yield and water use of Millet (*Panicum miliaceum*) and Sorghum (*Sorghum bicolor* L. Moench). *Austr J Crop Sci*. 5:1486–1492
- Fay PA, Polley HW, Jin VL, Aspinwall MJ (2012) Productivity of well-watered *Panicum virgatum* does not increase with CO₂ enrichment. *J Plant Ecol* 5:366–375

- Fladung M, Hesselbach J (1986) Callus induction and plant regeneration in *Panicum bisulcatum* and *Panicum milioides*. *Plant Cell Rep* 5:169–173
- Frohman MA, Dush MK, Martin GR (1988) Rapid production of full-length cDNAs from rare transcripts: amplification using a single gene-specific oligonucleotide primer. *Proc Natl Acad Sci* 85:8998–9002
- Furihata T, Maruyama K, Fujita Y, Umezawa T, Yoshida R, Shinozaki K, Yamaguchi-Shinozaki K (2006) Abscisic acid-dependent multisite phosphorylation regulates the activity of a transcription activator AREB1. *Proc Natl Acad Sci USA* 103:1988–93
- Galau GA, Hughes DW, Dure III (1986) Abscisic acid induction of cloned cotton late embryogenesis-abundant (Lea) mRNAs. *Plant Mol Biol* 7:155–170
- Gao MJ, Allard G, Byass L, Flanagan AM, Singh J (2002) Regulation and characterization of four CBF transcription factors from *Brassica napus*. *Plant Mol Biol* 49:459–71
- Ghannoum O (2009) C₄ photosynthesis and water stress. *Ann Bot* 103:635–644
- Ghannoum O, Evans JR, von Caemmerer S (2011) Nitrogen and water use efficiency of C₄ Plants. In: Raghavendra AS, Sage RF (Eds) C₄ photosynthesis and related CO₂ concentrating mechanisms. Springer: Dordrecht, NL. 129–146
- Ghannoum O, von Caemmerer S, Conroy JP (2001) Carbon and water economy of Australian NAD-ME and NADP-ME C₄ grasses. *Funct Plant Biol* 28:213–223
- Ghannoum O, von Caemmerer S, Conroy JP (2002) The effect of drought on plant water use efficiency of nine NAD-ME and nine NADP-ME Australian C₄ grasses. *Funct Plant Biol* 29:1337–1348
- Gomes MTG, da Luz AC, dos Santos MR, Pimentel Batitucci MC, Silva DM, Falquetto AR (2012) Drought tolerance of passion fruit plants assessed by the OJIP chlorophyll a fluorescence transient. *Scientia Horticulturae* 142:49–56
- Grudkowska M, Zagdańska B (2004) Multifunctional role of plant cysteine proteinases. *Acta Biochim Pol* 51:609–24
- Guha A, Sengupta D, Reddy AR (2013) Polyphasic chlorophyll a fluorescence kinetics and leaf protein analyses to track dynamics of photosynthetic performance in mulberry during progressive drought. *J Photochem Photobiol B* 119:71–83
- Guisé B, Srivastava A, Strasser RJ (1995) The polyphasic rise of the chlorophyll a fluorescence (O-K-J-I-P) in heat-stressed leaves. *Arch Sci Genève* 48:147–160
- Haberlandt G (1884) Physiological plant anatomy. *Acta Bot Croat* 68:127–146
- Hatch MD (1987) C₄-Photosynthesis: A unique blend of modified biochemistry, anatomy and ultrastructure. *BBA-Rev Bioenergetics* 2:81–106

- Himmelbach A, Yang Y, Grill E (2003) Relay and control of abscisic acid signalling. *Curr Opin Plant Biol* 6:470–79
- Holaday AS, Ritchie SW, Nguyen HT (1992) Effect of water deficit on gas-exchange parameters and ribulose 1,5-bisphosphate carboxylase activation in wheat. *Environ Ex Bot* 32:403–410
- Hu B, Liu X, Hong L, Li L, Luo GY (2010 b) Expression and localization of *Arachis hypogaea* 9-cis epoxy-carotenoid dioxygenase 1 (AhNCED1) of peanut under water stress. *Biotechnol* 24:1562–1568
- Hu WH, Xiao YA, Zeng JJ, Hu XH (2010 a) Photosynthesis, respiration and antioxidant enzymes in pepper leaves under drought and heat stresses. *Biol Plantarum* 54:761–765
- Hu Y-G, Lin F-Y, Wang S-Q, He B-R (2008) Cloning and expression analyses of drought-tolerant and water-saving related gene PmMYB in broomcorn millet. *Hereditas* 30:373
- Huh SM, Noh EK, Kim HG, Jeon BW, Bae K, Hu H-C, Kwak JM, Park OK (2010) *Arabidopsis* Annexins AnnAt1 and AnnAt4 interact with each other and regulate drought and salt stress responses. *Plant Cell Physiol* 51:1499–1514
- Ichimura K, Shinozaki K, Tina G, Sheen J, Henry Y, Champion A, Kreis M, Zhang S, Hirt H, Wilson C, Heberle-Bors E, Ellis BE, Morris PC, Innes RW, Ecker JE, Scheel D, Klessig DF, Machida Y, Mundy J, Ohashi Y, Walker JC (2002) Mitogen-activated protein kinase cascades in plants: A new nomenclature. *Trends Plant Sci* 7:301–308
- Ingram J, Bartels D (1996) The molecular basis of dehydration tolerance in plants. *Annu Rev Plant Physiol Plant Mol Biol* 47:377–403
- IPCC, 2013: Summary for Policymakers. In: *Climate Change 2013: The Physical Science Basis. Contribution of Working Group I to the Fifth Assessment Report of the Intergovernmental Panel on Climate Change* [Stocker, T.F., D. Qin, G.-K. Plattner, M. Tignor, S.K. Allen, J. Boschung, A. Nauels, Y. Xia, V. Bex and P.M. Midgley (eds.)]. Cambridge University Press, Cambridge, United Kingdom and New York, NY, USA
- Irvine FR (1955) Supplementary and emergency food plants of West Africa. *Econ Bot* 6:23–40
- Iuchi S, Kobayashi M, Taji T, Naramoto M, Seki M, Kato T, Tabata S, Kakubari Y, Yamaguchi-Shinozaki K, Shinozaki K (2001) Regulation of drought tolerance by gene manipulation of 9-cis-epoxycarotenoid dioxygenase, a key enzyme in abscisic acid biosynthesis in *Arabidopsis*. *Plant J* 27:325–33

- Ivanov AG, Sane PV, Krol M, Gray GR., Balseris A, Savitch LV, Öquist G, Hüner NPA (2006) Acclimation to temperature and irradiance modulates PSII charge recombination. *FEBS Lett* 580:2797–2802
- Jacoby T, Flanagan H, Faykin A, Seto AG, Mattison C, Ota I (1997) Two protein-tyrosine phosphatases inactivate the osmotic stress response pathway in yeast by targeting the mitogen activated protein kinase, HOG1. *J Biol Chem* 272:17749–17755
- Jakoby M, Weisshaar B, Droge-Laser W, Vicente-Carbajosa J, Tiedemann J, Kroj T, Parcy F (2002) bZIP transcription factors in *Arabidopsis*. *Trends Plant Sci* 7:106–111
- Jedrowski C, Ashoub A, Brüggemann W (2012) Reactions of Egyptian landraces of *Hordeum vulgare* and *Sorghum bicolor* to drought stress, evaluated by the OJIP fluorescence transient analyses. *Acta Physiol Plant* 35:345–354
- Jiang C-D, Jiang G-M, Wang X, Li L-H, Biswas DK, Li Y-G (2006) Increased photosynthetic activities and thermostability of photosystem II with leaf development of elm seedlings (*Ulmus pumila*) probed by the fast fluorescence rise OJIP. *Environ Exp Bot* 58:261–268
- Jones-Rhoades MW, Bartels DP (2004) Computational identification of plant microRNAs and their targets, including a stress-induced miRNA. *Mol Cell* 14:787–99
- Kaiser WM (1987) Effects of water deficit on photosynthetic capacity. *Physiol Plant* 71:142–149
- Kamalay C, Goldberg RB (1980) Regulation of structural gene expression in tobacco. *Cell* 19:935–946
- Kanai R, Edwards GE (1999) The biochemistry of C₄ photosynthesis. In: Sage RF, Monson RK (Eds) C₄-plant biology. Academic Press: San Diego, CA.
- Karyudi, Fletcher RJ (2002) Osmoregulative capacity in birdseed millet under conditions of water stress. I. Variation in *Setaria italica* and *Panicum miliaceum*. *Euphytica* 125:337–348
- Kido EA, Ferreira Neto JRC, Lane de Oliveira Silva R, Pandolfi V, Ribeiro Guimarães AC, Truffi Veiga D, Moutinho Chabregas S, Crovella S, Benko-Iseppon AM (2012) New insights in the sugarcane transcriptome responding to drought stress as revealed by Supersage. *Sci World J Article ID* 821062
- Kiper M, Bartels D, Herzfeld F, Richter G (1979) The expression of a plant genome in hnRNA and mRNA. *Nucleic Acids Res* 6:1961–1978
- Kobayashi Y, Yamamoto S, Minami H, Kagaya Y, Hattori T (2004) Differential activation of the rice sucrose nonfermenting1-related protein kinase2 family by hyperosmotic stress and abscisic acid. *Plant Cell* 16:1163–1177

- Konopka-Postupolska D, Clark G, Goch G, Debski J, Floras K, Cantero A, Fijolek B, Roux S, Hennig J (2009) The role of Annexin 1 in drought stress in *Arabidopsis*. *Plant Physiol* 150:1394–1410
- Körner C, Scheel JA, Bauer H (1979) Maximum leaf diffusive conductance in vascular plants. *Photosynthetica* 13:45–82
- Koyama T (1987) Grasses of Japan and its neighbouring regions. An identification manual. Tokyo, Kodansha Ltd.
- Kramer PJ (1974) Fifty years of progress in water relations research. *Plant Physiol* 54:463–471.
- Krause GH, Weis E (1991) Chlorophyll fluorescence and photosynthesis: the basics. *Annu Rev Plant Physiol Plant Mol Biol* 42:313–349
- Kyriakis JM, Avruch J (2001) Mammalian mitogen-activated protein kinase signal transduction pathways activated by stress and inflammation. *Physiol Rev* 81:807–869
- Laemmli UK (1970) Cleavage of structural proteins during the assembly of the head of bacteriophage T4. *Nature* 227:680–685
- Lawlor DW (2002) Limitation to photosynthesis in water-stressed leaves: stomata vs. metabolism and the role of ATP. *Ann Bot* 89:871–885
- Lawlor DW (2009) Musings about the effects of environment on photosynthesis. *Ann Bot* 103:543–549
- Lawlor DW, Tezara W (2009) Causes of decreased photosynthetic rate and metabolic capacity in water-deficient leaf cells: a critical evaluation of mechanisms and integration of processes. *Ann Bot* 103:561–579
- Lazar D, Schansker G (2009) Models of chlorophyll a fluorescence transients. In: Laisk A, Nedbal L, Govindjee (Eds) *Photosynthesis in silico: Understanding complexity from molecules to ecosystems*. Springer Science + Business Media B.V. 85–123
- Lazarides M, Hince B (1993) CSIRO Handbook of Economic Plants of Australia
- Lindemose S, O’Shea C, Krogh Jensen M, Skriver K (2013) Structure, function and networks of transcription factors involved in abiotic stress responses. *Int J Mol Sci* 14:5842–5878
- Lloyd J, Farquhar GD (1994) ¹³C discrimination during CO₂ assimilation by the terrestrial biosphere. *Oecologia* 3:201–215
- Lodish HF, Berk A, Kaiser CA, Krieger M, Scott MP, Bretscher A, Ploegh H (2008) *Molecular cell biology*. 6th edition. Freeman WH & Co., New York

- Long SP (1999) Environmental responses. In: Sage RF, Monson R (Eds) *C₄ Plant Biology*. Academic Press: San Diego, CA. 215–250
- Longxing H, Zhaolong W, Bingru H (2010) Diffusion limitations and metabolic factors associated with inhibition and recovery of photosynthesis from drought stress in a C₃ perennial grass species. *Physiol Plantarum* 139:93–106
- Lord DK, Cross NCP, Bevilacqua MA, Rider SH, Gorman PA, Groves AV, Moss DW, Sheer D, Cox TM (1990) Type 5 acid phosphatase. Sequence, expression and chromosomal localization of a differentiation-associated protein of the human macrophage. *Eur J Biochem* 189:287–293
- Mache R, Jalliffier-Verne M, Rozier C, Loiseaux S (1978) Molecular weight determination of precursor, mature and post-mature plastid ribosomal RNA from spinach using fully denaturing conditions. *Biochim Biophys Acta* 517:390–399
- MacRobbie EAC (2002) Evidence for a role for protein tyrosine phosphatase in the cytosol of ion release from the guard cell vacuole in stomatal closure. *Proc Natl Acad Sci* 99:11963–11968
- Mahajan S, Tuteja N (2005) Cold, salinity and drought stresses: An overview. *Arch Biochem Biophys* 444:139–158
- Martin RC, Hollenbeck VG, Dombrowski JE (2007) Evaluation of reference genes for quantitative RT-PCR in *Lolium perenne*. *Crop Sci* 48:1881–1887
- Matsumura H, Reich S, Ito A, Saitoh H, Kamoun S, Winter P, Kahl G, Reuter M, Krüger DH, Terauchi R (2003) Gene expression analyses of plant host–pathogen interactions by SuperSAGE. *Proc Natl Acad Sci USA* 100:15718–15723
- Matsumura H, Yoshida K, Luo S, Kimura E, Fujibe T, Albertyn Z, Barrero RA, Krüger DH, Kahl G, Schroth GP, Terauchi R (2010) High-Throughput SuperSAGE for digital gene expression analyses of multiple samples using next generation sequencing. *PLoS ONE* 5:e12010
- Miyazaki S, Koga R, Bohnert HJ, Fukuhara T (1999) Tissue- and environmental response-specific expression of 10PP2C transcripts in *Mesembryanthemum crystallinum*. *Mol Gen Genet* 261:307–316
- Morrone O, Aagesen I, Scataglini MA, Salariato DL, Denham SS, Chemisquy MA, Sede SM, Giussani LM, Kellogg EA, Zuloaga FO (2012) Phylogeny of the Paniceae (Poaceae: Panicoideae): integrating plastid DNA sequences and morphology into a new classification. *Cladistics* 28:333–356

- Moss DN, Krenzer Jr EG, Brun WA (1969) Carbon dioxide compensation points in related plant species. *Science* 164:187–188
- Nakashima K, Takasakia H, Mizoi J, Shinozaki K, Yamaguchi-Shinozakia K (2012) NAC transcription factors in plant abiotic stress responses. *Biochim Biophys Acta* 1819:97–103
- Nakashima K, Yamaguchi-Shinozaki K (2013) ABA signalling in stress-response and seed development. *Plant Cell Rep* 32:959–970
- Nippert JB, Fay PA, Knapp AK (2007) Photosynthetic traits in C₃ and C₄ grassland species in mesocosm and field environments. *Environ Exp Bot* 60:412–420
- Oh SJ, Song SI, Kim YS, Jang HJ, Kim SY, Kim M, Kim YK, Nahm BH, Kim JK (2005) *Arabidopsis* CBF3/DREB1A and ABF3 in transgenic rice increased tolerance to abiotic stress without stunting growth. *Plant Physiol* 138:341–51
- Osmond CB, Winter K, Ziegler H (1982) Functional significance of different pathways of CO₂ fixation in photosynthesis. In: Lange OL, Noble PS, Osmond CB, Ziegler H (Eds) *Encyclopaedia of plant physiology, New Series, Vol. 12B*. Berlin: Springer Verlag 479–547
- Oukarroum A, El Madidi S, Schansker G, Strasser RJ (2007) Probing the responses of barley cultivars (*Hordeum vulgare* L.) by chlorophyll a fluorescence OLKJIP under drought stress and re-watering. *Environ Ex Bot* 60:438–446
- Oukarroum A, Schansker G, Strasser RJ (2009) Drought stress effects on photosystem I content and photosystem II thermotolerance analysed using Chl a fluorescence kinetics in barley varieties differing in their drought tolerance. *Physiol Plantarum* 137:188–199
- Pawłowicz I, Kosmala A, Rapacz M (2012) Expression pattern of the psbO gene and its involvement in acclimation of the photosynthetic apparatus during abiotic stresses in *Festuca arundinacea* and *F. pratensis*. *Acta Physiol Plant* 34:1915–1924
- Pinto H, Tissue DT, Ghannoum O (2011) *Panicum milioides* (C₃–C₄) does not have improved water or nitrogen economies relative to C₃ and C₄ congeners exposed to industrial-age climate change. *J Exp Bot* 62:3223–3234
- Qin F, Sakuma Y, Li J, Liu Q, Li YQ, Shinozaki K, Yamaguchi-Shinozaki K (2004) Cloning and functional analyses of a novel DREB1/CBF transcription factor involved in cold-responsive gene expression in *Zea mays* L. *Plant Cell Physiol* 45:1042–52

- Ripley B, Frole K, Gilbert M (2010) Differences in drought sensitivities and photosynthetic limitations between co-occurring C₃ and C₄ (NADP-ME) Panicoid grasses. *Ann Bot* 105:493–503
- Rozen S, Skaletsky HJ (2000) Primer3 on the WWW for general users and for biologist programmers. In: Krawetz S, Misener S (Eds) *Bioinformatics methods and protocols: Methods in molecular biology*. Humana Press, Totowa, NJ 365–386
- Sage RF (2004) The evolution of C₄ photosynthesis. *New Phytol* 161:341–370
- Saha S, Spark AB, Rago C, Akmaev V, Wang CJ, Vogelstein B, Kinzler KW, Velculescu VE (2002) Using the transcriptome to annotate the genome. *Nature Biotech* 20:508–512
- Saijo Y, Kinoshita N, Ishiyama K, Hata S, Kyojuka J, Hayakawa T, Nakamura T, Shimamoto K, Yamaya T, Izui K (2001) A Ca²⁺-dependent protein kinase that endows rice plants with cold- and saltstress tolerance functions in vascular bundles. *Plant Cell Physiol* 42:1228–1233
- Sakuma Y, Liu Q, Dubouzet JG, Abe H, Shinozaki K, Yamaguchi-Shinozaki K (2002) DNA-binding specificity of the ERF/AP2 domain of *Arabidopsis* DREBs, transcription factors involved in dehydration- and cold-inducible gene expression. *Biochem Biophys Res Commun* 290:998–1009
- Satoh R, Fujita Y, Nakashima K, Shinozaki K, Yamaguchi-Shinozaki K (2004) A novel subgroup of bZIP proteins function as transcriptional activators in hypoosmolarity responsive expression of the *ProDH* gene in *Arabidopsis*. *Plant Cell Physiol* 45:309–17
- Schansker G, Tóth SZ, Strasser RJ (2005) Methylviologen and dibromothymoquinone treatments of pea leaves reveal the role of photosystem I in the Chl a fluorescence rise OJIP. *BBABioenergetics* 1706:250–261
- Sede, SM, Zuloaga FO, Morrone O(2009) Phylogenetic studies in the Paniceae (Poaceae-Panicoideae): *Ocellochloa*, a new genus from the New World. *Syst Bot* 34:684–692
- Seki M, Narusaka M, Ishida J, Nanjo T, Fujita M, Oono Y, Kamiya A, Nakajima M, Enju A, Sakurai T, Satou M, Akiyama K, Taji T, Yamaguchi-Shinozaki K, Carninci P, Kawai J, Hayashizaki Y, and Shinozaki K (2002) Monitoring the expression profiles of ca. 7000 *Arabidopsis* genes under drought, cold, and high-salinity stresses using a full-length cDNA microarray. *Plant J* 31:279–292
- Shinozaki K, Yamaguchi-Shinozaki K (2000) Molecular responses to dehydration and low temperature: differences and cross-talk between two stress signalling pathways. *Curr Opin Plant Biol* 3:217–23

- Shinozaki K, Yamaguchi-Shinozaki K (2007): Gene networks involved in drought stress response and tolerance. *J Exp Bot* 58:221–227
- Shinozaki K, Yamaguchi-Shinozaki K, Seki M (2003) Regulatory network of gene expression in the drought and cold stress responses. *Curr Opin Plant Biol* 6:410–17
- Souza RP, Machado EC, Silva JAB, Lagoa AMMA, Silveira JAG (2004) Photosynthetic gas exchange, chlorophyll fluorescence and some associated metabolic changes in cowpea (*Vigna unguiculata*) during water stress and recovery. *Environ Exp Bot* 51:45–56
- Stefl R, Skrisovska L, Allain FH-T (2005) RNA sequence- and shape-dependent recognition by proteins in the ribonucleoprotein particle. *EMBO Reports* (Nature Publishing Group) 6:33–38
- Still CJ, Berry JA, Collatz GJ, DeFries RS (2003) Global distribution of C₃ and C₄ vegetation: carbon cycle implications. *Global Biogeochem Cy* 17:6–16
- Strasser BJ (1997) Donor side capacity of photosystem II probed by chlorophyll a fluorescence transients. *Photosynth Res* 52:147–155
- Strasser BJ, Strasser RJ (1995) Measuring fast fluorescence transients to address environmental questions: The JIP test. In: Mathis P (Ed) *Photosynthesis: From light to biosphere*, Vol 5. Kluwer Academic, The Netherlands 977–980
- Strasser RJ, Srivastava A, Govindjee (1995) Polyphasic chlorophyll a fluorescence transients in plants and cyanobacteria. *Photochem Photobiol* 61:32–42
- Strasser RJ, Srivastava A, Tsimilli-Michael M (1999) Screening the vitality and photosynthetic activity of plants by the fluorescence transient. In: Behl RK, Punia MS and Lather BPS (Eds) *Crop improvement for food security*. SSARM, Hisar, India 72–115
- Strasser RJ, Srivastava A, Tsimilli-Michael M (2000) The fluorescence transient as a tool to characterize and screen photosynthetic samples. In: Yunus M, Pathre U, Mohanty P (Eds) *Probing photosynthesis: Mechanism, regulation and adaptation*. Taylor and Francis, London, UK 443–480
- Strasser RJ, Stirbet AD (2001) Estimation of the energetic connectivity of PS II centres in plants using the fluorescence rise O-J-I-P. Fitting of experimental data to three different PS II models. *Mathem Comput Simulat* 56:451–461
- Strasser RJ, Tsimilli-Michael M, Qiang S, Goltsev V (2010) Simultaneous in vivo recording of prompt and delayed fluorescence and 820-nm reflection changes during drying and after rehydration of the resurrection plant *Haberlea rhodopensis*. *Biochim Biophys Acta* 1797:1313–1326

- Strasser RJ, Tsimilli-Michael M, Srivastava A (2004) Analysis of the chlorophyll fluorescence transient. In: Papageorgiou GC, Govindjee (Eds) Chlorophyll fluorescence: A signature of photosynthesis, advances in photosynthesis and respiration. Springer, Dordrecht, The Netherlands 321–362
- Sun W, Bernard C, Van De Cotte B, Van Montagu M, Verbruggen N (2001) *At-HSP17.6A*, encoding a small heat-shock protein in *Arabidopsis*, can enhance osmotolerance upon overexpression. *Plant J* 27:407–415
- Sunkar R, Zhu JK (2004) Novel and stress-regulated microRNAs and other small RNAs from *Arabidopsis*. *Plant Cell* 16:2001–19
- Thiombiano A, Schmidt M, Dressler S, Ouédraogo A, Hahn K, Zizka G (2012) Catalogue des plantes vasculaires du Burkina Faso. *Boissiera* 1–391
- Towbin H, Staehelin T, Gordon J (1979) Electrophoretic transfer of proteins from polyacrylamide gels to nitrocellulose sheets: procedure and some applications. *Proc Natl Acad Sci USA* 76:4350–4354
- Tran LSP, Nakashima K, Sakuma Y, Simpson SD, Fujita Y, Shinozaki K, Yamaguchi-Shinozaki K (2004) Functional analyses of *Arabidopsis* NAC transcription factors controlling expression of *erd1* gene under drought stress. *Plant Cell* 16:2482–98
- Triesmann R (1996) Regulation of transcription by MAP kinase cascades. *Curr Opin Cell Biol* 8:205–215
- Uno Y, Furihata T, Abe H, Yoshida R, Shinozaki K, Yamaguchi-Shinozaki K (2000) *Arabidopsis* basic leucine zipper transcription factors involved in an abscisic acid-dependent signal transduction pathway under drought and high-salinity conditions. *Proc Natl Acad Sci USA* 97:11632–37
- van Heerden PDR, Swanepoel JW, Krüger GHJ (2007) Modulation of photosynthesis by drought in two desert scrub species exhibiting C₃-mode CO₂ assimilation. *Environ Ex Bot* 61:124–136
- van Heerden PDR, Tsimilli-Michael M, Krüger GHJ, Strasser RJ (2003) Dark chilling effects on soybean genotypes during vegetative development: Parallel studies of CO₂ assimilation, chlorophyll-a fluorescence kinetics O-J-I-P and nitrogen fixation. *Physiol Plant* 117:476–491
- Velculescu VE, Zhang L, Vogelstein B, Kinzler KW (1995) Serial analyses of gene expression. *Science* 270:484–487

- Vicré M, Farrant JM, Driouich A (2004) Insights into the cellular mechanisms of desiccation tolerance among angiosperm resurrection plant species. *Plant Cell Environ* 27:1329–1340
- Webster RD (1988) Genera of the North American Paniceae (Poaceae: Panicoideae). *Syst Bot* 13:576–609
- William JT, Farias RM (1972) Utilisation and taxonomy of the desert grass *Panicum turgidum*. *Econ Bot* 26:13–20
- Xu C, Huang B (2010) Differential proteomic responses to water stress induced by PEG in two creeping bentgrass cultivars differing in stress tolerance. *J Plant Physiol* 167:1477–1485
- Yamada S, Komori T, Myers PN, Kuwata S, Kubo T, Imaseki H (1997) Expression of plasma membrane water channel genes under water stress in *Nicotiana excelsior*. *Plant Cell Physiol* 25:1226–1231
- Yamaguchi-Shinozaki K, Koizumi M, Urao S, Shinozaki K (1992) Molecular cloning and characterization of 9 cDNAs for genes that are responsive to desiccation in *Arabidopsis thaliana*: Sequence analysis of one cDNA that encodes a putative transmembrane channel protein. *Plant Cell Physiol* 25:217–224
- Yamaguchi-Shinozaki K, Shinozaki K (2005) Organization of *cis*-acting regulatory elements in osmotic- and cold-stress-responsive promoters. *Trends Plant Sci* 10:88–94
- Yamaguchi-Shinozaki K, Shinozaki K (2006) Transcriptional regulatory networks in cellular responses and tolerance to dehydration and cold stresses. *Annu Rev Plant Biol* 57:781–803
- Yang T, Poovaiah BW (2003) Calcium/Calmodulin-mediated signal network in plants. *Trends Plant Sci* 8:505–512
- Yordanov I, Goltsev V, Stefanov D, Chernev P, Zaharieva I, Kirova M, Gecheva V, Strasser RJ (2008) Preservation of photosynthetic electron transport from senescence-induced inactivation in primary leaves after decapitation and defoliation of bean plants. *J Plant Phys* 165:1954–1963
- Zimmermann T, Bocksberger G, Brüggemann W, Berberich T (2013) Phylogenetic relationship and molecular taxonomy of African grasses of the genus *Panicum* inferred from four chloroplast DNA-barcodes and nuclear gene sequences. *J Plant Res* 126:363–371
- Zivcak M, Brestic M, Olsovska K, Slamka P (2008) Performance Index as a sensitive indicator of water stress in *Triticum aestivum* L. *Plant Soil Environ* 54:133–139

8 List of figures

Fig. 1: Maps of annual mean surface temperature change and average percent change in annual mean precipitation	2
Fig. 2: Anatomy of a C ₄ leaf (Kranz anatomy)	3
Fig. 3: NAD-ME subtype of C ₄ photosynthesis	5
Fig. 4: Summary of the main effects of water stress on the photosynthetic parameters of C ₄ leaves.	9
Fig. 5: Transcriptional regulatory networks involved in drought-stress-responsive gene expression.	10
Fig. 6: Selected steps of the HT-SuperSAGE method	25
Fig. 7: Selected steps of the 3' RACE method.....	31
Fig. 8: Overview of the BLAST searches.....	32
Fig. 9: Schematic description of Primer efficiency measurement setup.....	34
Fig. 10: Plate setup for a qPCR experiment.....	35
Fig. 11: Drought stress treatment.....	38
Fig. 12: Photosynthesis rate (P_N) recorded in three <i>Panicum</i> species under drought stress...39	
Fig. 13: Stomatal conductance (g_{H_2O}) recorded in three <i>Panicum</i> species under drought stress.	40
Fig. 14: Water use efficiency (WUE) of <i>Panicum</i> species under different water regimes.	42
Fig. 15: Averaged polyphasic chlorophyll a fluorescence transients normalized to $F_0 = 50\mu s$ applied on a logarithmic time scale.	43
Fig. 16: Averaged chlorophyll a transients double normalized to $F_{50\mu s} = 0$ and $F_M = 1$ applied on a logarithmic time scale.....	44
Fig. 17: ΔV_{OJ} curves applied on a logarithmic time scale.	45
Fig. 18: Spider Plot of selected relative JIP-test fluorescence parameters.	47
Fig. 19: Correlation of P_N and PI_{tot}	48
Fig. 20: SDS-PAG with C ₃ (<i>P. bisulcatum</i>) and C ₄ (<i>P. laetum</i>) samples	49
Fig. 21: Immunodetection of PEPC, RubisCO LSU and SSU, OEC and Dehydrin 1.....	49
Fig. 22: Isolated, DNA-digested and purified RNA.....	51
Fig. 23: HT-SuperSAGE tag regulation (≥ 2 -fold).....	53
Fig. 24: Differential regulation of HT-SuperSAGE tags.....	54
Fig. 25: Species-comprehensive comparison of the total number of differentially regulated tags.....	55

Fig. 26: Species-comprehensive comparison of the differentially regulated tags (group 1-4)	56
Fig. 27: Species-comprehensive comparison of the differentially regulated tags (group 5-8).	57
Fig. 28: Number of tags ≥ 2 -fold and < 5 -fold expressed under the different regulation schemata	59
Fig. 29: Number of tags ≥ 5 -fold differentially expressed (groups 1-4)	60
Fig. 30: Number of tags ≥ 5 -fold differentially expressed (groups 5-8)	61
Fig. 31: Overview of elected genes concerning coding region, 26 bp tag and 3' RACE sequence	66
Fig. 32: Exemplary qPCR amplification plot for primer efficiency	67
Fig. 33: Exemplary samples from the primer efficiency qPCR run on a 2 % agarose gel	68
Fig. 34: qPCR amplification plots of the reference gene CPB20	69
Fig. 35: Exemplary amplification plot of a comprehensive qPCR run	70
Fig. 36: Exemplary samples from the comparative qPCR run on a 2 % agarose gel	71
Fig. 37: Differential regulation of gene expression in <i>P. laetum</i> , <i>P. miliaceum</i> and <i>P. turgidum</i> detected by qPCR analyses	71
Fig. 38: Transcriptional regulatory networks of abiotic stress signals and gene expression	93
Fig. 39: Agarose gel with 3' RACE samples	139

9 List of tables

Table 1: Origin of seeds / plants.....	13
Table 2: Climate chamber setup	13
Table 3: Sampling scheme	15
Table 4: Experimental values provided by the JIP-test.....	18
Table 5: Pipetting scheme for the standard curve of the Bradford protein assay.....	20
Table 6: Pipetting scheme for different SDS-PAGs	21
Table 7: List of primary antibodies used for immunodetection	22
Table 8: Adapter 1 indices.....	28
Table 9: RWC values of samples.....	37
Table 10: Water use efficiency (WUE) [$\mu\text{mol CO}_2/\text{mmol H}_2\text{O}$] of analysed <i>Panicum</i> species under different water regimes	41
Table 11: Relative OJIP parameters measured during control, stress and recover.....	46
Table 12: Number of counted pixels for protein bands	50
Table 13: HT-SuperSAGE results	52
Table 14: Differentially regulated tags in the four <i>Panicum</i> species	55
Table 15: Exemplary analyses of tags shared by all four <i>Panicum</i> species (C<S>R).....	58
Table 16: Differential tag expression with appending tag amounts	59
Table 17: Tags differentially regulated ≥ 50 -fold and the appending number of tags	62
Table 18: BLAST search outcome.	63
Table 19: Summary of the 3' RACE outcome	64
Table 20: Annotation of the (via 3' RACE) elongated sequences by BLAST search.....	65
Table 21: Genes chosen for the qPCR analyses.....	67
Table 22: Standard curve results for the chosen target genes	68
Table 23: Standard curve results for the reference gene primer efficiency qPCR run	69
Table 24: Differential gene regulation recorded by HT-SuperSAGE and qPCR analyses...	72
Table 25: Species-comprehensive analyses of the genes used to conduct qPCR analyses ...	73
Table 26: Primers generated from the 26 bp tags for 3' RACE (1 – 12).....	137
Table 27: Primers generated from the 26 bp tags for 3' RACE (13 – 24)	138

10 Abbreviations

SI units as well as fluorescence parameters (Table 4) are not explained.

a.s.l.	above sea level
ABA	abscisic acid
ABRE	ABA-responsive element
ADP	Adenosine diphosphate
Ala	alanine
AMP	adenosine monophosphate
APR	adenosine 5'-phosphosulfate reductase 2
APS	ammonium persulfate
AREB	ABRE-binding proteins
Asp	aspartate
ATP	adenosine triphosphate
B&W	bind and wash
BiK-F	Biodiversität und Klimaforschungszentrum Frankfurt
BLAST	Basic Local Alignment Search Tool
BLAST _n	nucleotide BLAST
BLAST _p	protein BLAST
bp	base pair
BSA	bovine serum albumin
BSC	bundle sheath cell
C	control
CAM	crassulacean acid metabolism
CBF	C-repeat binding factor
cDNA	copy DNA
CDPK	calcium-dependent protein kinase
Chl	chlorophyll
C _i	intercellular CO ₂ concentration
CMIP	Coupled Model Intercomparison Project Phase
CO ₂	carbon dioxide
CP	cysteine proteinase
CPB 20	cap-binding protein 20
CRT	C-repeat
C _t	Cycle threshold
DCMU	3-(3,4-dichlorophenyl)-1,1-dimethylurea
DMSO	Dimethyl sulfoxide
DNA	deoxyribonucleic acid
dNTP	deoxyribonucleotide
DRE	drought-responsive element
DREB	DRE binding proteins
ds	double-stranded
DTT	Dithiothreitol
DW	dry weight
ECL	enhanced chemiluminescence
EDTA	ethylenediaminetetraacetic acid
EST	expressed sequence tag
F	fluorescence
Fig.	Figure
Forsk.	Forskål

F_t	fluorescence values at a given time
FW	fresh weight
GDP	Guanosine diphosphate
g_{H_2O}	stomatal conductance to water vapour
GTP	Guanosine triphosphate
h	hour
H_2O	water
HCl	hydrogen chloride
HCO_3^-	hydrogen carbonate
HD-ZF	homeo domain-zink finger
HRP	horseradish peroxidase
HSP	Heat shock protein
HT-SuperSAGE	high throughput-serial analysis of gene expression
IPCC	Intergovernmental Panel on Climate Change
IPTG	Isopropyl β -D-1-thiogalactopyranoside
L.	Linnaeus
LEA	late embryogenesis abundant
LSU	large subunit
MA	malate
MAPK	mitogen-activated protein kinase
MAPKK	MAPK kinase
MAPKKK	MAPKK kinase
MC	mesophyll cell
MIP	major intrinsic protein
mRNA	messenger RNA
n	number of samples
NaCl	sodium chloride
NAD	nicotinamidadeninedinucleotide
NAD-ME	NAD-malate enzyme
NADP	nicotinamidadeninedinucleotidephosphate
NADP-ME	NADP-malate enzyme
NCBI	National Centre for Biotechnology Information
NCED 1	9-cis-epoxacarotenoid dioxygenase 1
NGS	next generation sequencing
NORM	normalizing assay
NP-40	nonidet P-40
nr / nt	non-redundant / nucleotide
NRT	no real-time
ns	not significant
NTC	no template control
OAA	oxaloacetate
OEC	oxygen evolving complex
PA	pyruvate
PAG	polyacrylamide gel
PAGE	polyacrylamide gel electrophoresis
PAP	purple acid phosphatase
PCK	phospho <i>eno</i> pyruvate carboxykinase
pCO_2	partial pressures of carbon dioxide
PEP	phospho <i>eno</i> pyruvate
PEPC	phospho <i>eno</i> pyruvate carboxylase
pH	$-\log [H_3O^+]$

Phe	pheophytine
Pi	orthophosphate
P_N	photosynthesis rate
PPase	phosphoprotein (serine/threonine) phosphatase
PPi	pyrophosphate
ppm	parts per million
PS	photosystem
PTPase	protein tyrosine phosphatases
PVDF	polyvinylidene difluoride
QA	quinone A B
QB	quinone B
qPCR	quantitative polymerase chain reaction
R	recovery
RACE	rapid amplification of cDNA ends
RC	reaction centre
RCP	Representative Concentration Pathway
RE	restriction enzyme
RNA	ribonucleic acid
RNA-Seq	Whole Transcriptome Shotgun Sequencing
RNP	ribonuclease precursor
ROS	reactive oxygen species
rpm	rounds per minute
rRNA	ribosomal RNA
RT	room temperature
RubisCO	ribulose-1,5-bisphosphate carboxylase/oxygenase
RuBP	ribulose-1,5-bosphosphate
RWC	relative water content
S	stress
SD	standard deviation
SDS	Sodium dodecyl sulphate
SSU	small subunit
<i>T</i>	transpiration rate
TBST	Tris-buffered saline tween-20
TEMED	N,N,N',N'-tetramethylethyldiamin
TF	transcription factor
Thunb.	Thunberg
TIL	temperature-induced lipocaline
Tris	Tris-(hydroxymethyl-)aminomethan
TW	turgid weight
TyrZ	tyrosinZ
UTR	untranslated region
v / v	volume per volume
w / v	weight per volume
WUE	water use efficiency
X-gal	5-bromo-4-chloro-3-indolyl- β -D-galactopyranoside

11 Appendix

11.1 3' RACE

Primers designed by tags generated through HT-SuperSAGE and used to conduct 3' RACE.

Table 26: Primers generated from the 26 bp tags for 3' RACE. Listed are primers 1 - 12 generated from highly differentially regulated HT-SuperSAGE tags. Primers were used for 3' RACE (forward primers). Control (C), stress (S) and recovery (R), down-regulation (>), up-regulation (<), no differential regulation (=), melting temperature (T_m).

	C > S < R	T _m [°C]	C < S > R	T _m [°C]	C > S = R	T _m [°C]				
<i>P. bisulcatus</i>	1	CATGATCCAGTGTGAGTTTGTG	55,7	5	CATGGATCTGACATCTTTTGGGT	58	11	CATCTCCTCCCCCAACC	60	
	2	CATGTACGTGTAGGAGTCAAGGTG	59,5	6	CATGTATGCAATGGCACTGTATATA	53,2	12	CATGTTACTACTCTGGTAGACGC	57,4	
	3	GGTGAGGAGAGTGGAGTGTAT	56,7	7	CATGGTGGTGGTTCAAATTTGCATA	56,4				
	4	CATGTTCCGGTGGGTGCCAAAAAAA	58	8	CATGAACCCCAACGATGAAGGAAAAAT	58				
				9	GAGACACGTGTTCCGGAATCCG	58,6				
				10	CATGAAGGATAGGGGGTTCGGATAGA	59,5				
	<i>P. lactum</i>	1	CATGAGCAAATTAATGCTACCAATGG	54,8	5	CATGAATAAGGCCAGCTTAATTAATT	53,2	11	GCGTGGACCGGATCAATGGAAAT	58,8
		2	AACGGCCTGTGCTGTCTG	57,6	6	CATGTATGTATCTCAAGCATCCAGAT	54,8	12	CATGAACTAGTAGCTAGTGTCTCGT	56,4
		3	CCGGGGCTTGTAGTTTCGCTA	58,6	7	CATGCCATCTGATATAGAGATATA	51,7			
		4	CATGAGCAAACAATGCTACCAATGGCT	58	8	CATGTACTCTTAAAGATGACTTCA CA	54,8			
				9	CATGTTTGGTTCCTCAAGTGGAAAT	54,8				
				10	CATGATCAITTTGTAATTTGAAAAATTTG	48,5				
<i>P. miltaceum</i>		1	TTCCTGTACGGCGCTCGCG	60	5	ATGACGGCGCCGGTGTCTGT	59,7	11	AGCGCTGGCCAAAGCGCG	59,4
		2	CATGTTTCTCGCCTGTATATCCAG	58	6	CACCCGGCCACCGTCTGTCT	59,7	12	AGCACAACTCCGGCCACTGGG	60,2
		3	CATGGCAGCAGGATTCCAAGAGATTA	59,5	7	AACCGCGCTCCGGGGTGT	59,4			
		4	CTCAAGATGGGGGCCATCGAG	58,3	8	AGGAGGCCACCGGGGTGC	59,4			
				9	GATCGGGCCAGCACGTCC	59,7				
				10	GCCCGCCGACAGATAGAAATGT	58,8				
	<i>P. turgidum</i>	1	CTCAAGTGAACGGACCGGATCG	60,4	5	CGCGTGAATATGTACCCGGG	58,3	11	GGAGCGCTGTGATCTCTCAG	60,2
		2	GTGCTTTGTCTGGGCTTCT	56,7	6	CATGCTCGACACGGTTGTCTTTTAG	57,7	12	CATGGAAATAATGTCCCTGCTTTG	58
		3	CATGAAGCGGCCACGGCGC	59,7	7	GGGGGTAGCTTGTGTTCAGC	60,4			
		4	CATGCATACAGCTACGGGTTGG	56,7	8	GGGGGGGTAGTTTGTGTTCAGC	60,6			
			9	CATGTGATCTGTCTTTTGTCTTTG	58					
			10	GGCTATGGGATCGGAAATCGTA	58,8					

Table 27: Primers generated from the 26 bp tags for 3' RACE. Listed are primers 13 – 24 generated from highly differentially regulated HT-SuperSAGE tags. Primers were used for 3' RACE (forward primers). Control (C), stress (S) and recovery (R), down-regulation (>), up-regulation (<), no differential regulation (=), melting temperature (T_m).

	C < S = R	T _m [°C]	C = S < R	T _m [°C]	C < S < R	T _m [°C]	
<i>P. bisulcatum</i>	13	54,8	CATGTCGATCGTGGACTGTAGAACT	59,5	23	CATGTAATAATTTGAGCAAAAAAAAAAAAA	46,9
	14	51,7	GTAATATCGTCCCTCTCTCTGCC	58,8	24	CATGAACATATCTATAGAGAGTTGCA	53,2
	15	59,5	CATGAGCAGGCAAGAGAAAACTGCTG	46,9			
	16	54,8	CATGTCCGCTACTCAGGTAAAAAAA	53,2			
	17	48,5	CATGTATATCAAAATAAAATGCTAAAC	58,8			
<i>P. lactum</i>	13	59,4	TGGGGCTCGTCGGCTCG	59,7	23	GTACCAGGCCTAGGGCAGCGAACT	60,6
	14	60,4	CCACGGGCTTGCTGTAGCTA	60,4	24	AGAGCGGGCACGGCGGACG	59,4
	15	59,7	TGGGGCTTGTCGGCTCGC	60,4			
	16	60,4	CTCACCAACTTCTGCCAGCGCC	60,6			
	17	58,5	GCTCCAGGCCAGCGTATGAAGAA	59,7			
<i>P. millicecum</i>	13	59,4	ATGGCTGCGGGCGGAGG	58	23	GGCCGTGTCAAAGGTCAAAGGCTAT	58,8
	14	58,8	GTGCCAACCCGTAATCGACTTGC	59,7	24	ATACGCATCGCCCGCCGCCAC	60
	15	60,4	CGTGGGCAGCCAAAGCTGCTAG	59,7			
	16	59,7	AAGCGGTGCTCGCGCTCC	58,8			
	17	59,4	ACCGGACGGGAGGCTG	59,7			
<i>P. turfidum</i>	13	53,2	CATGAATACAATTGTTCTCTGCT	60,4	23	CATGCCGGTCGGCGCTGG	59,4
	14	58	CATGCGGTGTGATTCGATGGTTCT	59,7	24	GAACATAAACCGCGCGCCGCTAG	59,8
	15	59,4	AGGGCCGCCATCGACGCG	56,4			
	16	59,5	CATGCTGCAAGACTGCAACGGATTG	60,6			
	17	59,4	CGGCGTTAGGGGGGGCT	56,4			

Agarose gel with applied 3' RACE samples. Orange rectangles mark bands which were cut out, purified and sequenced.

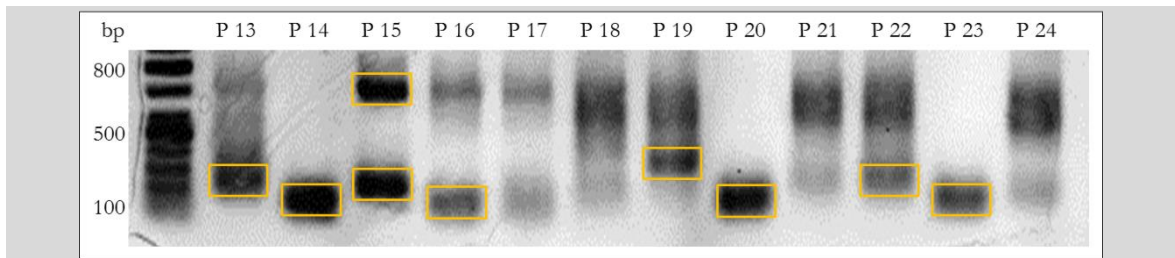


Fig. 39: Agarose gel with 3' RACE samples. Exemplary, the 3' RACE reactions carried out with *P. laetum*, primers (P) 13 – 24 is shown. The orange rectangles mark the bands cut out of the gel, diluted and send for sequencing.

Sequences generated by 3' RACE (5' – 3'). Numbers in brackets refer to Primers (Table 26, Table 27).

P. bisulcatum (2) 138 bp

TAGTTAAGGCAGCAATCTGCCGTGCATATATAGTCTGCTACTACGTGTACGT
ACTGTATACGTAACAAAATACTTATAAAAAGCAGAGCAGATAGGTTTATACAG
AGACGACGACCCCTGTAGTCCCAAAAAAAAAAAAAA

P. bisulcatum (3) 66 bp

GGTTAGGGTAGAGATTGTTTAATCAGTATCTATCTCGATGGGGTTCGTTCCTG
TGCCTTAAAAATGC

P. bisulcatum (5) 74 bp

TGGTACCAACCTTGTATTTGCACTARTAAAAAGGGAACCTCAGTTGTGCTCGT
GGCGTAAAAAAAAAAAAAAAAA

P. bisulcatum (9) 153 bp

TGCCACGTTACTTTAGCTAGGCGAGTCATCAGGATAGTAGGATAGTGAGTTC
TTT*TAGTTTCGCCCTGTGCTCAGCACGTTCCACGCAGCTGCATATGGTACCGC
GCCGTGTCGATGTGTCGTTCTCGGAAAAGGGTCAGGGAGTCGTGGTGTG

P. bisulcatum (11) 103 bp

GTTGGGTGAGGACATGTGAATGCAAGCTCCGGCTATGATATGTAATATGGA
TACTAGAGCACATCTGTCACAATCCGCCGACAATACTAGATCGTGTAAATA

P. bisulcatum (11) 108 bp

TATCGTTGGGTGAGGAACATGTGAATGCAAGCTCCGGCTATGATATGTAATA
TGGATACTAGAGCACATCTGTCACAATCCGCCGACAATACTAGATCGTGTTA
ATTA

P. laetum (2) 106 bp

CGTCCTCGGCCGCCGCGCCTCCCTCCTTCGCCGTCGTCTGCGGCACCGGCAAG
AAGATCAAGACCGACAAGCCCTTCGGGATYGGGGGTGGCCTCACCGTCGAC
AAA

P. laetum (14) 55 bp

TCTCTGCTATATGATGCGTCTCGCGCGCAGCGAATAAAAAGCTGATTCCGACT
TAC

P. laetum (17) 104 bp

AGGCCTACGCTAGAAGCTTGTGTGTATTGAGTTTGACRATGTATGCAACTA
TCTACTGAAATAAGAGATATATCATACATGTGCAATTTCTTCAAAAAAAAAAAAA

P. laetum (19) 95 bp

TGGTGTCTRTTGGTGGGCTAATGTACGTCGTTTCTTCTTTCGGTCGCAACGCA
ACATTTGCAACTGCTGTAATGTAATTGGGTGTATTGATTTATGT

P. laetum (24) 211bp

AGTTATCTTTTCTGCTTAACGGCCTGCCAACCCCTGGAAACGGTTCAGCCGGA
GGTAGGGTCCAGCGGTTCGGAAGAGCACCGCACGTCGCGCGGTGTCCGGTG
CGCCCCGGCGGCCCATGAAAATCCGGAGGACCGAGTACCGTCCACGCCCCG
GTCATACTCATAACCGCATCAGGTCTCCAAGGTGAACAGCCTCTGGCCAATG
GAACAA

P. miliaceum (3) 134 bp

CTGATACTAGGTCATAGTATGAACAAAACCTGTAGGTCTCGTATAGCATTTCGA
GTGTACGAATTGTTGTATTGAAAATGTAGCAGAACCATACAAGGGTTTAGA
GTTGATATGGAAACGCAAAGATTTTAACGA

P. miliaceum (9) 124 bp

CGGAGCTCATCGCCGGCTTCACTGTGCAGTACGGCCGCGACGGATCCAACCTT
CATCGACATGAGCGTCCGGAAGCAGATTGAGGAGATCGCCTCAGAGTTTCGA
GCTGCCCTCCGTCGCCCTCTA

P. miliaceum (10) 171 bp

GTGTTCTGTACTGTATAGTGCAAGAGAAGGTGGTGTAAATTGGGGGGCGTAA
TGTAATCTCGAACATTGTGCGTCGTTCTTCTTTCGGTCGCAACGCAGCATTG
CAACTGCTGTAATGTAATTGGGTGTACTGATTTATGTGCGGGTTGCTTATGG
TGTGTTTTAAAAAAAAA

P. miliaceum (17) 200 bp

CTGATCTCCCTAATCTAGGAGAGCTGGCTAGTCTCGCAGGACGCTGCGCGGC
ATGGCCTTCGTGGAGCAATGGCAGAATAGCACCCCTTGCTAGTGTCCGGTGCT
CTTCGGAGCAGCAAGGCCGGCGATCAGACCAGCCATTGCAAGTCCAGCTACC
CGACTTCAGGCCAAAGCAGTCATGCTGACCCCTGTGGATCTGAA

P. miliaceum (20) 102 bp

GCTTCTGTTCGAGCCGCACCGCCAGGCCATCAAGTACCCGTCCGAGAAGA
GGGACGTCTACTCGCTCGTCGCCTTCGTCAACAGCCTCCGGTGAGAGGCC

P. miliaceum (22) 69 bp

TGCACAAGAACATTCGCCATCAGCTCTTGAAGCATCTAGCTAGCACTCTCACA
AAAAAAAAAAAAAAAAAAAA

P. turgidum (2) 132 bp

TGTCCCCTCTGTAATCCATTGCTATGATGAGATCTTGTGCTAAAATATTCGCC

GGTGAGGGCTATCCTATGGCATTATCTGAAACTGTTTTTCGATGAATGTATTG
TACGTTTTGGATCMGTTATAAAAAAAAAA

*P. turgidum*_(12) 103 bp

CTCCTCGCGGAGCATAATGTACTGTGCGTGTAGTAATCCTCGACAAATAAGC
TAGTGTGGCTAGCATTTGTTGCTTCACGCGCCTTCGTGTCATCCTTTCAAGG

P. turgidum (14) 164 bp

AGGATAGGTTCTGATTTGTCCTCGTCTGTATATAACCATTGCATATGATGTGAT
CTTGTGCTAGAATATTCGCCGGTGAGGGCTATCCTATGGCATTATCTGAAAC
TGTTTTTCGATGAATGTATTGTACGTTTGGATCAAGTTATTGTGGATGTTTGT
CACACCA

P. turgidum (17) 189 bp

CCTGTGTTTGGTGTCTGTTTCGIGTTCGTTGTTGCCCATCIGTGTTTTTGATC
GCAAGCTCGTTCGTCTAGTGGTTGTGTTGTTGTCTGTCAGAGCTATCTTGAT
CTCCGTCCCATGAACTGGGGTGTGGATTGGATGCTGTTGTCTTGTGTAAC
TGTTCCCGTTTCAGTTAATCAAATGGAAAAA

Acknowledgments

I would like to thank Prof. Dr. Wolfgang Brüggemann for the great opportunity to do my doctorate degree in his laboratory. I would also like to thank him for the allocation of the very interesting working question and the chemicals, the equipment and financial support.

PD Dr. Thomas Berberich I would like to thank for the assistance and supervision during my dissertation. Furthermore I would like to thank him for the great support achieving the “Short-Term Post-doctoral fellowship” from the “*Japan Society for the Promotion of Science*” and the scientific contacts.

I would also like to thank Prof. Dr. Hideo Matsumura from the Shinshu-University, Ueda, Japan for his great support during my stay and the allocation of a working place, all the necessary chemicals and equipment to carry out my analysis. Furthermore I would also like to thank him for his great engagement to help me feel warmly welcome.

I would also like to thank Dr. Ryohei Terauchi from the Iwate Biotechnology Research Institute (IBRC), Kitakami, Japan for his great support during my stay and the allocation of a working place and the opportunity for the sequencing of my samples. Furthermore I would also like to thank him for his great engagement to help me feel warmly welcome.

Dr. Hiromasa Saitoh I would like to thank for his great supervision during my stay in Kitakami and the numerous times taking me around Kitakami.

I would also like to thank the “Japan Society for the Promotion of Science” for the allocation of three month “Post-doctoral fellowship” and the possibility to carry out research in Japan.

The “Stiftung Polytechnische Gesellschaft Frankfurt” I would like to thank for the allocation of the „MainCampus doctus“ fellowship during my dissertation and the many workshops and extra-curricular activities.

Prof. Dr. Claudia Büchel I would like to thank for the allocation of the Real-Time PCR Thermo Cyclers.

I would also like to say thank you to all members of the working group for the great support during my time in the working group, especially Vera and Stefan, for the great times we had in our office.

I would also like to thank Rike, Sarah and Stella for always supporting and motivating me during the whole time, it has helped me a lot!

And last but not least I would like to thank my wonderful small and big family for everything; I would have never made it without you!

Curriculum vitae

Tanja Jungcurt born Zimmermann, * 17.12.1983 Frankfurt/Main, Germany
t.jungcurt@sciencemail.org



Tertiary Education

since 01.11.2010	Doctorate thesis „ Analysis on the Diversity of Drought Tolerance in Grasses of the Genus <i>Panicum</i> “ in the Group of Prof. Dr. W. Brüggemann under the supervision of PD Dr. T. Berberich at the Goethe University Frankfurt/Main
SS 09 – SS 2010	Diploma thesis „Phylogenetic Relationship and Drought Tolerance in West African Grasses“ in the Group of Prof. Dr. W. Brüggemann under the supervision of PD Dr. T. Berberich at the Goethe University Frankfurt (Diploma, degree: 1,1)

Conferences and internships

2013	Conference of the German Botanical Society, Germany
2013	UK plant science conference, Scotland
2011	Shinshu University and Iwate Biotechnology Research Institute (IBRC), Japan (3 month JSPS internship)
2011	SPPS conference, Norway
2011	Field trip, Mongolia (2 weeks)
2009	Conference of the German Botanical Society, Germany
2007 – 2008	Universidad de Granada, Spain (ERASMUS)
2000 – 2001	Orewa College, New Zealand

Publications

Zimmermann T, Bocksberger G, Brüggemann W, Berberich T (2013) Phylogenetic relationship and molecular taxonomy of African grasses of the genus *Panicum* inferred from four chloroplast DNA-barcodes and nuclear gene sequences. J Plant Res 126:363–371

